ACOUSTIC WAVE-GUIDE MEASUREMENTS IN AIR FILLED AND WATER-FILLED TUBES

Submitted to

THE UNIVERSITY OF LONDON

For the degree of

MASTER OF PHILOSOPHY

by

ÜMİT ÜLKÜ

Department of Physics

Imperial Colloge of Science and Technology

October, 1968.

ACKNOWLEGEMENT

The author wishes to express his gratitude to Dr. R. W. B. Stephens for his advice and encouragement given during the preparation of this thesis.

CONTENTS:

ABSTRACT.

Employing the standing wave method, the attenuation coefficient of the (0,0), (I,0), and (2,0) mode sound waves in two different rigid walled rectangular wave-guides filled with air have been measured in the frequency range from I.2 to 4.7 Kc/s. Experimental values of attenuation coefficient are in good agreement (about 3%) with the theoretical values.

Measurements of the attenuation coefficient with a helium filled guide were also carried out and good agreement with theory was obtained.

The specific acoustic impedance of a sample of mineral wool and absorption coefficients of the mineral wool and an artifical sample were measured at normal and oblique incidence.

The variation of the reflection coefficient of some pressure -release materials under high hydrostatic pressures at frequencies up to 5.5 Kc/s has been measured.

In these experiments a column of water contained in a cylindirical, vertical steel tube was excited into resonance by a sound source situated at the bottom of the tube, both with and without the samples. Resistance and reactance ratios have been obtained for the samples at different frequencies and for hydrostatic pressures from zero to 25 atmospheres.

The theory of the pressure-release materials under high

hydrostatic pressure indicates that it is possible to make good pressure-release materials capable of operating in deep water. It appears that the materials should have adequate resistance to high hydrostatic pressure and must contain air-filled voids.

The results indicate the reflecting properties of the samples and so can help in the design of efficent reflectors.

CHAPTER I

GENERAL SURVEY

Details of propagation of higher order mode sound waves in rigid walled, gas filled, rectangular wave-guides will be explained in chapter II.

Two different rectangular wave-guides have been used for measurements of tube attenuation and the impedance and absorption coefficient of porous materials. The details of the apparatus will be given in chapter III.

Theoretical values of the coefficients of (0,0),(m,0), (0,n) and (m,n) type modes will be given in chapter IV. It appears that for wave-guides with the transverse dimensions less than I5cm. sound attenuation in the body of the medium is small compared with the tube wall losses. (about I%).

Applying the boundary layer theory, the theoretical values of attenuation coefficients for air and helium are calculated. Experimental values of attenuation coefficient were determined by employing the standing wave method.

Although, measurements with (0,0) and (I,0) modes were carried out by many authors, less attention was given for (2,0) mode .

The results of measurements with (2,0),(I,0) and(0,0) modes for air filled waveguides have been given in chapter V. Re-

sults of measurements with helium filled guide are also included in the same chapter.

In chapter VI, the methods and determination of the specific acoustic impedance of porous materials at oblique incidence are explained and the specific acoustic impedance of a sample of mineral wool was measured at normal and oblique incidence.

In chapter VII, the properties of sound absorbing materials will be explained. Absorption coefficients of mineral wool and an artifical sample at normal and oblique incidence have been measured.

In underwater acoustics, at shallow depths, it is easy to make a good reflector using different materials which contain air. For deep water, however, there are other conditions which require to be fulfilled and these are dealt within chapter VIII.

Very little attention has been paid to the construction of reflectors in water-borne sound, especially in deep water. Thus, one of the main aim of this work was to examine the acoustic properties of some available pressure-release materials in water at high hydrostatic pressures and at audible frequencies. Some forms of medium are proposed for testing and two artifical materials were made for experiment.

The measurements were carried out with a water filled steel tube and details are given in chapter IX.

The method of resonance analysis was applied for the measurement of the specific acoustic impedance of the pressure-release materials. This method is explained in chapter X.

Apparatus which were used for measurements and the experimental results for the two artifical samples, three different foamed plastic and a sample of rubber with closed pores, are given in chapter XI.

It was found that at zero hydrostatic pressure, all samples have a reflection coefficient of about 90% or above. However, at high hydrostatic pressures the reflection coefficient of the samples are reduced. This reduction is depends on the type of material.

CHAPTER II

PROPAGATION OF SOUND IN RECTANGULAR FLUID WAVE-GUIDES. CASE OF RIGID WALLS AND WITHOUT ENERGY DISSIPATION.

2.1. INTRODUCTION.

The phenomenon of wave propagation within wave-guides has been known for more than 9o years. Lord Rayleigh[1], has given a theoretical account of the higher order acoustic waves which are possible within rigid-walled tubes of rectangular and circular cross-section. Morse[2], Rogers[3], and more recently Redwood[4], Budden[5], Rschevein[6] and Bate and Stephens[7] also dealt with this subject in more detail.

In wave-guide propagation the boundaries of the guide have a considerable influence on the types of wave that may be propagated. If the boundaries are rigid and impervious, plane waves are possible within the guide as well as higher order modes. This may be achieved by enclosing the fluid between solid plates made of an extremely rigid material, which prevents any appreciable displacement at the boundaries.

If the guide has zero pressure at the boundary, however, plane wave propagation is not possible. For most purposes a water-air surface can be regarded as a zero pressure boundary.

In rigid circular tubes, if the radius of the tube is sufficiently small, only plane sound waves can propagate for a given frequency.

This condition is given by,

$$\frac{c_o}{f} \geq 3.413\, D$$

where D: Internal radius of the tube,

c_o: velocity of sound in free gas,

f: the frequency.

In rectangular tubes it is possible to excite plane waves alone by using frequencies less than the cut-off frequency of the (1,0) mode. (See equation 2.23).

Therefore it is easy to propagate plane waves alone, but excitation of a particular higher order mode in the absence of all other modes is more complicated.

The analysis of circular tubes involves Bessel functions and for rectangular tubes sine and cosine functions.

In 1938, Hartig and Swanson[8] realized that a sound source having a pressure distribution corresponding to a particular mode could be used to excite that mode alone.

In this work, rigid and impervious walled rectangular wave-guides, filled with gas were used. In order to make measurements of attenuation of transmitted waves and in particular to know how the transmitted mode affects the wave attenuation, it will be necessary to know the acoustic charac teristics of higher order modes in rectangular wave-guides. This will also be useful in measuring the absorption coefficient of materials at oblique angles of

incidence.

In this chapter, energy losses within the guide for the higher order modes will be considered to be zero.

2.2 RECTANGULAR WAVE-GUIDES WITHOUT LOSSES: (m,n) MODES.

Consider a rectangular wave-guide with transverse dimensions (2a) and (2b) in y- and z- directions, respectively. The axis is located centrally, as shown in figure 2.1.

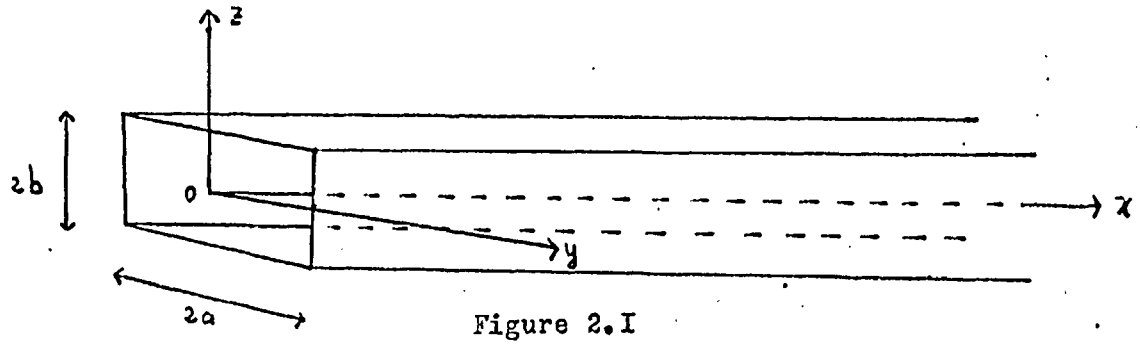

Figure 2.I

Introducing the time factor exp(jwt) , the wave equation may be written,

$$\frac{\partial^2\phi}{\partial x^2}+\frac{\partial^2\phi}{\partial y^2}+\frac{\partial^2\phi}{\partial z^2}=-\left(\frac{w}{c_0}\right)^2\phi \qquad (2.1)$$

where, ϕ: velocity potential,

w: angular frequency ($w=2\pi f$).

The solution of this equation gives the velocity potential for propagation in x direction,

$$\phi=\sum_{m=0}^{\infty}\sum_{n=0}^{\infty}\phi_{mn}=\sum_{m=0}^{\infty}\sum_{n=0}^{\infty}A_{mn}\begin{matrix}\cos\\ \sin\end{matrix}\left(\frac{m\pi}{2a}y\right)\begin{matrix}\cos\\ \sin\end{matrix}\left(\frac{n\pi}{2b}z\right)\exp\left(-j\beta_{mn}x\right)\times\exp(jwt) \qquad (2.2)$$

where, m,n: integers,

A_{mn}: the amplitude constant,

β_{mn}: wavelength constant of the (m,n) th mode.

β_{mn} is given by,

$$\left(\frac{\omega}{c_0}\right)^2 = \left(\frac{m\pi}{2a}\right)^2 + \left(\frac{n\pi}{2b}\right)^2 + \beta_{mn}^2 \qquad (2.3)$$

It can be seen that, there are serious restrictions on the forms of wave which may propagate. Each value of m and n describes a "mode" of propagation. The important features of these modes may be listed as below,

a) Each mode can be considered as four plane waves, each of which is obliquely incident with respect to all the four containing walls and travelling along the guide in a zig-zag path. Each mode is distinguished by a variation of pressure across a transverse-section. The nodal lines of pressure inside the guide should be noted; the number and nature of such lines provide a basis for distinguishing between modes. Position of nodal lines of pressure in a transverse-section for a few of the higher order modes of acoustic waves in rectangular tubes are shown in figure 2.2.

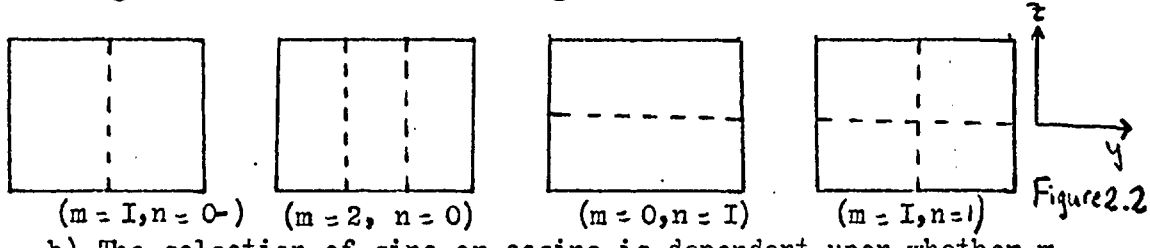

Figure 2.2

b) The selection of sine or cosine is dependent upon whether m and n are odd or even numbers. If, for example, m is even and n is odd number, the mode is symmetrical in y but is antisymmetrical in z direction.

The $\begin{matrix}\cos\\ \sin\end{matrix}\left(\frac{m\pi}{2a}y\right)$ and $\begin{matrix}\cos\\ \sin\end{matrix}\left(\frac{n\pi}{2b}z\right)$ terms correspond to the varia-

tion in the y- and z- axis, respectively.

c) The acoustic pressure (p) and particle velocities in particular directions (u_x, u_y, u_z) determined for a single mode ϕ_{mn} are,

$$P = \rho_o \frac{\partial \phi}{\partial t} = j\omega \rho_o \phi_{mn}$$

$$u_x = -\frac{\partial \phi_{mn}}{\partial x} = j\beta_{mn}\phi_{mn} = \gamma_{mn}\phi_{mn} \qquad (2.4)$$

$$u_y = -\frac{\partial \phi_{mn}}{\partial y} = A_{mn}\frac{m\pi}{2a}\begin{matrix}-\sin \\ \cos\end{matrix}\left(\frac{m\pi}{2a}y\right)\begin{matrix}\cos \\ \sin\end{matrix}\left(\frac{n\pi}{2b}z\right)\exp\left(-j\beta_{mn}x\right)\exp\left(j\omega t\right) = \frac{m\pi}{2a}\begin{matrix}-\tan \\ \cot\end{matrix}\left(\frac{m\pi}{2a}y\right)\phi_{mn}$$

$$u_z = -\frac{\partial \phi_{mn}}{\partial z} = A_{mn}\frac{n\pi}{2b}\begin{matrix}\cos \\ \sin\end{matrix}\left(\frac{m\pi}{2a}y\right)\begin{matrix}-\sin \\ \cos\end{matrix}\left(\frac{n\pi}{2b}z\right)\exp\left(-j\beta_{mn}x\right)\exp\left(j\omega t\right) = \frac{n\pi}{2b}\begin{matrix}-\tan \\ \cot\end{matrix}\left(\frac{n\pi}{2b}z\right)\phi_{mn}$$

where, ρ_o: undisturbed density of the gas in the wave-guide,

γ_{mn}: propagation constant of the (m,n) th modes.

In the loss free case, the propagation constant is given by,

$$\gamma_{mn} = j\beta_{mn} \qquad (2.5)$$

d) At any given frequency only those modes, for which β_{mn} is real are propagated. When β_{mn} is imaginary for any frequency, corresponding mode attenuate rapidly in the x direction according to the term $\exp\left(-j\beta_{mn}x\right)$. The mode is than described as "evanescent" and there is no transmission of energy along the guide for such modes. The frequency for which β_{mn} is zero, is called the cut-off frequency of that mode. The cut-off frequency of the (m,n) th mode can be determined from equation(2.3), and is given by,

$$\left(f_c\right)_{(m,n)} = \frac{c_o}{2}\left[\left(\frac{m}{2a}\right)^2 + \left(\frac{n}{2b}\right)^2\right]^{\frac{1}{2}} \qquad (2.6)$$

Using the equations (2.3) and (2.6), β_{mn} may be written in terms of

cut-off frequency,

$$\beta_{mn} = \frac{\omega}{c_0}\left[1 - \frac{(f_c)^2_{(m,n)}}{f^2}\right]^{\frac{1}{2}} \qquad (2.7)$$

e) When m=n = o, the velocity potential equation reduces to,

$$\phi = \phi_{00} = A_{00}\exp(-j\beta_{00}x)\exp(j\omega t) \qquad (2.8)$$

This represents a plane wave. In rigid walled wave-guides, the four oblique plane waves are now equivalent to a single plane wave travelling in the direction of the x axis. From equation (2.3), the wavelength constant for plane waves,

$$\beta_{00} = \frac{\omega}{c_0} \qquad (2.9)$$

The cut-off frequency of plane waves, from equation(2.6) is now,

$$(f_c)_{(0,0)} = 0 \qquad (2.10)$$

Therefore, plane waves can be propagated at all frequencies.

f) The charateristic impedance of the (m,n) th mode is defined as,

$$W^{c}_{mn} = \frac{p}{u_x} = \frac{j\omega\rho_0}{\gamma_{mn}} \qquad (2.11)$$

W_{mn}, is real for a propagating mode(γ_{mn} is imaginary); and W_{mn}, is imaginary for an evanescent mode.

In the case of plane waves, for example,

$$\gamma_{00} = j\beta_{00} = \frac{j\omega}{c_0}, \quad \text{and} \quad W_{00} = \rho_0 c_0 \qquad (2.11.a)$$

g) The value of wavelength constant, in terms of wavelength is given by,

$$\beta_{mn} = \frac{2\pi}{\lambda^{\circ}_{mn}} \qquad (2.12)$$

where, λ°_{mn}: the wavelength of propagation in the tube in the absence of attenuation.

Angular frequency,

$$\omega = \frac{2\pi C_o}{\lambda^{\circ}_{oo}} \qquad (2.13)$$

where, λ°_{oo}: the wavelength of the plane wave in the tube in the absence of attenuation.

Substituting the equations (2.12) and (2.13) into the equation (2.3) gives,

$$\left(\frac{1}{\lambda^{\circ}_{oo}}\right)^2 - \left(\frac{1}{\lambda^{\circ}_{mn}}\right)^2 = \left(\frac{m}{4a}\right)^2 + \left(\frac{n}{4b}\right)^2 \qquad (2.14)$$

This equation gives the relation between λ°_{mn}, λ°_{oo}, mode numbers and the transverse dimensions of the tube and called as the " wave-guide equation".

2.3. RECTANGULAR WAVE-GUIDES WITHOUT LOSSES: (m,o) MODES.

In this present work plane waves, (1,o) mode and (2,o) mode have been excited and measurements have been carried out by using the appropriate sound sources.

In the case of (m,o) modes the velocity potential reduces to,

$$\phi = \sum_{m=o}^{\infty} \phi_{mo} = A_{mo} \begin{matrix}\cos \\ \sin\end{matrix}\left(\frac{m\pi}{2a} y\right) \exp\left(-j\beta_{mo} x\right) \exp\left(j\omega t\right) \qquad (2.15)$$

where,

$$\beta^2_{mo} = \left(\frac{\omega}{C_o}\right)^2 - \left(\frac{m\pi}{2a}\right)^2 \qquad (2.16)$$

Equation (2.15) may be considered to be a superposition of two travelling waves along the guide obliquely incident with respect tothe side walls ($y=\pm a$), and making the angle θ with the axis x where,

$$\cos\theta = \frac{\beta_{mo}}{\beta_{oo}} = \frac{\lambda^{\circ}_{oo}}{\lambda^{\circ}_{mo}} = \left[1 - \frac{(f_c)^2_{(m,o)}}{f^2}\right]^{\frac{1}{2}} \qquad (2.17)$$

For a propagating mode β_{mo} is real number, therefore θ is a

real angle. At high frequencies i.e. $f \gg (f_c)_{(m,0)}$, θ has lower values, but at a cut-off frequency of a mode, $\theta \rightarrow 90^\circ$ and the waves do not progress in x direction but reflect between the boundaries striking them at normal incidence. Variation of θ with the frequency is shown in figure (2.3),

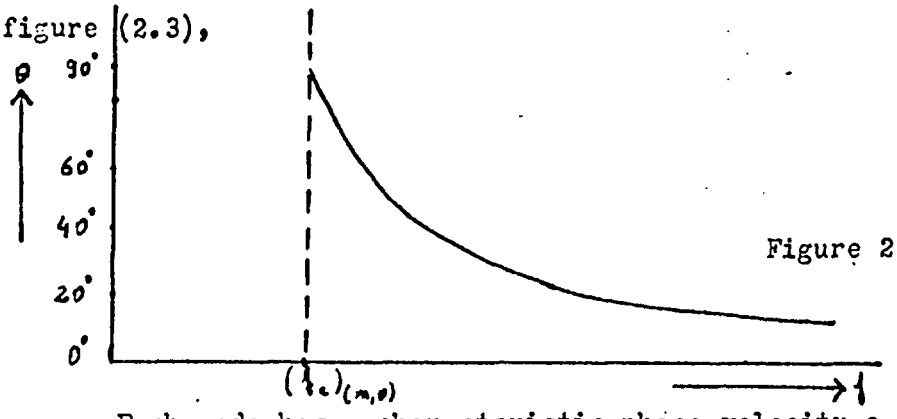

Figure 2.3

Each mode has a characteristic phase velocity c_p. c_p is the rate at which a point of constant phase travels along the boundary of the guide and is given by,

$$c_p = \frac{\omega}{\beta_{m0}} = \frac{c_0}{\cos\theta} = c_0 \left[1 - \frac{(f_c)^2_{(m,0)}}{f^2}\right]^{-\frac{1}{2}} \qquad (2.18)$$

c_p, is always greater than c_0, except when $\theta = 0$. For a propagating mode, the relationship between c_0, c_p, $(f_c)_{(m,0)}$, and f is,

$$\left(\frac{(f_c)^2_{(m,0)}}{f^2}\right)^2 + \left(\frac{c_0}{c_p}\right)^2 = 1 \qquad (2.19)$$

Energy propagates at a group velocity c_g, which is given by,

$$c_g = c_0 \cos\theta = c_0 \left[1 - \frac{(f_c)^2_{(m,0)}}{f^2}\right]^{\frac{1}{2}} \qquad (2.20)$$

From, equations (2.18) and (2.20),

$$c_0^2 = c_p \cdot c_g \qquad (2.21)$$

For a propagating mode c_g is real and always less than c_0; so, $c_p > c_0 > c_g$. For an evanescent mode c_g is imaginary, but this result has no useful physical interpretation. Variations of c_p and c_g

with the frequency is shown in figure (2.4),

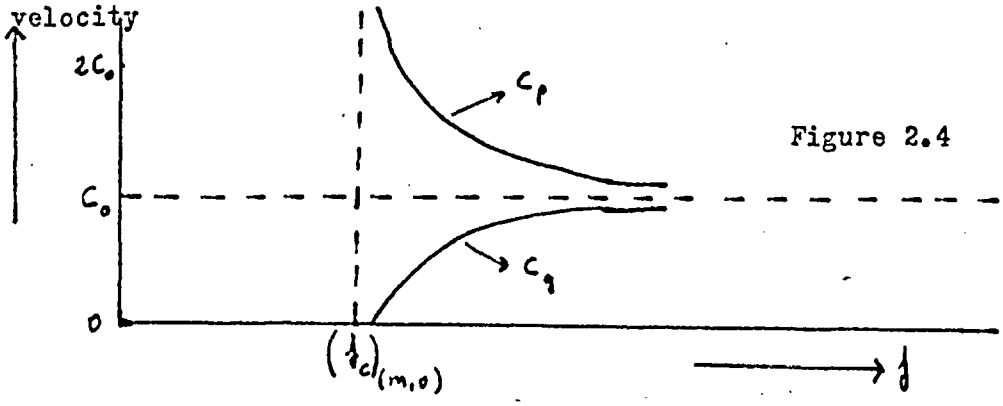

Figure 2.4

The acoustic pressure and particle velocities for (m,o) modes becomes,

$$p = j\omega\rho_o \phi_{mo}$$

$$u_x = j\beta_{mo}\phi_{mo} = \gamma_{mo}\phi_{mo} \qquad (2.22)$$

$$u_y = A_{mo}\frac{m\pi}{2a}\begin{matrix}-\sin\\ \cos\end{matrix}\left(\frac{m\pi}{2a}y\right)\exp\left(-j\beta_{mo}x\right)\exp\left(j\omega t\right)$$

$$= \frac{m\pi}{2a}\begin{matrix}-\tan\\ \cot\end{matrix}\left(\frac{m\pi}{2a}y\right)\phi_{mo}$$

$u_z = o$, (i.e. all functions are independent of z).

The cut-off frequency of (m,o)) modes are,

$$(f_c)_{(m,o)} = \frac{mc_o}{4a} \qquad (2.23)$$

From this equation, the cut-off wavelength of (m,o) modes are given by, $(\lambda_c)_{(m,o)} = \frac{4a}{m}$ (2.24)

The pressure distribution in the xy plane corresponding to some lower modes are illustrated in figure (2.5).

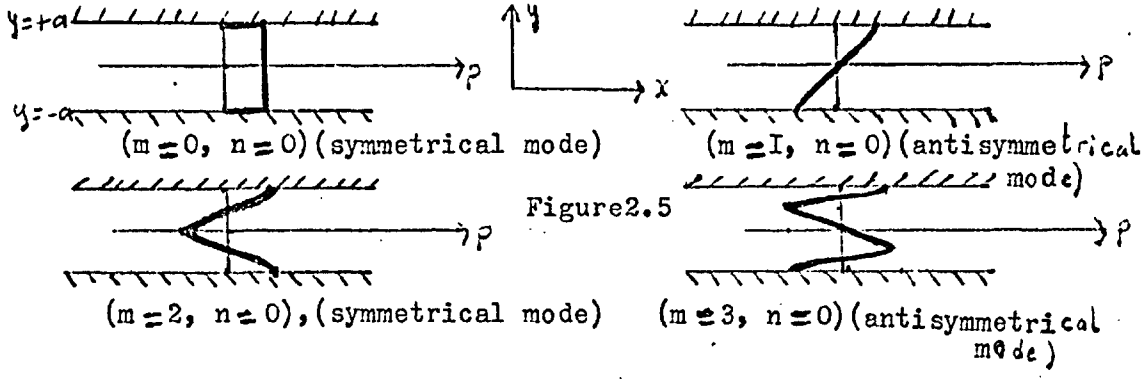

Figure2.5

For a propagated mode u_x and p are in phase and u_y is in phase quadrature with them. Particle displacements in x and y directions are in quadrature. Thus, particles of fluid traverse ellipses in the xy plane as shown in figure (2.6), for (1,o) mode.

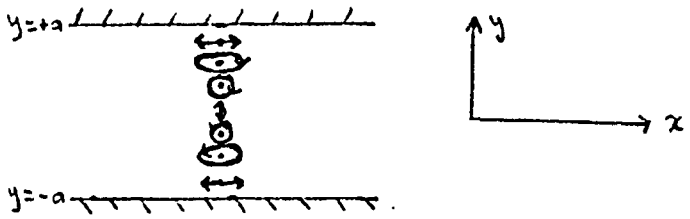

Figure 2.6

For an evanescent mode, however, u_x and u_y are in phase and p is in phase quadrature with them. Particle displacements in x and y directions are in phase now and both are antiphase with the pressure. Thus, the particles of fluid traverse straight lines, as shown in figure (2.7) for (1,o) mode.

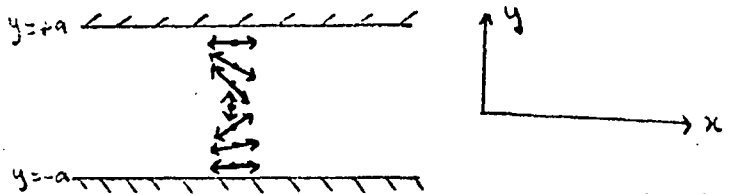

Figure 2.7

The wave-guide equation for (m,o) modes becomes (from equation 2.14),

$$\left(\frac{1}{\lambda_{oo}}\right)^2 - \left(\frac{1}{\lambda_{mo}}\right)^2 = \left(\frac{m}{4a}\right)^2 \qquad (2.25)$$

2.4. CONDITIONS FOR THE EXCITATION OF A GIVEN MODE.

In order to excite a pure mode it is necessary to satisfy two conditions,

a) The guide should be excited by a sound source configuration producing a pressure distribution identical with that corresponding to the particular mode. If, this condition is not precisely satisfied several modes may be excited simultaneously.

b) The frequency of excitation, must be greater than the cut-off frequency of that particular mode.

By choosing a wave-guide which has a sufficiently large ratio of major to minor transverse dimensions; (i.e. a>b), the cut-off frequencies of the modes can be put in the order of,

$$\frac{mc_0}{4a} = (\lambda_c)_{(m,0)} < (\lambda_c)_{(0,n)} = \frac{nc_0}{4b} \qquad (2.26)$$

where, m = 0,1,2,3 in this experiment.

Therefore, if the frequencies less than the cut-off frequency of the (0,1) mode are used, only (m,0) modes can be excited.

The amplitude constants A_{mo}, are determined by the character of the sound source. If the source gives a known velocity distribution in the plane x=0, A_{mo} can be obtained. If, in the plane x=0 there is a sinusoidal source of velocity in x direction,

$$V \exp(j\omega t) \qquad (2.27)$$

Particle velocity at x=0 for (m,o) mode is,

$$(u_x)_{x=0} = -\frac{\partial \phi}{\partial x} = \sum_{m=0}^{\infty} j \beta_{mo} A_{mo} \begin{matrix}\cos \\ \sin\end{matrix}\left(\frac{m\pi}{2a} y\right) \exp(j\omega t) \qquad (2.28)$$

This may be equated to equation (2.27), and,

$$V = \sum_{m=0}^{\infty} j \beta_{mo} A_{mo} \begin{matrix}\cos \\ \sin\end{matrix}\left(\frac{m\pi}{2a} y\right) \qquad (2.29)$$

In order to find A_{mo} both sides of this equation are multiplied by $\cos\left(\frac{m'\pi}{2a} y\right)$, (m' is an integer) and integrate between y=-a and y=+a,

$$\int_{-a}^{+a} V \begin{matrix}\cos \\ \sin\end{matrix}\left(\frac{m'\pi}{2a} y\right) dy = \sum_{m=0}^{\infty} j \beta_{mo} A_{mo} \int_{-a}^{+a} \begin{matrix}\cos \\ \sin\end{matrix}\left(\frac{m\pi}{2a} y\right) \begin{matrix}\cos \\ \sin\end{matrix}\left(\frac{m'\pi}{2a} y\right) dy$$

The right-hand side of this equation is zero, except when m = m'. Hence,

$$A_{mo} = \frac{B}{j\beta_{mo} a} \int_{-a}^{+a} V \begin{matrix}\cos \\ \sin\end{matrix}\left(\frac{m\pi}{2a} y\right) dy \qquad (2.30)$$

where, B=1 if $m \neq o$; B= 2 if $m = o$.

By means of this equation it is possible to determine the condition for elimination of any higher order mode in the wave-guide. (i.e. $A_{mo} = o$).

A symmetrical source, for which V(y)= V(-y) will excite onlymodes of zero or even order, while an antisymmetrical source for which V(y)= -V(-y) will excite only odd orders.

Thus, it is possible to eliminate one set of modes by the choice of symmetrical or antisymmetrical source configuration. Discrimination between odd or between even modes requires greater complexity of source and frequency limits.

Using frequencies f such that,

$$(f_c)_{(1,0)} < f < (f_c)_{(2,0)} \qquad (2.31)$$

then only (o,o) mode and (1,0) mode may be propagated. Elimination of one of these modes is possible by using a symmetrical or antisymmetrical source. A symmetrical source has a pair of symmetrically located pistons of equal amplitude and in phase synchronism, while an antisymmetrical source has a pair of symmetrically located pistons of equal amplitude but in phase opposition. An antisymmetrical source may be described as a dipole.

In order to excite the (2,0) mode alone, two conditions must be satisfied:

a) The frequencies which satisfies the equation

$$(f_c)_{(2,0)} < f < (f_c)_{(3,0)} \qquad (2.32)$$

must be used.

b) A symmetrical sound source must be used, but plane waves can also be propagated at the same time with the (2,0) modes, so, a further condition has to be satisfied.

From equation (2.30), the condition for elimination of plane wave is,

$$\int_{-a}^{+a} V \, dy = 0 \qquad (2.33)$$

This equation requires a minimum of three pistons, a pair of equal amplitude located at equal distances $y = \pm a$, and a third of double amplitude operating in antiphase at $y = o$. Such a source is described as a quadrupole.

CHAPTER III

APPARATUS FOR FLUID WAVE-GUIDE MEASUREMENTS.

3.I. INTRODUCTION. Scott[9] (I946), has given six conditions, and Beranek[10] (I949), has added a seventh which must be fulfilled for accurate plane wave impedance tube measurements.

Corresponding conditions which must be satisfied for measurements with higher order modes may be given as follows:

(i) The cross-sectional area of the tube must be constant and the walls should be rigid,

(ii) Only the desired mode of sound waves should be propagated free from the others,

(iii) The microphone orifice must be accurately located to about 0.I mm.

(iv) The face of the sample must be plane and mounted accurately perpendicular to the central axis of the tube,

(v) The microphone used for exploration of the sound field must not appreciably effect the field and must be sensitive and stable,

(vi) A single frequency must be used for each measurement,

(vii) The temperature in the tube must not alter.

In order to satisfy these conditions the following apparatus has been designed.

3.2. DESCRIPTION OF APPARATUS. The degree to which the above seven conditions have been satisfied by the present apparatus can be best

understood by examining them one by one as follows:

(i) The Rectangular Wave-Guides: Two rectangular guides have been used, which are:

The Large Wave-Guide: The internal dimensions of this guide are I4.36 cm. and 4.8 cm. By substituting in equation (2.23) the cut-off frequencies of the (I,0), (2,0) , (3,0) and (0,I) modes are found.

$$(f_c)_{(1,0)} = 1204 \text{ c/s}. \qquad (f_c)_{(3,0)} = 3612 \text{ c/s}.$$

$$(f_c)_{(2,0)} = 2408 \text{ c/s}. \qquad (f_c)_{(0,1)} = 3583 \text{ c/s}.$$

Thus, at the frequencies less than 3583 c/s, condition (2.26) is satisfied for the values of m = I,2,3 and (0,n) type modes cannot be propagated. In fact, the (2,0) mode is the highest order in this experiment and when frequencies less than 36I2c/s, are used, discrimination between the modes depend only on the source configuration.

The length of the guide is 2I0 cm. and it was made from tufnol plates. The rigidity of tufnol plates are poor and it was surrounded with sand and put in a strong wooden box.

The Small Wave-Guide. The small waveguide has a wall thickness of 0.22cm. and internal transverse dimensions of 7.2cm. and 3.4cm. The length of the guide is IIOcm. and it was made from brass.

The cut-off frequencies of the (I,0),(2,0) and (0,I) modes are:

$$(f_c)_{(1,0)} = 2390 \text{ c/s}.$$

$$(f_c)_{(2,0)} = 4780 \text{ c/s}.$$

$$(f_c)_{(0,1)} = 5080 \text{ c/s}.$$

Thus, at frequencies less than 4780c/s, only (0,0) and (I,0) modes can be propagated in the tube. This tube was also surrounded with sand constrained in a wooden box.

After these preparations the two wave-guides satisfied condition (i), with no indications of wall vibration as explained in chapter five.

One end of both guides is fitted to a heavy brass specimen holder, the other end being connected to the loudspeaker units by means of two rubber tubes.

From the cut-off frequencies of the (I,0) and (2,0) modes it can be seen that the oblique incidence measurements are limited to about one octave, within which the angle of incidence varies from 30° to 90° as the frequency decreases. (see equation 2.I7)

(ii) Excitation of a particular mode free from the others requires a particular sound generator system. The systems were used are:

(0,0) and (I,0) System: Two identical loudspeaker units, each of resistance I5 ohms, are coupled by two rubber tubes to about I.5 cm. diameter orifices in the end plate of the wave-guide. The units are fed via a balance network which in conjunction with a variable length device in one driving tube, permits the adjustment of the

two acoustic source current to equal strengths with a phase difference of zero or π. These two conditions of driving the wave-guide produce pure (0,0) and pure (I,0) waves, respectively, provided that the cut-off frequencies of higher order modes are not exceeded as explained before in this section.

The acoustic pressure distribution in the wave-guide is detected by a multiple probe system. Three stainless steel probe tubes, one against each narrow wall of the wave-guide and a third mid-way between these two. They are fixed at one end to the movable stage carrying also a Rochelle Salt microphone. The microphone may be connected by a small rubber connection to any of the probe tubes and the pressure variation along the guide observed by moving the optical slide. The probes serve both for the initial generator adjustment and for the subsequent standing wave measurements. When the microphone is connected to the centre probe, which lies in the (I,0) nodal plane, it responds only to plane waves which may be eliminated by adjustment of the sound source. When a condition of balance has been attained (i.e. zero pressure at the centre probe), the microphone is transferred to the outer probe which then may be used to explore the standing wave pattern of the (I,0) mode. For (0,0) waves the input to one of the speaker units is reversed and standing wave measurements are made with the centre probe. This is important, because, although the (I,0) mode could be eliminated by operating the sound source system in perfectly symmetrical manner, it is difficult

to satisfy this condition and centre probe does not respond to the (I,0) mode.

(0,0) and (2,0) System: For an available wave-guide due to the limitation on frequency for the (I,o) mode, the possibility of measurements of acoustic impedances at normal incidence is also limited. Using a sound source as will be described later in this section pure (0,0) and pure (2,0) modes can be propagated. Therefore, normal incidence measurements at higher frequencies become possible for that particular wave-guide. In this experiment (2,0) sound source system has been used for the large wave-guide only.

It has been shown in chapter two that, the (2,0) mode may be generated by a symmetrical source (to eliminate the antisymmetrical (I,0) mode) which satisfies the equation (2.33). Three pistons the outside pair operating with equal amplitude and phase and the centre piston with double amplitude and in antiphase. The device has been designed by Shaw[11].

The two outer orifices are fed from one of the units through one of the rubber tubes, a concealed semicircular channel ensuring that the sound energy divides equally. The centre orifice is fed from the second unit through the other rubber tube. If the units are fed in phase, which may be adjusted by the balance network, pure plane waves in the wave-guide propagated. The acoustic pressure distribution in the wave-guide is now detected by using four probe tubes. Outer pair which fit into the lower corners of the guide and

an inner pair located at the positions of $y=\pm\frac{a}{2}$ which are the two nodal planes.

Adjustment of the sound source is carried out by connecting one of the inner probes to the microphone and adjusting for zero pressure. Thus the (I,0) waves are eliminated. Measurements of pressure in the tube for the (2,0) mode may be obtained using one of the outside probes (i.e. near the tube wall). Plane wave measurements are carried out with an inner probe when all three orifices are adjusted to operate in phase since any residual (2,0) mode will have no effect at the nodal plane.

(iii) Spacers: In order to keep the orifices of the probe tubes in their proper places, spacers which are of 0.75mm. diameter steel pivot wire have been used. They have been punched in the probe tube walls and so orifices of the probe tubes have been kept in their proper places with an accuracy of about 0.Imm.

(iv) Specimen Holders: For attenuation measurements a brass plate I.2 cm. thick for the small wave-guide and I.9 cm. for the large, with a plane face has been used. For impedance measurements, however, specimen holders which provide a rectangular cavity for the specimens and of transverse dimensions equal to those of the wave-guide have been used. The end of the guide may be closed, either by the plate or the specimen holder. The face of the specimens were smooth and plane. In order to mount the specimens perpendicular to the axis of the tube, the distance between the specimen face and

the rim of the specimen holder have been read using a ruler and a hand lens to about 0.I mm. When same readings have been obtained for about eight different ruler positions, this condition may assumed to be fulfilled.

(v) Reference Microphone: For the large wave-guide, probe tubes, 250 cm. in length, of inside diameter 2.3 mm. and outside diameter 3.0 mm. are used while for the small wave-guide the respective dimensions are I50 cm, I.8 mm. and 2.3 mm. The guides are supported by resting on the lower wall of the wave-guide. Presence of probe tubes cause a slight increase in the mode wave-length, and change the balance conditions at the sound source end. The absorption by the probe orifices is less important.

The reference microphone is used to correct for variations in the incident sound amplitude reaching the reflecting surface, when the probe tubes are moved. The reference microphone is coupled to a very small orifice in the wave-guide wall, near the specimen face. Three such orifices are provided at different transverse positions ($y=0, y=\frac{a}{2}, y=a$), so that the microphone may read sound pressure at desired positions.

In all standing wave measurements in this work, each reading on the travelling microphone was followed by one on the reference microphone, and the ratio of the two was used in the subsequent analysis.

(vi) Frequency Stability: The angle of incidence is a function

of frequency. Therefore, the frequency of excitation must be held constant within one part in several thousand if an accuracy of 2% is required.

The frequency stability of the Signal Generator, which was used in this work (see section 3.3), maintained a constancy better than one part in a thousand for an hour. At a given frequency the observation of the standing wave pattern in the tube takes about I5 minutes, furthermore, the frequency of the generator was checked continuously on the frequency counter, and only the observations for which the frequency kept constant were accepted. As a result it is assumed that this condition has also been fulfilled.

(vii) The Stability of Temperature: The discussion with regard to frequency stability applies equally to the temperature of the gas inside the wave-guide. During the measurements, the temperature of the gas should be constant to within 0.I C: If the gas temperature is changing, the standing wave pattern will also shift.

However, The laboratory air temperature did not change more than 0.I C per half hour and the large thermal capacity of the wave-guide also assisted in maintaining stability the I5 minute period required for a standing wave measurement. Furthermore, the positions of minima of the standing wave pattern were read in the possible shortest time which is only about two minutes. This consideration is important because the mode wave-length is directly obtained from the positions of the pressure minima.

3.3. GENERAL ARRAGEMENT OF THE APPARATUS. The apparatus which have been used in this experiment are shown in figure 3.I. The details of some individual components having been dealt with in section 3.2 (i.e. the two microphones, loudspeaker units, wave-guides and probe tubes.).

The Advance Audio Frequency Signal Generator J2C has an output impedance of 600 ohm with a frequency range of I5c/s to 50kc It provides an output into 600 ohm, 0.I mW. to I W. (0.25V to 25V) with a low distortion level. Overall distortion at full output is less than 2% (34 dB down on fundamental). If the output is kept below 0.I W distortion is less than I% (40 dB down on fundemental). Normally a power of about 0.I5 W required to drive the loudspeaker units. The signal generator has been used at a low output level and a power amplifier which has an output impedance of I6 ohms was employed to couple the Signal Generator with the loudspeaker units.

The AF Spectrometer Type 2III has a frequency range of 35 c/s to 35 Kc/s and consist basically of an input amplifier, a filter system and an output amplifier. It has I/3 and I/I octave filters. The indicating instrument is equipped with rectifier circuits so enabling the true r.m.s. value of the signal to be measured. The input impedance of the instrument is 2.2 megohms. which allows direct connection to the microphone. The standing wave pattern can be plotted directly from the meter. Microphone amplifier is also used when balancing the sound source and when measuring the reference

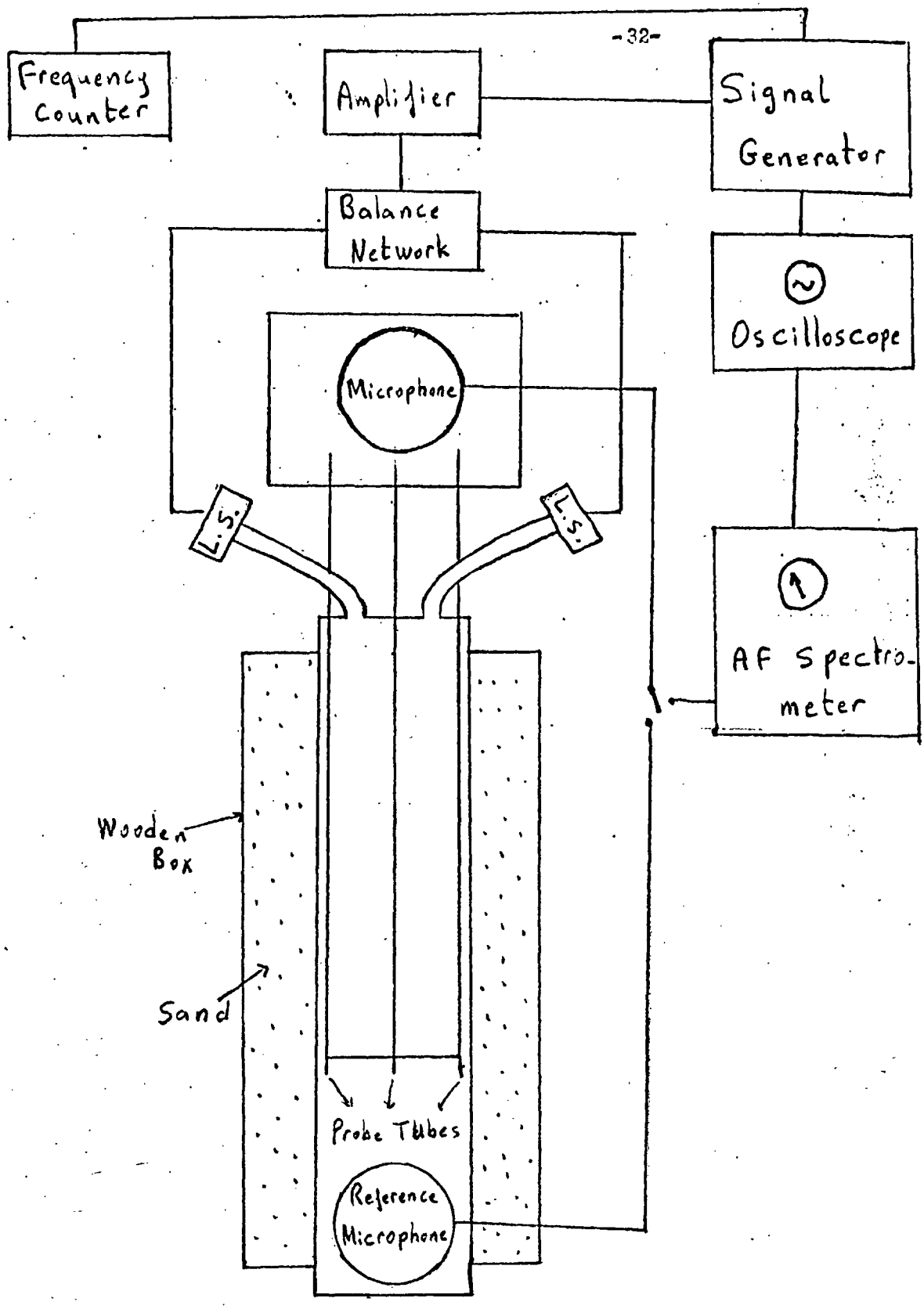
Frequency Counter
Amplifier
Signal Generator
Balance Network
Oscilloscope
Microphone
L.S.
L.S.
AF Spectro-meter
Wooden Box
Sand
Probe Tubes
Reference Microphone

Figure 3.1.

microphone voltage. The maximum voltage gain of the amplifier is 100 dB. The balanging of sound source requires a filter which has a narrow bandwith in order to avoid the influence of noise and harmonic distortion and therefore a I/3 octave filter has been used in this experiment.

The direct measurement of the absorption coefficient of the test material with the aid of this AF Spectrometer is also possible. The indicating meter of the Spectrometer contains scales in addition to the normal calibrations. This permit direct reading of the absorption coefficient in percent.

A Cathode Ray Oscilloscope (CRO) has been used to detect the microphone signal. The input signal from the Signal Generator was also displayed on the screen of the oscilloscope to ascertain the wave form.

An Advange Frequency Counter has been used to read the frequency of the Signal Generator more precisely, which was necessary in order to determine accurately the angle of incidence and to be sure that the frequency of the Generator did not change during the readings.

The movable probe microphone which can be seen in figure (3.2) has a massive brass housing set in rubber. This was remounted more flexibly with pieces of rubber tube and enclosed in a hard board box filled with sound absorbing materials. Such preparations were necessary to reduce the stray signal level of the travelling mic-

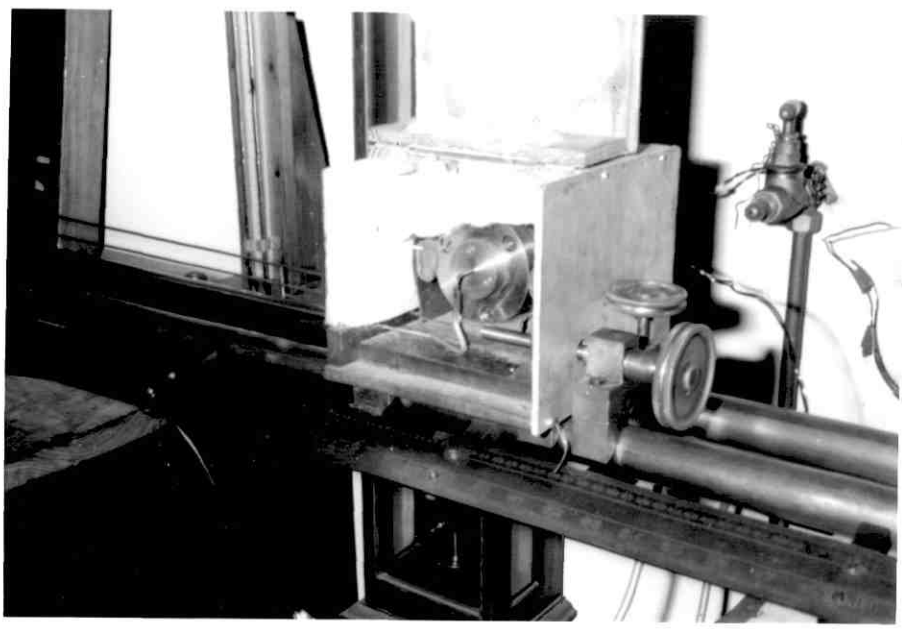

Figure 3.2

rophone, due to unwanted sound penetrating the microphone housing and to isolate the mechanical vibration entering via the optical bench. The stray level was about 80 dB below the signal level of a pressure maxima and was not important even when measuring the pressure minima. There was no need to cover the reference microphone which was always actuated with a large signal.

CHAPTER IV

THE ATTENUATION OF THE HIGHER ORDER MODES OF ACOUSTIC WAVES IN GAS-FILLED RECTANGULAR TUBES.

4.I. INTRODUCTION.

In chapter two no consideration has been given to the attenuation of the sound waves during propagation in the tube. The source of dissipation in tubes may be divided into three general categories which are: body losses; boundary layer losses; and losses due to tube wall vibrations.

a) Body Losses: This type of loss comprises four basic types,

(i) Viscosity losses,

(ii) Thermal conductivity losses,

(iii) Losses due to molecular exchanges of energy,

(iv) Losses due to turbulence and inhomogeneity of the fluid medium.

(i) Viscosity Losses. This type of loss results from relative motion occurring between various portions of the medium during the compressions and expansions that accompany a sound wave.

Stokes[12] (I845), has theoretically developed a mechanism for sound attenuation by using the property of viscosity of the medium.

For plane waves, he has modified the wave equation to include viscosity as below,

$$\frac{\partial^2 u_x}{\partial t^2} = c_o^2 \frac{\partial^2 u_x}{\partial x^2} + \frac{4\mu}{3} \frac{\partial^3 u_x}{\partial^2 x \, \partial t} \qquad (4.1)$$

where, μ is the shear coefficient of viscosity.

The attenuation coefficient due to viscosity in the medium is then given by,

$$\alpha_{vis} = \frac{2\,\omega^2\,\mu}{3\,\rho_0\,c_0^3} \qquad (4.2)$$

where, c_0 is the velocity of sound in the medium.

It appears that for all normal frequencies the velocity of propagation is unaffected by the viscosity.

(ii) Thermal Conductivity Losses. For acoustic waves, the pressure fluctiations in the body of the gas are accompanied by density fluctuations slightly out of phase, due to the low thermal conductivity of the gas. Consequently, there is an energy loss in the gas thus reducing the amplitude of the wave.

Kirchhoff[13] (1868), utilized the property of thermal conductivity of the medium and developed a theory for this type of loss in fluids. The theoretical equation associated with the thermal conduction is given by,

$$\alpha_{ther} = \frac{K\,(\chi-1)\,\omega^2}{2\,\rho_0\,c_0^3\,\chi_p} \qquad (4.3)$$

where, K :thermal conductivity of the gas,

χ_p: specific heat of the fluid at constant pressure,

χ: the ratio of principal specific heats.

Attenuation due to viscosity and to thermal conductivity act independently, when the attenuation is small. Thus equations (4.2) and (4.3) may be added to give the theoretical " classical coefficient of attenuation" for acoustic waves in a medium, i.e.

$$\alpha_{cla.} = \alpha_{vis.} + \alpha_{ther.} = \frac{w^2}{2\rho_0 c_0^3}\left(\frac{4\mu}{3} + \frac{K(\chi-1)}{\chi_p}\right) \qquad (4.4)$$

(iii) Losses Due To Molecular Exchanges of Energy. The dissipation of acoustic energy that is associated with changes in the molecular structure of the medium results in a finite time being required for these changes to take place.

When a monoatomic gas, such as argon and helium, is compressed adiabatically, all the work done in compressing the gas goes into increasing the temperature of the gas. Since, this take place almost instantaneously, changes in temperature, pressure and density are all in phase, consequently, when sound waves are propagated in such gases no excess absorption is present apart from the losses due to viscosity and thermal conductivity.

For polyatomic gases the internal energies of rotation and vibration of the molecules must also be considered as well as the energy of translation. During the propagation of sound waves, a characteristic time or relaxation time is required for molecular energy changes to occur. This finite time causes density changes in a fluid to lag behind pressure changes. Thus, molecular relaxation tends to attenuate the sound wave. When the frequency of sound wave is so low that the relaxation time is much smaller than a period of the acoustic cycle, equilibrium among the various states exist virtually at all times and the attendant difference in phase between pressure and temperature changes is small. Similarly,

when the frequency of sound wave is so high, the relaxation time is much larger than a period of the acoustic cycle. Almost no interchange of energy takes place between external translational states and the internal states. Therefore, this type of loss will produce a maximum excess attenuation when the period of the acoustic cycle is equal to the relaxation time.

Affect of Relative Humidity. Attenuation of sound is also depends on the relative humidity. Sivian[14] (1947), has measured the attenuation coefficient for dry air and for air with 37% relative humidity, as a function of frequency. Results showed that there is some excess attenuation of sound in humid air at the frequencies up to 100 kc/s. This excess absorption is temperature dependent and caused by the presence of a small percentage of water-vapor molecules. In dry air the relaxation time for oxygen molecules is several m. seconds and therefore the vibrational mode is not excited by sound waves. However, the presence of water-vapor reduces the relaxation time to 10^{-3} to 10^{-5} seconds and so causes excess attenuation at frequencies from one to hundred kc/s. The vibrational energy of nitrogen molecules is very small at room temperatures and does not contribute to the anomalous absorption.

(iv) Losses Due to Turbulence and Inhomogeneity of The Fluid Medium. When the fluid contains inhomogeneities, such as suspended particles or regions of turbulence, an additional attenuation takes place apart from that occuring in an isotropic medium. In tube measurements, these types of loss can be neglected.

b) Boundary Layer Losses: During the propagation of sound waves in tubes there is a loss of energy arising from heat conduction and viscosity at the tube walls. These losses occur in a thin layer of gas at the wall, which is known as the "Boundary Layer". This type of loss will be explained in more detail later in this chapter. In this section and only the historical introduction will be given here.

The influence of viscosity on the propagation of plane waves has been studied by Helmholtz[15] (I863), in cylindrical tubes. The more general problem including thermal conductivity effects was solved by Kirchhoff[13] (I868), He has given the value for the coefficient of attenuation of plane waves in a tube, which is inversely proportional to the radius of the tube. The attenuation of plane waves in rigid cylindrical tubes have been measured by several writers, such as, Mason[16] (I928), Beranek[17] (I940), and Fay[18] (I940), but they found the value IO-I5 % above that predicted by the theory of Kirchhoff. Scott[19] (I946), used a standing wave tube and found the value only 3% above the theory.

Attenuation of higher order modes in tubes has been investigated theoretically by Morse[20], considering the admittance of the wall to be small.

Cremer[21] (I948), used the boundary layer acoustic impedance method. He pointed out that the reflection of a plane wave striking a rigid impervious plane surface and making an angle θ with the sur-

face of the walls, may be treated by the acoustic impedance concept where the wall impedance Z has the value,

$$\frac{1}{Z} = \frac{(1+j)}{\rho_0 c_0}\left(\frac{n\mu}{\rho_0 c_0^2}\right)^{\frac{1}{2}}\left[\sin^2\theta + \frac{\chi-1}{\chi^{\frac{1}{2}}}\left(\frac{K}{\mu\chi_v}\right)^{\frac{1}{2}}\right]^{-\frac{1}{2}} \qquad (4.5)$$

Nielsen[22] (I949), has given expressions for the viscous and thermal conduction losses at the walls of the acoustic resonators of circular cross-section.

Attenuation of (I,0) modes in rigid rectangular tubes has been investigated experimentally by Hartig and Lambert[23] (I950) for the first time. Their analysis led them to an expression for the attenuation due to thermal conductivity and viscosity at the tube walls which was equivalent to Kirchhoff's result, multiplied by a factor which was a function of the cut-off frequency of the (I,0) mode. Shaw[24] (I950), commenting on the work of Hartig and Lambert, has given a theoretical formula which was different.

Bogert[25] (I950), has applied electromagnetic wave-guide techniques to the calculation of the attenuation of the (I,0) mode in a rectangular tube but included viscous losses only.

Beatty[26,27] (I950), calculated the boundary layer attenuation caused by viscous and thermal affects of all higher order modes of propagation in both rigid walled rectangular and circular tubes, using Morse's duct formulas and the concept of boundary layer admittance introduced by Cremer. He has obtained the same result as obtained by Shaw.

Lambert[28](I95I), has found a solution by applying Slater's[29]

energy relations. His results were similar to Beatty and Shaw.

Shaw[30] (I953), has found a theoretical solution for the attenuation of the (m,0) modes between two parellel plates, using the fundemental equations given by Kirchhoff for plane waves. His experimental results for the (I,0) modes were in good agreement with theory.

Campbell[31] (I953), has given more information about boundary layer phenomenna.

Ghabrial[32] (I955), has measured the attenuation coefficient of the (2,0) mode. His results agree to I% with the theory given by Beatty, Lambert and Shaw.

Lambert[33] (I953) and Weston[34] (I953), have given more detail about attenuation in tubes; and Lambert[35] (I957), has made further investigation about sound attenuation in rigid tubes near cut-off frequency.

c) Losses Due to Tube Wall Vibations: A third loss mechanism is by coupling of the fluid vibrations with the walls of the tube. If the walls of the tube are rigid this type of loss could be neglected. However, the character of the antisymmetrical mode can cause some excess attenuation if the walls of the tube are not infinitely rigid. This will be explained in more detail in the next chapter.

Comparison of the Body Losses under the defining conditions of the present experiment:

In this experiment, the experimental conditions were as follows:

a) The walls of the tube are rigid,

b) The relative humidity was always above 40%,

c) The transverse dimensions of the tubes are less than I5 cm.

The measurements have been carried out at the frequencies from I to 4.6 kc/s at laboratory temperatures, and the tubes were filled with air and helium.

The body losses are of particular significance when the volume of the fluid is large in comparison with the area of its boundaries.

Knudsen[36]'s measurements indicates that, as the relative humidity increases, the frequency of the maximum attenuation is increased. At the normal relative humidities of 40% or more, this frequency is in the lower ultrasonic range and consequently, the attenuation due to water-vapor[u] in air at normal laboratory temperatures is very small for frequencies between I to 5 kc/s.

Body losses, for dry air in 20° C is given by,

$$\alpha_{body} = \alpha_{vis.} + \alpha_{ther.} + \alpha_{mol.} = 2.0 \times 10^{-13} f^2 \quad \frac{nepers}{cm}$$

where, f is the frequency in c/s.

Thus α_{body} is proportional to (frequency)^2 and its value is more significant at ultrasonic frequencies and in large volumes.

Boundary layer losses (see equation 4.40) are proportional to the square root of the frequency and inversely proportional to the transverse dimensions of the tube. Therefore, at low frequ-

encies and with the present dimensions, the body losses become negligible being about 1% less than the total attenuation.

On the other hand, to apply the boundary layer approach, the thickness of the boundary layer (see equation 4.9) should be small compared with the transverse dimensions of the tube, as is the case with the present apparatus.

Hence, only the boundary layer losses will be taken into account which is the usual procedure when using small tubes.

4.2. ATTENUATION OF HIGHER ORDER MODES IN RIGID, RECTANGULAR TUBES:

It is assumed that the effects of viscosity and thermal conduction at the walls of a tube may be considered independently, the two contribution may than be superposed.

Viscous Losses: The effect of viscosity in modifying the motion of a gas in contact with the walls has been treated by Stokes.[12] Consider an alternating gas current of velocity

$$U_0 \exp(j\omega t) \qquad (4.6)$$

and moving parallel to an infinite rigid plane located at $h = 0$, where, the axis of h is normal to the plane (see figure 4.I). This

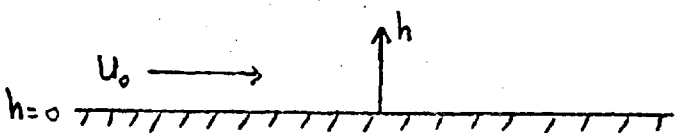

Figure.4.1

velocity of gas will be influenced by friction near the wall. If, U_t is defined as the tangential particle velocity at the wall, Stokes has shown that the velocity must satisfy the viscous wave equation: i.e.

$$\frac{\partial^2 U_t}{\partial h^2} = j \frac{\omega \rho_0}{\mu} U_t \qquad (4.7)$$

The solution of the viscous wave equation is given by:

$$u_t = (U_o)_t \left\{ 1 - \exp\left[-(1+j) \frac{h}{\sqrt{\frac{2\nu}{\omega \rho_o}}} \right] \right\} \exp(j\omega t) \quad (4.8)$$

In this equation,

$$\xi_{vis.} = \sqrt{\frac{2\nu}{\omega \rho_o}} \quad (4.9)$$

has the dimensions of length and is known as " The viscous boundary layer thickness". u_t reduces to zero at the wall (Lamb)[37]. The tangential velocity is built up in the distance of $\xi_{vis.}$ from the wall. For 20° C and I atmosphere pressure in air,

$$\xi_{vis} = \frac{0.219}{\sqrt{f}} \text{ cm.}$$

where, f is the frequency in cycle per second. So, at f = I600 c/s, $\xi_{vis.} = 0.0055$ cm. After several multiples of $\xi_{vis.}$ the motion of gas is uninfluenced by the wall.

The energy dissipation per second within an elemental volume of the boundary layer of area (dA) and thickness dh due to viscosity is:

$$\nu \, dA \left(\frac{\partial u_t}{\partial x} \right)^2_{real} dh \quad (4.10)$$

Substituting from equation (4.8) into the above equation and integrating between h = 0 and $h \to \infty$, gives the mean power loss $dW_{vis.}$, associated with an area dA of the boundary layer, due to viscosity, i.e.

$$dW_{vis.} = \frac{1}{4} \rho_o \, \omega \, \xi_{vis.} \, (U_o)^2_t \, dA \quad (4.11)$$

Therefore, the viscous loss at the walls is proportional to the square of thetangential particle velocity amplitude. Thus,

the power loss in a length of the tube dx due to viscosity is:

$$dW_{vis.} = \int_l \frac{1}{4} \rho_o \omega \varepsilon_{vis.} (u_o)_t^2 \, dx \, dl \qquad (4.12)$$

where, the integration is to be performed around the perimeter of the cross-section of the tube. (see figure 4.2).

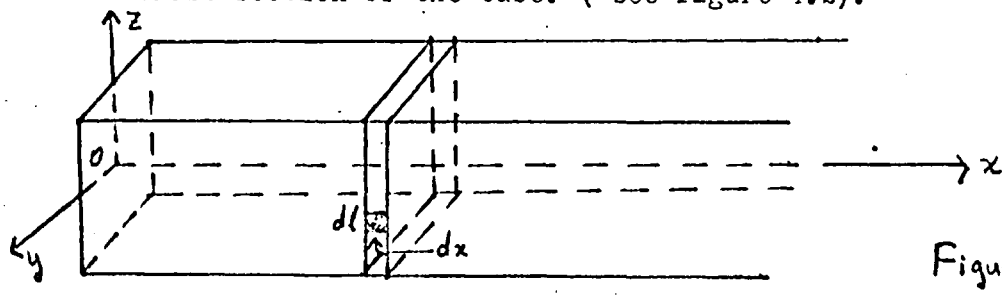

Figure 4.2.

Thermal Conduction Losses. The presence of a solid wall modifies the thermal fluctuations caused by an acoustic disturbance in the layer of gas nearest the wall. When the pressure rises to a maximum, heat is generated and the density of the gas increases. But, because of the infinite thermal capacity of the wall compared to that of the gas, heat generated in the gas absorbed by the wall causing a cooling of the gas. In the succeeding half cycle, acoustic pressure falls to a minimum value and the heat previously absorbed is given back. Thus, approximately an isothermal condition is maintained. On the other hand, the flow of heat is not quite in phase with pressure fluctuations and the gasdensity lags behind the pressure.

As a consequence of the phase difference in density and pressure there is a net heating of layer of gas at the wall which is subsequently communicated to the body of the gas. This layer of gas is known as "The thermal boundary layer".

The energy loss, which occurs when a wall is subjected to a periodic pressure variation:

$$p = p_0 \exp(j\omega t) \qquad (4.13)$$

can be calculated. Since the boundary layer is thin the pressure may be considered constant throughout. Outside the boundary layer there is a temperature variation θ', but in the proximity of the wall $\theta' = 0$. Thus the solution of the thermal wave equation must satisfy the boundary conditions, (i.e. at $h = 0, \theta' = 0$ and at $h \to \infty, \theta' = \theta_0'$) and it is given by

$$\theta' = \theta_0' \left[1 - \exp\left(-(1+j)\, h / \sqrt{2K/\rho_0 \omega \chi_p} \right) \right] \exp(j\omega t) \qquad (4.14)$$

where, K : Thermal conductivity of gas,

χ_p : specific heatof the gas at constant pressure,

h, is measured along the axis normal to the surface of the wall, and θ_0' is given by:

$$\theta_0' = \frac{\chi - 1}{\chi} \frac{T_0}{P_0'} p_0 \qquad (4.15)$$

where, χ : the ratio of principal specific heats (χ_p / χ_v) of the gas,

P_0' : the static pressure,

T_0 : the ambient absolute temperature,

p_0 : amplitude of the acoustic periodic pressure.

In equation (4.I4) the quantity,

$$\xi_{th.} = \sqrt{\frac{2K}{\rho_0 \omega \chi_p}} \qquad (4.16)$$

has the dimensions of length and is known as " the thermal boundary layer thickness". For 20° C and I atmosphere pressure in air, $\xi_{th.} = \frac{0.260}{\sqrt{f}}$ cm, where, f is the frequency in cycles per second. Hence for f = I600c/s,

$\varepsilon_{th.} = 0.0065$ cm.

The quantities θ' and excess pressure p are small, so the equation of state may be written in the form of:

$$dv = v_o \left(\frac{\theta'}{T_o} - \frac{p}{p_o'} \right) \qquad (4.17)$$

where, dv is the change in the volume element of v_o.

Writing $v_o = dA.dh$, equation (4.17) may be rewritten,

$$dv = \left(\frac{\theta'}{T_o} - \frac{p}{p_o'} \right) dA . dh \qquad (4.18)$$

Substituting from equation (4.14) and remembering that

$$c_o = \sqrt{\frac{\chi p_o'}{\rho_o}} ,$$

(4.18) becomes:

$$dv = (\chi - 1) \left\{ 1 - \left[\exp\left(- (1+j)h \Big/ \sqrt{2K/\omega\rho_o\chi_p} \right) - \chi \right] \right\} \frac{p_o \exp(j\omega t)}{\rho_o c_o^2} dA dh \qquad (4.19)$$

The product of the real part of the rate of reduction in volume $-\left(\frac{\partial v}{\partial t}\right)_{real}$ and the real part of the pressure gives the rate of energy loss: where,

$$\left[- \frac{\partial v}{\partial t} \right]_{real} = - \left\{ (\chi - 1) \sin\left[\omega t - \sqrt{\frac{\omega \chi_p}{2}}\, h \right] \exp\left(-h \sqrt{\chi_p \rho_o \omega / 2K} \right) + \sin \omega t \right\} \left(\frac{\omega p_o}{\rho_o c_o^2} \right) dA\, dh \qquad (4.20)$$

and, $\left[p \right]_{real} = p_o \cos \omega t$ (4.21).

Taking the mean value with respect to time and integrating the result between $h = 0$ and $h \to \infty$ gives the mean power loss, associated with the area dA of the boundary layer, i.e.

$$dW_{th.} = \frac{1}{4} \frac{\chi - 1}{\rho_o c_o^2} \omega \varepsilon_{th.} p_o^2 \, dA \qquad (4.22)$$

Therefore, this type of loss is proportional to the square of the pressure amplitude.

It is evident from equations (4.9) and (4.16) that the two boundary layer thicknesses are nearly equal, i.e. $\xi = \xi_{vis.} \cong \xi_{th.}$. Thus it may be considered that the thermal and viscous processes occur in a single boundary layer. Also ξ is negligible compared with the transverse dimensions of the tube.

The power loss in a length of tube dx, due to thermal conductivity is (cf.4.12), (see figure 4.2).

$$dW_{th.} = \int_l \frac{1}{4} \frac{\chi - 1}{\rho_o c_o^2} \omega \xi_{th.} p_o^2 \, dx \, dl \qquad (4.23)$$

Determination of The Attenuation Coefficient: In the case of acoustic wave propagation in a rectangular tube without attenuation, the velocity potential (ϕ) and the propagation constant (γ_{mn}) of any mode, are given by the equations (2.2) and (2.5), respectively.

The effect of viscosity and thermal conduction losses is assumed to add a small real part to the propagation constant, so that,

$$\gamma_{mn} = \alpha_{mn} + j\beta_{mn} \qquad (4.24)$$

where, α_{mn} : the attenuation coefficient of the (m,n) th mode.

Velocity potential is now multiplied by $\exp(-\alpha_{mn} x)$, but is otherwise unchanged from equation (2.2), i.e.

$$\phi = \sum_{m=0}^{\infty} \sum_{n=0}^{\infty} A_{mn} \exp(-\alpha_{mn} x) \begin{matrix} \cos \\ \sin \end{matrix} \left(\frac{m\pi}{2a} y\right) \begin{matrix} \cos \\ \sin \end{matrix} \left(\frac{n\pi}{2b} z\right) \cos(\omega t - \beta_{mn} x) \qquad (4.25)$$

For a particular mode the rate at which the acoustic energy crossing the section at $x = 0$ is,

$$W = \frac{1}{2}\int_{-a}^{+a}\int_{-b}^{+b}\int_{0}^{2} p\, u_x \, dy\, dz\, dt \qquad (4.26)$$

where, 2 is the period of the acoustic cycle ($2 = 2\pi/\omega$),

$$p = \rho_0 \frac{\partial \phi}{\partial t} = -\rho_0 \omega A_{mn} \begin{matrix}\mathrm{Cos}\\ \mathrm{Sin}\end{matrix}\left(\frac{m\pi}{2a} y\right) \begin{matrix}\mathrm{Cos}\\ \mathrm{Sin}\end{matrix}\left(\frac{n\pi}{2b} z\right) \mathrm{Sin}\,\omega t \qquad (4.27)$$

and:

$$u_x = -\frac{\partial \phi}{\partial x} = -\beta_{mn} A_{mn} \begin{matrix}\mathrm{Cos}\\ \mathrm{Sin}\end{matrix}\left(\frac{m\pi}{2a} y\right) \begin{matrix}\mathrm{Cos}\\ \mathrm{Sin}\end{matrix}\left(\frac{n\pi}{2b} z\right) \mathrm{Sin}\,\omega t \qquad (4.28)$$

The total power loss is:

$$dW = dW_{vis.} + dW_{th} \qquad (4.29)$$

The attenuation coefficient α_{mn}, is related to dW and W by the equation: $\alpha_{mn}\, dx = \frac{1}{2}\frac{dW}{W}$

or:

$$\alpha_{mn} = \frac{1}{2}\frac{(dW_{vis.}/dx)_{mn} + (dW_{th}/dx)_{mn}}{W_{mn}} = \frac{1}{2}\frac{\int \frac{1}{4}\rho_0 \omega \varepsilon_{vis.} (u_0)_t^2\, dl + \int \frac{1}{4}\frac{\chi-1}{\rho_0 c_0^2}\omega \varepsilon_{th.} p_0^2\, dl}{\frac{1}{2}\int_{-a}^{+a}\int_{-b}^{+b}\int_{0}^{2} p\, u_x\, dy\, dz\, dt} \qquad (4.30)$$

The values of p, P_0 and u_x are given by the equations (4.27) and (4.28). The value of the amplitude of the tangential velocity is:

$$(u_0)_t^2 = (u_0)_x^2 + (u_0)_y^2 + (u_0)_z^2 \qquad (4.31)$$

At the walls $y = \pm a$, $(u_0)_y = 0$ and at $z = \pm b$, $(u_0)_z = 0$.

where, $$(u_0)_x = -A_{mn}\beta_{mn} \begin{matrix}\mathrm{Cos}\\ \mathrm{Sin}\end{matrix}\left(\frac{m\pi}{2a} y\right) \begin{matrix}\mathrm{Cos}\\ \mathrm{Sin}\end{matrix}\left(\frac{n\pi}{2b} z\right) \qquad (4.32)$$

$$(u_0)_y = A_{mn}\frac{m\pi}{2a} \begin{matrix}-\mathrm{Sin}\\ \mathrm{Cos}\end{matrix}\left(\frac{m\pi}{2a} y\right) \begin{matrix}\mathrm{Cos}\\ \mathrm{Sin}\end{matrix}\left(\frac{n\pi}{2b} z\right) \qquad (4.33)$$

$$(u_0)_z = A_{mn}\frac{n\pi}{2b} \begin{matrix}\mathrm{Cos}\\ \mathrm{Sin}\end{matrix}\left(\frac{m\pi}{2a} y\right) \begin{matrix}-\mathrm{Sin}\\ \mathrm{Cos}\end{matrix}\left(\frac{n\pi}{2b} z\right) \qquad (4.34)$$

Therefore, all values are known in the equation (4.30) and evaluating the integrals of this equation the value of attenu-

ation coefficient can be found.

Now, for perfectly rigid walls,

$$\frac{dW_{vis}}{dx} = \int_l \frac{1}{4} w \varepsilon_{vis.} \rho_o (u_o)_t^2 dl = \frac{1}{4} \rho_o w \varepsilon_{vis} \left\{ 2 \int_{-a}^{+a} \left[(u_o)_x^2 + (u_o)_y^2 + (u_o)_z^2 \right]_{y=b} dy + 2 \int_{b}^{+b} \left[(u_o)_x^2 + (u_o)_y^2 + (u_o)_z^2 \right]_{z=a} dz \right\}$$

The result of this integration depends on the values of m and n and may be written for convenience as four different conditions, (i) $m = 0$, $n = 0$

$$\left[\frac{dW_{vis.}}{dx} \right]_{(0,0)} = \rho_o w \varepsilon_{vis.} A_{00}^2 \beta_{00}^2 (a+b) \quad (4.35)$$

(ii) $m \neq 0$, $n = 0$

$$\left[\frac{dW_{vis.}}{dx} \right]_{(m,0)} = \frac{1}{2} \rho_o w A_{m0}^2 \varepsilon_{vis.} \left\{ \left[\beta_{m0}^2 + \left(\frac{m\pi}{2a} \right)^2 \right] a + 2 \beta_{m0}^2 b \right\} \quad (4.36)$$

(iii) $m = 0$, $n \neq 0$

$$\left[\frac{dW_{vis.}}{dx} \right]_{(0,n)} = \frac{1}{2} \rho_o w A_{0n}^2 \varepsilon_{vis.} \left\{ 2 \beta_{0n}^2 a + \left[\left(\frac{n\pi}{2b} \right)^2 + \beta_{0n}^2 \right] b \right\} \quad (4.37)$$

and (iv) $m \neq 0$, $n \neq 0$,

$$\left[\frac{dW_{vis.}}{dx} \right]_{(m,n)} = \frac{1}{2} \rho_o w A_{mn}^2 \varepsilon_{vis} \left\{ \left[\beta_{mn}^2 + \left(\frac{m\pi}{2a} \right)^2 \right] a + \left[\beta_{mn}^2 + \left(\frac{n\pi}{2b} \right)^2 \right] b \right\} \quad (4.38)$$

Again,

$$\left[\frac{dW_{th.}}{dx} \right] = \int_l \frac{1}{4} \frac{\chi - 1}{\rho_o c_o^2} w \varepsilon_{th.} p_o^2 dl$$

$$= \frac{1}{4} \frac{\chi - 1}{\rho_o c_o^2} w \varepsilon_{th.} \left[2 \int_{-a}^{+a} (p_o)_{z=b}^2 dy + 2 \int_{-b}^{+b} (p_o)_{y=a}^2 dz \right]$$

and the results for four different cases are set below, (i) $m = 0$, $n = 0$

$$\left[\frac{dW_{th.}}{dx} \right]_{(0,0)} = \frac{\chi - 1}{c_o^2} \rho_o w^3 A_{00}^2 \varepsilon_{th.} (a+b) \quad (4.39)$$

(ii) $m \neq 0$, $n = 0$,

$$\left[\frac{dW_{th}}{dx} \right]_{(m,0)} = \frac{\chi - 1}{2 c_o^2} \rho_o w^3 A_{m0}^2 \varepsilon_{th.} (a + 2b) \quad (4.40)$$

(iii) $m = 0$, $n \neq 0$

$$\left[\frac{dW_{th.}}{dx} \right]_{(0,n)} = \frac{\chi - 1}{2 c_o^2} \rho_o w^3 A_{0n}^2 \varepsilon_{th} (2a + b) \quad (4.41)$$

(iv) $m \neq 0$, $n \neq 0$,

$$\left[\frac{dW_{th.}}{dx}\right]_{(m,n)} = \frac{\chi-1}{2c_o^2}\rho_o \omega^3 A_{mn}^2 \varepsilon_{th.}(a+b) \quad (4.42)$$

Finally,

$$W = \frac{1}{2}\int_{-a}^{+a}\int_{-b}^{+b}\int_{0}^{2} \rho u_x \, dy \, dz \, dt$$

$$= \frac{\rho_o \omega A_{mn}^2 \beta_{mn}^2}{2}\int_{-a}^{+a}\begin{matrix}\cos^2 \\ \sin^2\end{matrix}\left(\frac{m\pi}{2a}y\right)dy\int_{-b}^{+b}\begin{matrix}\cos^2 \\ \sin^2\end{matrix}\left(\frac{n\pi}{2b}z\right)dz\int_{0}^{2}\sin^2 \omega t \, dt$$

and the four resulting cases are: (i) $m = 0$, $n = 0$,

$$W_{(0,0)} = 2\omega\rho_o A_{oo}^2 \beta_{oo} \, a \, b \quad (4.43)$$

(ii) $m \neq 0$, $n = 0$,

$$W_{(m,0)} = \omega\rho_o A_{mo}^2 \beta_{ma} \, a \, b \quad (4.44)$$

(iii) $m = 0$, $n \neq 0$,

$$W_{(0,n)} = \omega\rho_o A_{on}^2 \beta_{on} \, a \, b \quad (4.45)$$

(iv) $m \neq 0$, $n \neq 0$,

$$W_{(m,n)} = \frac{1}{2}\omega\rho_o A_{mn}^2 \beta_{mn} \, a \, b \quad (4.46)$$

Substitution of the equations, (4.35), (4.39) and (4.43) into equation (4.30) gives the attenuation coefficient for plane waves in the tube viz.

$$\alpha_{(0,0)} = \frac{1}{4}\beta_{oo}\left(\frac{1}{a}+\frac{1}{b}\right)\left[\varepsilon_{vis.} + (\chi-1)\varepsilon_{th.}\right] \quad (4.47)$$

Substitution of equations, (4.36), (4.40) and (4.44) into equation (4.30) leads to,

$$\alpha_{(m,0)} = \frac{\varepsilon_{vis.}}{4\beta_{mo}}\left\{\left[\beta_{mo}^2 + \left(\frac{m\pi}{2a}\right)^2\right]\frac{1}{b} + \beta_{mo}^2\frac{2}{a}\right\}$$

$$+\frac{(\chi-1)\omega^2\varepsilon_{th.}}{2c_o^2\beta_{mo}}\left(\frac{1}{a}+\frac{1}{2b}\right) \quad (4.48)$$

The case $b \to \infty$ corresponds to propagation between parallel planes at $y = \pm a$, which was considered by Shaw[20], who derived an identical expression for α_{mo} applying Kirchhoff's method. He has also found that, the wave-length constantis increased by the magnitude of the attenuation coefficient which is due to the attenuation of the sound waves.

Pyett[38], using the perturbed mode numbers where dissipation exists, derived the same expression for a rectangular tube. i.e.

$$\beta_{mn} = \frac{2\pi}{\lambda_{mn}} = \frac{2\pi}{\lambda^{o}_{mn}} + \alpha_{mn} \qquad (4.49)$$

where, λ_{mn} is the wavelength of the (m,n) th mode in the tube.

Substitution of the equations (4.37) , (4.41) and (4.45) into equation (4.30) gives:

$$\alpha_{(o,n)} = \frac{\Sigma_{vis.}}{4\beta_{on}} \left\{ \beta_{on}^2 \frac{2}{b} + \left[\beta_{on}^2 + \left(\frac{n\pi}{2b} \right)^2 \right] \frac{1}{a} \right\} + \frac{(\chi - 1)\, \omega^2\, \Sigma_{th.}}{2\, c_o^2\, \beta_{on}} \left(\frac{1}{2a} + \frac{1}{b} \right) \qquad (4.50)$$

Finally, substitution of the equations (4.38) , (4.42) and (4.46)into equation (4.30) gives:

$$\alpha_{(m,n)} = \frac{\Sigma_{vis.}}{4\beta_{mn}} \left\{ \left[\beta_{mn}^2 + \left(\frac{m\pi}{2a} \right)^2 \right] \frac{2}{b} + \left\{ \beta_{mn}^2 + \left(\frac{n\pi}{2b} \right) \frac{2}{a} \right\} \right\} + \frac{(\chi - 1)\, \omega^2\, \Sigma_{th.}}{2\, c_o^2\, \beta_{mn}} \left(\frac{1}{a} + \frac{1}{b} \right) \qquad (4.51)$$

CHAPTER V

MEASUREMENT OF THE ATTENUATION COEFFICIENT FOR PLANE WAVES, (I,0) AND (2,0) MODES IN GAS FILLED, RECTANGULAR TUBES.

5.I. INTRODUCTION. In chapterIV, theoretical expressions of attenuation coefficients for any type of mode have been given. In these expressions, a, b, $c_o, \mu, \kappa, \chi, \chi_\beta$ are all constants which depend on the tube dimensions and the properties of the gas filling the tube. Therefore, for a given frequency, theoretical values of the attenuation coefficient for plane waves in the tube can be obtained from equation (4.47). For (m,0) type modes, however, it is necessary to find the value of β_{m_o} which thus requires the determination of $\lambda^o_{m_o}$.

From equation (4.49), $\lambda^o_{m_o}$ may be written in terms of α_{m_o} and $\lambda^\alpha_{m_o}$, i.e.

$$\lambda^o_{m_o} = \frac{\lambda^\alpha_{m_o}}{1 - \alpha_{m_o}\lambda^\alpha_{m_o}/2\pi} \qquad (5.1)$$

$\lambda^\alpha_{m_o}$ is directly obtained by measurement and α_{m_o} is also derived from experiment. (see section 5.2).

Therefore, β_{m_o} can be obtained and substituting its value into equation (4.48 gives the theoretical value of attenuation coefficient for (m,0) type modes.

5.2. STANDING WAVE ANALYSIS. The theory of the exploration of the standing wave pattern along a tube was initiated by Scott[9](I946) and since considered by many others. In this method, the positions and the values of the pressure amplitudes at maxima and minima of the standing wave pattern along the tube are determined.

In making attenuation measurements, a smooth metal plate is used as the reflector at one end of the tube. This reflector may be assumed to be rigid so that there is no change in the value of the wave amplitude on reflection.

Now assume $e^{-2\psi}$ is the ratio of the amplitudes of reflected and incident waves at the reflecting surface and $\Delta = (2\delta - \pi)$ is the phase change accompanying reflection. Thus, for a rigid reflector, $\psi \cong 0$ and $\delta \cong \frac{\pi}{2}$.

Scott has shown that, with a standing wave pattern in the tube, pressure minima occur at distances from the reflector given by:

$$x_N = \frac{N\pi}{\beta_{mo}} - \frac{\delta}{\beta_{mo}} - \frac{\alpha_{mo}}{2\beta_{mo}^2} \sinh 2(\alpha_{mo} x + \psi) \quad (5.2)$$

where, $N = 1, 2, 3, \ldots$

Correspondingly, pressure maxima occur at distances from the reflector given by,

$$x_M = \frac{(2M+1)\pi}{2\beta_{mo}} - \frac{\delta}{\beta_{mo}} + \frac{\alpha_{mo}}{2\beta_{mo}^2} \sinh 2(\alpha_{mo} x + \psi) \quad (5.3)$$

where, $M = 0, 1, 2, 3, \ldots$

For a rigid reflector, (i.e. $\psi \cong 0, \delta \cong 0$) the above expressions reduce to,

$$x_N = (2N-1)\left(\frac{\pi}{2\beta_{mo}}\right) - \frac{\alpha_{mo}}{2\beta_{mo}^2} \sinh 2\alpha_{mo} x \quad (5.4)$$

$$x_M = 2M \frac{\pi}{2\beta_{mo}} + \frac{\alpha_{mo}}{2\beta_{mo}^2} \sinh 2\alpha_{mo} x \quad (5.5)$$

Considering now negligible energy dissipation in the tube (i.e. $\alpha_{mo} = 0$), then:

$$\left[x_N \right]_{\alpha_{mo}=0} = (2N-1) \frac{\pi}{2\beta_{mo}} \qquad (5.6)$$

$$\left[x_M \right]_{\alpha_{mo}=0} = 2M \frac{\pi}{2\beta_{mo}} \qquad (5.7)$$

Therefore, the effect of dissipation in the tube, is to decrease the distence between a pressure minimum and rigid reflector and to increase the distance between a pressure maximum and the rigid reflector by an amount

$$\frac{\alpha_{mo}}{2\beta_{mo}^2} \sinh 2\alpha_{mo} x .$$

The validity of above expressions depend on the condition $\frac{\alpha_{mo}}{\beta_{mo}} \ll \pi$. This condition is always fulfilled in this work for the values of $\frac{\alpha_{mo}}{\beta_{mo}}$ were less than 0.I.

The amplitudes of pressure minima and maxima are given by

$$P_{min} = C \left[\sinh^2(\alpha_{mo} x_N + \psi) + \frac{\alpha_{mo}^2}{4\beta_{mo}^2} \sinh^2 2(\alpha_{mo} x_N + \psi) \right]^{\frac{1}{2}} \qquad (5.8)$$

$$P_{max} = C \left[\cosh^2(\alpha_{mo} x_M + \psi) + \frac{\alpha_{mo}^2}{4\beta_{mo}^2} \sinh^2 2(\alpha_{mo} x_M + \psi) \right]^{\frac{1}{2}} \qquad (5.9)$$

where, C is constant.

In the present case, α_{mo} is very small (less than 0.003) and the second terms in the above equations may be neglected. Furthermore, $\psi \cong 0$ for a rigid reflector, thus equations (5.8) and (5.9) may be reduced respectively to

$$P_{min} = C \sinh \alpha_{mo} x \qquad (5.10)$$

$$P_{max} = C \cosh \alpha_{mo} x \qquad (5.11)$$

Generally, $\alpha_{mo} x$ is less than 0.2, so, $\cosh \alpha_{mo} x$ does not considerably differ from unity and the (sinh) function is nearly equal to its argument. Therefore, equations (5.I0) and (5.II) show that,

all pressure maxima become nearly equal and the pressure minima are a linear function of distance, in the case of the rigid reflector.

The standing wave ratio S is given by:

$$S = \frac{P_{min}}{P_{max}} = \tanh \alpha_{mo} x \qquad (5.12)$$

and,

$$\alpha_{mo} = \frac{1}{x} \tanh^{-1} S \qquad (5.13)$$

If, $(\tanh^{-1} S)$ is plotted against x, a straight line should be obtained, whose slope gives the attenuation coefficient.

5.3. NON RIGIDITY OF WAVE-GUIDE WALLS --EXISTANCE OF TRANSVERSE VIBRATIONS. At a pressure antinode, the (I,0) mode exerts a positive force on one of the minor sides of a transverse section of the tube and a negative force on the other opposite side. Thus the antisymmetrical character of the (I,0) mode tends to cause lateral displacement of the section in the same direction if the walls of the tube are not sufficiently rigid. However, such displacement also occurs when the whole tube vibrates transversly as a bar, so that, there may be coupling between the bar-type flexural resonances of the tube and the (I,0) mode. In such case, acoustic energy would be expected to pass most readely from gas to tube when the phase velocity (c_p) of the (I,0) mode coincides with that of a flexural wave in the tube.

Morse[39], gives the expression of the velocity of flexural wave in a bar, i.e.

$$c_f = \left(\frac{E_b}{\rho_b}\right)^{\frac{1}{4}} \left(\omega R_g\right)^{\frac{1}{2}} \qquad (5.14)$$

where,

E_b : Young modulus of the material of the wave-guide wall,

ρ_b : density of the material,

R_g : radius of gyration of the cross- section.

R_g For a rectangular, thin walled tube of transverse dimensions 2a and 2b, is,[40]

$$R_g = \frac{a}{\sqrt{3}} \left(\frac{a+3b}{a+b} \right)^{\frac{1}{2}} \qquad (5.15)$$

The allowed frequencies of the flexural vibration of an unsupported bar of length (l) vibrating freely are,[39]

$$\left(f_a\right)_N = \frac{\pi R_g}{2l} \left(\frac{E_b}{\rho_b} \right)^{\frac{1}{2}} \left(N + \frac{1}{2} \right)^2 \qquad (5.16)$$

where, $N = 1, 2, 3, \ldots$

Therefore, from equation (5.16), $\left(f_a\right)_N$ may be found and substituting these values into equation (5.14) gives the approximate values of c_1, at resonance. When one of the values of c_1, coincides with the phase velocity of the (1,0) mode, some excess attenuation of sound may be expected for non-rigid tube walls. In section (5.4) this possibility will be investigated by inserting numerical values in the analytical expressions.

5.4. EXPERIMENTAL WORK.

In order to find the theoretical values of attenuation coefficients, the values of gas coefficients c_o, ρ_o, χ, χ_ρ, μ and K must be known. (See references 41, 42, 43, 44, 45).

Gas constants for air:

The density of air (ρ_o) at an absolute temperature T (deg K)

and pressure P(cm. Hg.):

$$\rho_o = 0.001293 \left(\frac{P}{76}\right)\left(\frac{273}{T}\right) \cdot gm/cm^3 .$$

hence, at 22° C and I atmosphere, $\rho_o = 0.001293$ gm/cm.

The velocity of sound in air (c_o) at any ordinary temperature in degC, can be calculated from the formula:

$$C_o = 33145 + 60.7\,(\text{temperature}) \quad cm/sec.$$

So, at 22° C, $c_o = 34480$ cm/sec.

Specific heat at constant pressure (χ_p) and the ratio of the principal specific heats (χ) of air, at I atmosphere and 22° C are respectively $0.24 \frac{Cal}{gm.degC}$ and 1.403 .

The shear viscosity coefficient of air (μ) at 22° C is $\mu = 181\,\mu p$. . If the viscosity of a gas μ' at the temperature T' is known, the viscosity μ'' at T'' is given by:

$$\mu'' = \mu' \left(\frac{T' + C}{T'' + C}\right)\left(\frac{T''}{T'}\right)^{\frac{3}{2}}$$

where C is Sutherland constant and equal to 117 for air.

The thermal conductivity of a gas at normal pressures is independent of pressure and may be given by: $k = 0.25\,(9\chi - 5)\,\mu\,\chi_v$

At 22° C, I atmosphere, the thermal conductivity of air is: $6.212 \times 10^{-5} \frac{Cal}{cm.sec.degC.}$

Attenuation of (0,0) and (1,0) Modes: Measurements with (0,0) and (1,0) modes were carried out in the small wave-guide. The experimental values of attenuation coefficients were found about 10% above the theoretical values. The sand which covers the guide

Frequency	Temperature	Calculated $\alpha_{0,0} \times 10^{-5}$ (cm^{-1})	Observed $\alpha_{0,0} \times 10^{-5}$ (cm^{-1})
2418 c/s	21.8°C	61	62
2426 c/s	22.0°C	62	60
2444 c/s	21.6°C	62	65
2668 c/s	21.6°C	64	66
2938 c/s	21.8°C	66	67
3272 c/s	21.9°C	70	73

Table 5.1.

Frequency	Temperature	Calculated $\alpha_{1,0} \times 10^{-5}$ (cm^{-1})	Observed $\alpha_{1,0} \times 10^{-5}$ (cm^{-1})
2418 c/s	21.8°C	620	625
2426 c/s	22.0°C	386	394
2444 c/s	21.7°C	299	294
2668 c/s	21.6°C	159	165
2938 c/s	21.9°C	132	135
3272 c/s	21.9°C	113	114

Table 5.2

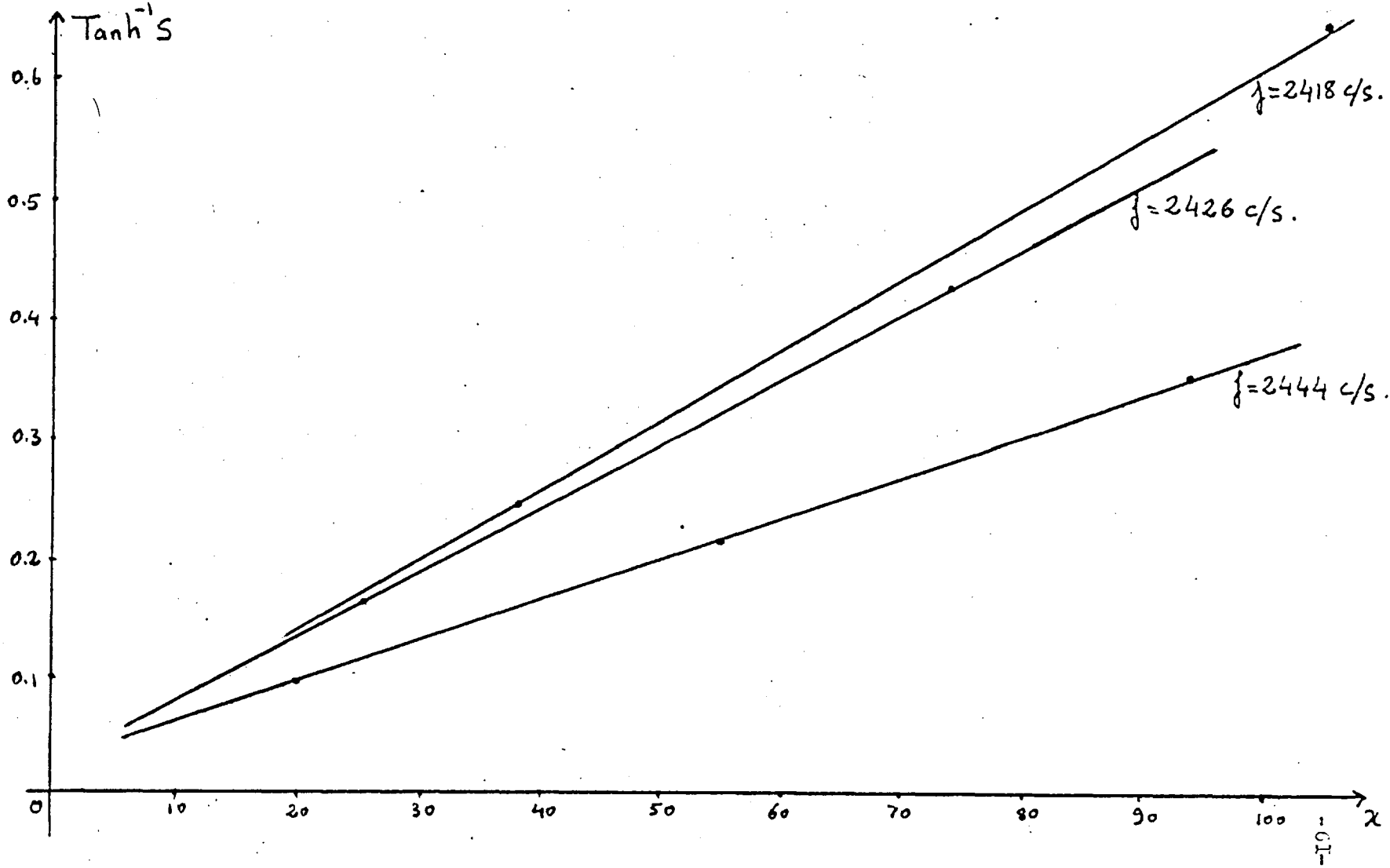
Tanh⁻¹S
0.6
0.5
0.4
0.3
0.2
0.1
0
10
20
30
40
50
60
70
80
90
100
x
f=2418 c/s.
f=2426 c/s.
f=2444 c/s.

Figure 5.1

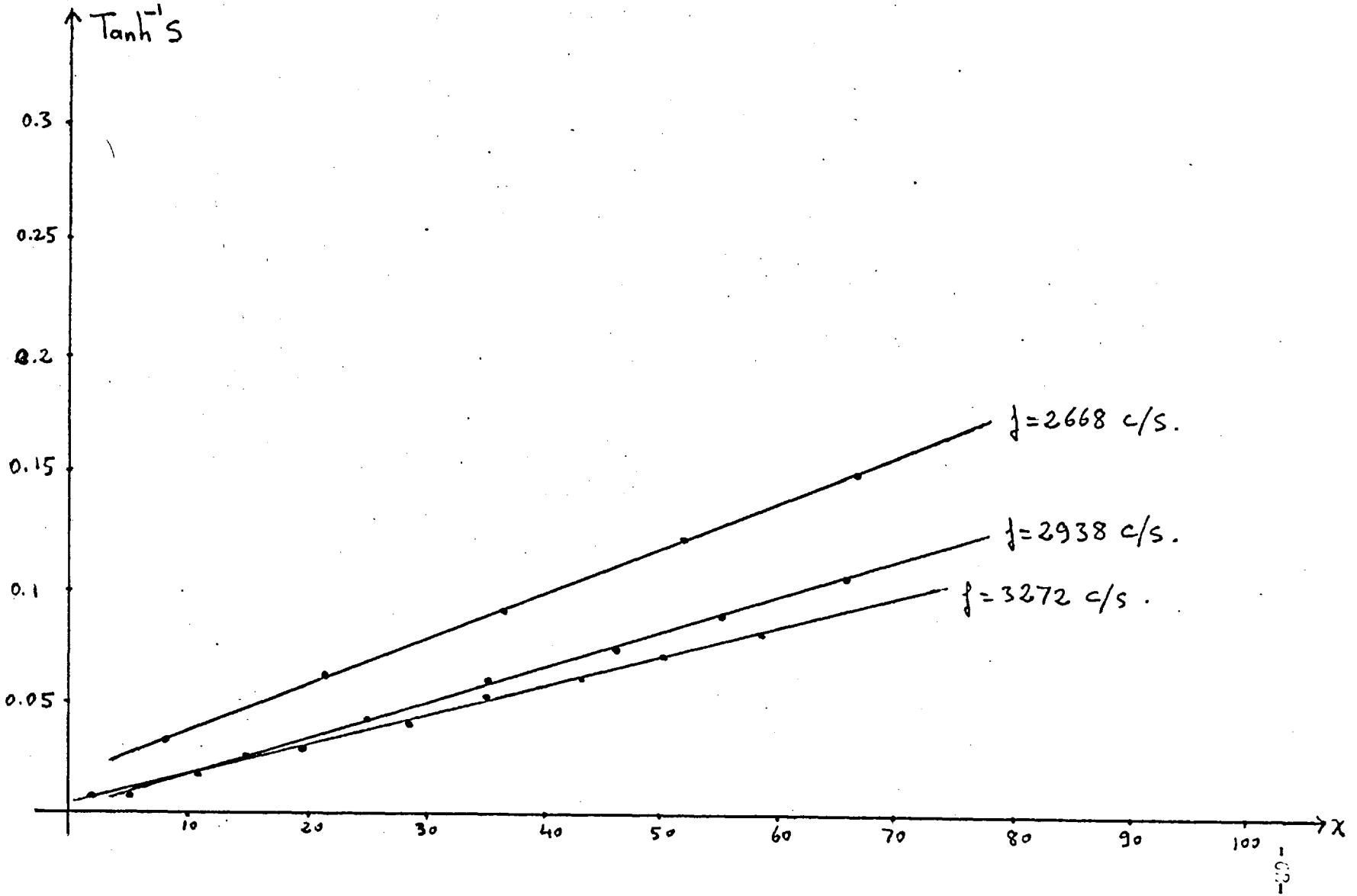
Tanh⁻¹S
0.3
0.25
0.2
0.15
0.1
0.05
10
20
30
40
50
60
70
80
90
100
X
f=2668 c/s.
f=2938 c/s.
f=3272 c/s.

Figure 5.2

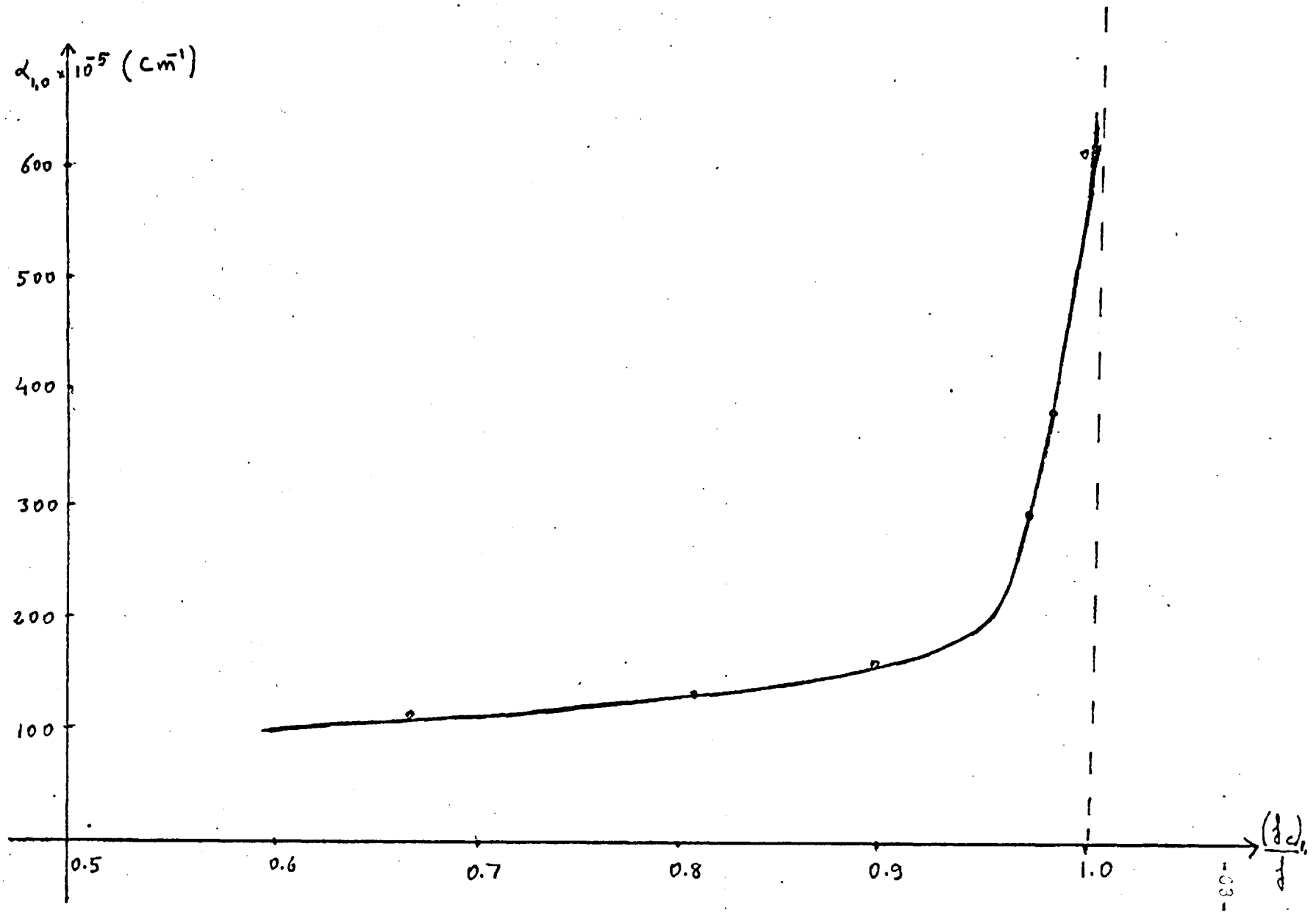
$\alpha_{1,0} \times 10^{-5}$ (cm^{-1})
600
500
400
300
200
100
0.5
0.6
0.7
0.8
0.9
1.0
$\frac{(\beta_c)_1}{\beta}$

Figure 5.3

caused this high values of attenuation coefficients because of its high internal firiction. On the other hand no wall vibration occurred, which means that the walls were effectively rigid.

The sand which covers the guide was then removed and the measurements were carried out with the tube free from sand but still contained within the covered box.

The results of plane wave measurements have been given in table 5.I. The theoretical values of attenuation coefficients have also been included for comparison. An agreement within 3% is found which should be within experimental error.

The values of attenuation coefficients obtained in (I,0) mode experiments have been given in table5.2. together with theoreticalvalues of $\alpha_{1,0}$. In figure 5.I and figure 5.2 $\tanh^{-1} S$ have been plotted against x. The results as expected were straight lines which ensures that the standing wave patterns follow the theoretical forms very closely.

The attenuation coefficient of the (I,0) mode against the ratio of $\left[(\delta_c)_{1,0}/\lambda\right]$ has been plotted in figure5.3. From this figure it can be seen that $\alpha_{1,0}$ has large values near the cut-off frequency of the (I,0) mode. This is because the wavelength of the (I,0) mode is very large when the excitation frequency approaches the cut-off frequency of the (I,0) mode.

During the standing wave measurements all pressure maxima

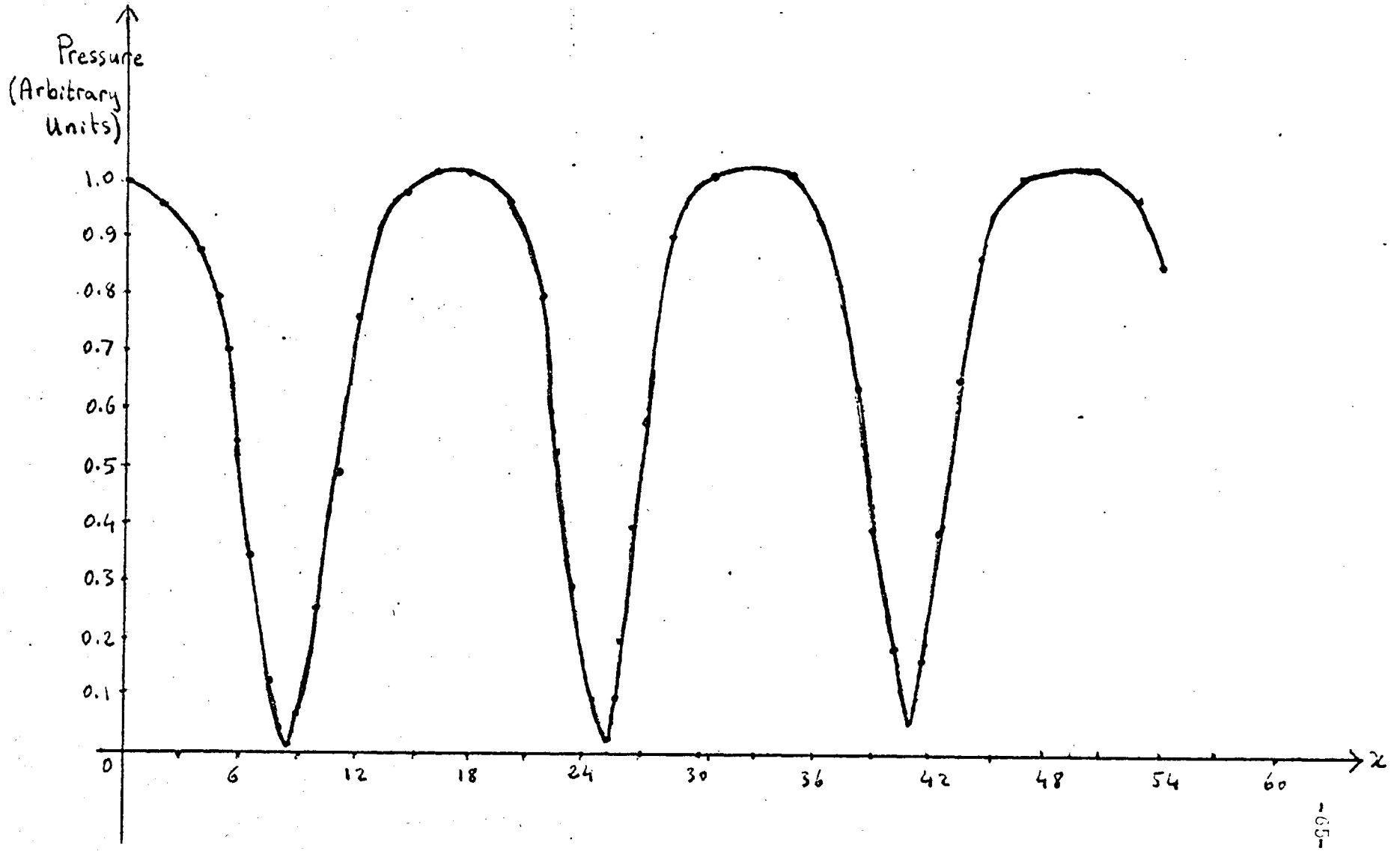
Pressure
(Arbitrary
Units)
1.0
0.9
0.8
0.7
0.6
0.5
0.4
0.3
0.2
0.1
0
6
12
18
24
30
36
42
48
54
60
x

Figure 5.4

were found to be approximately equal and the pressure minima increased with the distance measured from the face of the rigid reflector. This can be seen in figure 5.4 which shows the variation of pressure along the large wave-guide for the (I,0) mode at the frequency of I603 c/s.

The possibility of tube wall vibrations when the sand is removed should be considered. For brass tube, $E_b = 9.11 \times 10^{11}$ gm.cm/sec^2, $\rho_b = 8.6$ gm./cm^3. and $R_g = 2.75$cm. Thus the values of allowed frequencies of the flexural vibration of the tube may be found from equation (5.I6). When $N = 4$ in equation (5.I6), f_a is equal to 2427 c/s. Substituting this value into equation (5.I4) gives the velocity of flexural wave which is about $II9 \times I0^3$ cm/sec. On the other hand the phase velocity of the (I,0) mode in the tube is given by $c_p = c_o/\cos\theta$ (see equation 2.I8). When $c_p \cong c_1$ the value of $\cos\theta$ is 0.30. The value of $\cos\theta$ was also given in terms of the frequency (see equation 2.I7), i.e.

$$\cos\theta = \left[1 - \left(\frac{(f_c)_{1,0}}{f}\right)^2\right]^{\frac{1}{2}}$$

Substituting the value of $\cos\theta$ and $(f_c)_{1,0}$ into this equation gives the approximate frequency 2563 c/s. Therefore, at this frequency the twovelocities c_p and c_1 are coincide and this may cause some excess attenuation.

Experiments with f = 2563 c/s showed that observed value of $\alpha_{1,0}$ is about I3 % above the theoretical value which was caused by the tube wall vibrations.

Frequency	Temperature	Calculated $\alpha_{2,0} \times 10^{-5}$ (cm^{-1})	Observed $\alpha_{2,0} \times 10^{-5}$ (cm^{-1})
2423 c/s	22.0°c	260	280
2478 c/s	22.0°c	156	164
2538 c/s	21.9°c	111	116
2996 c/s	22.0°c	77	80
3286 c/s	21.8°c	76	80

Table 5.3

Frequency	Temperature	Calculated $\alpha_{0,0} \times 10^{-5}$ (cm^{-1})	Observed $\alpha_{0,0} \times 10^{-5}$ (cm^{-1})
6889 c/s	21.8°C	116	122
7003 c/s	21.8°c	118	122
7396 c/s	21.9°c	120	126
7512 c/s	21.9°c	124	129

Table 5.4

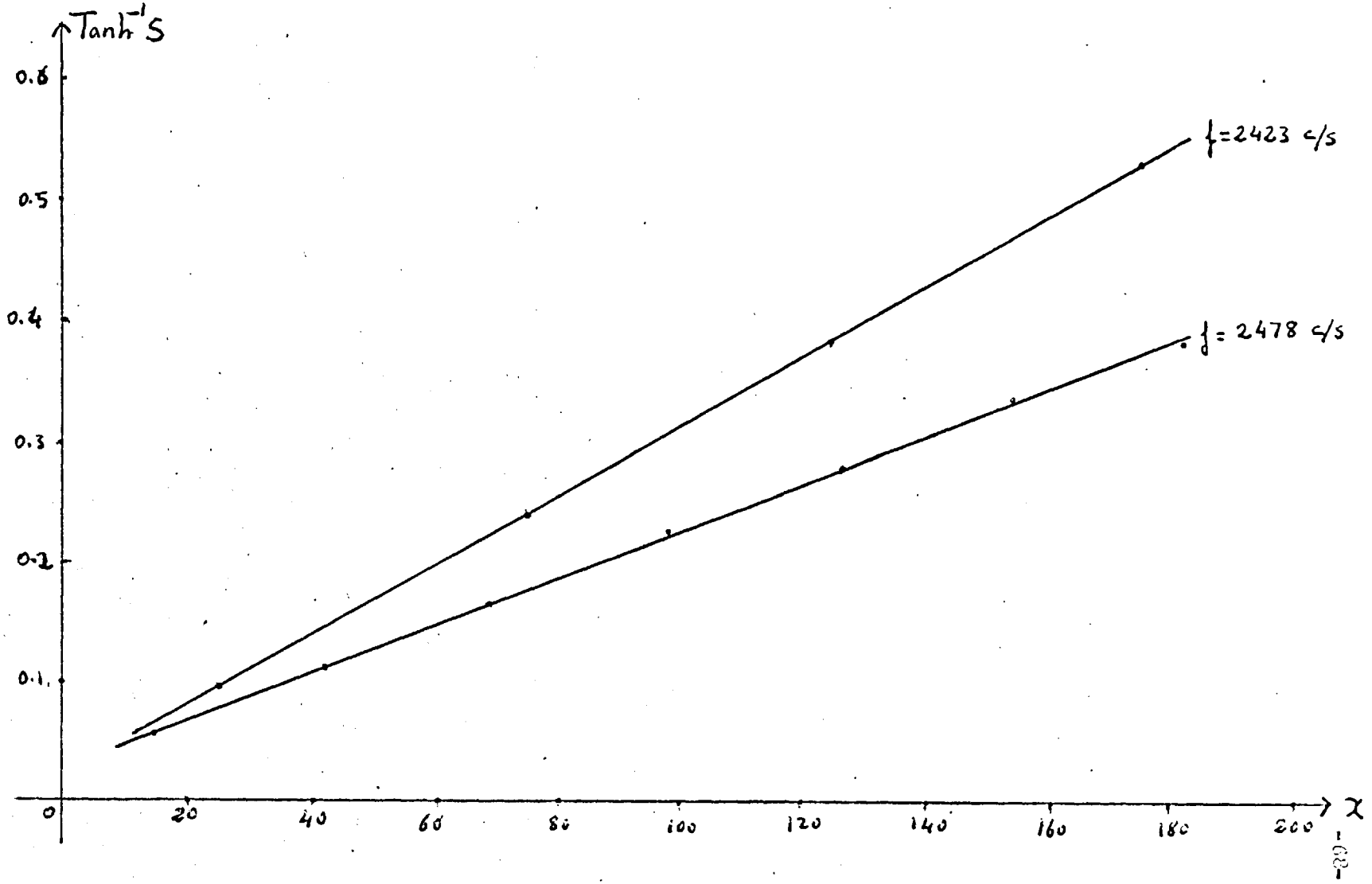
Tanh⁻¹S
0.6
0.5
0.4
0.3
0.2
0.1
0
20
40
60
80
100
120
140
160
180
200
x
f=2423 c/s
f = 2478 c/s

Figure 5.5

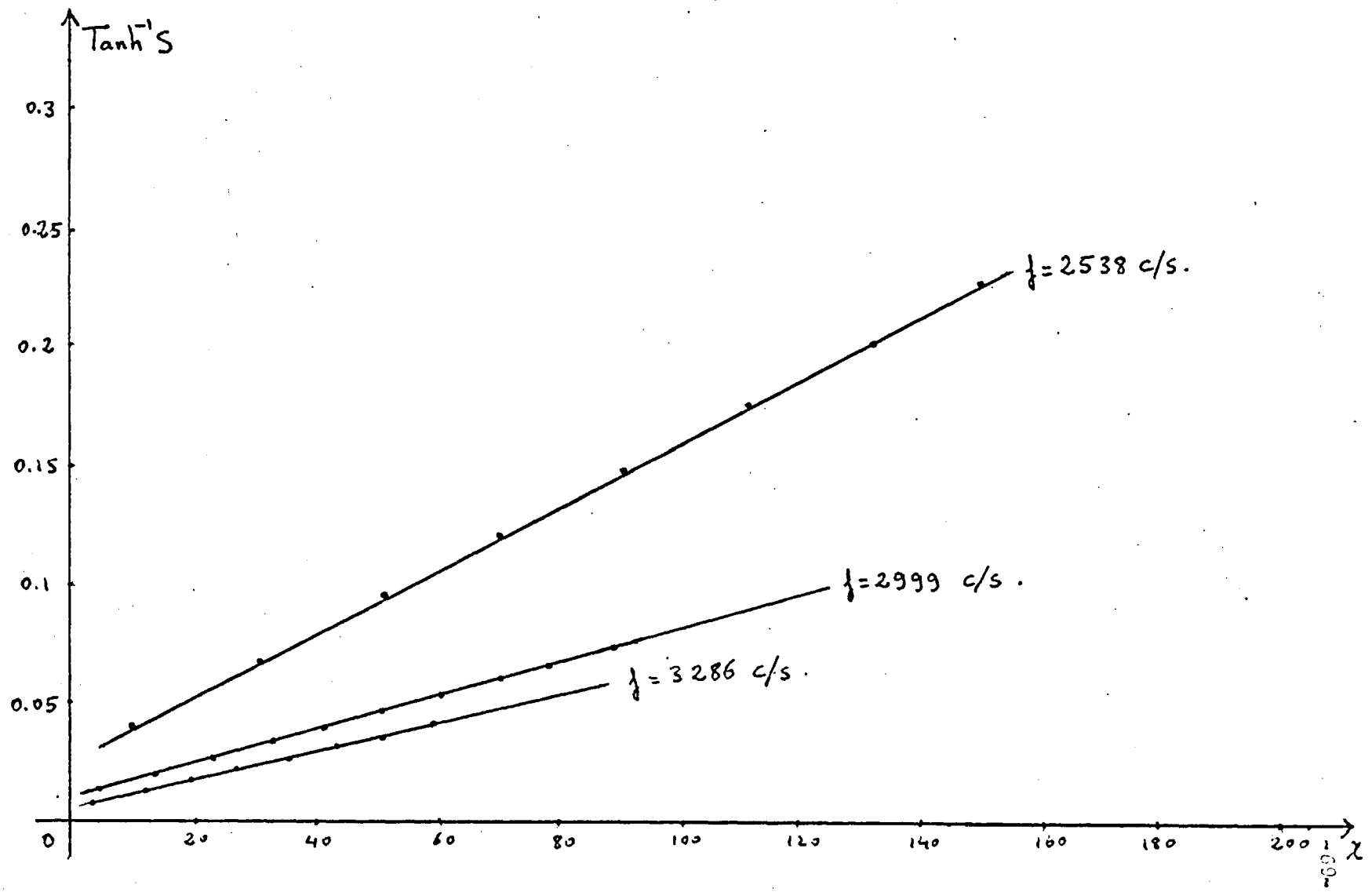
Tanh⁻¹S
0.3
0.25
0.2
0.15
0.1
0.05
0
20
40
60
80
100
120
140
160
180
200
χ
f = 2538 c/s.
f = 2999 c/s.
f = 3286 c/s.

Figure 5.6

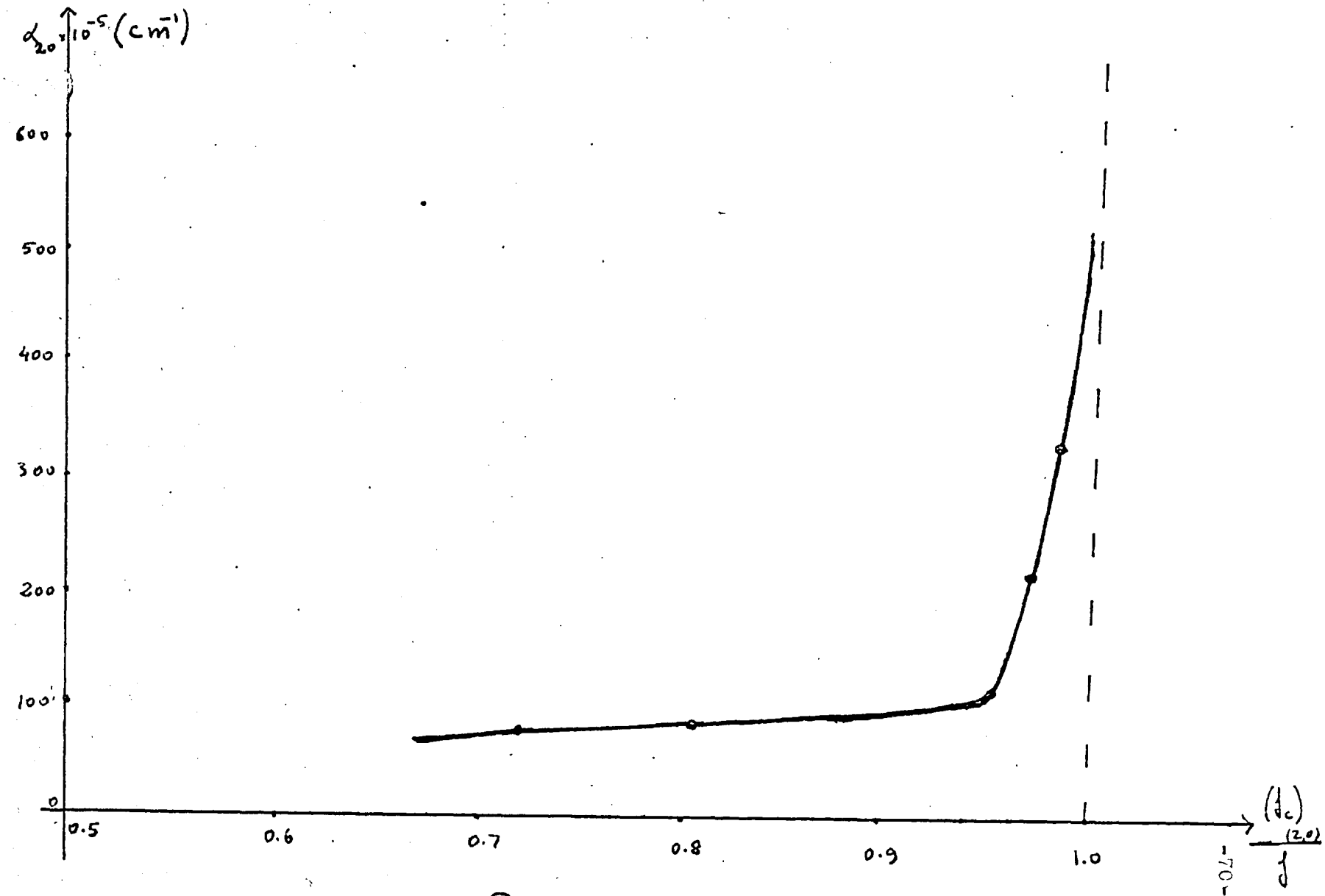
$\alpha_{20} \times 10^{-5} (cm^{-1})$
600
500
400
300
200
100
0
0.5
0.6
0.7
0.8
0.9
1.0
$\frac{(f_c)}{f}$
(20)

Figure 5.7.

Attenuation of The (2,0) Mode: Experiments with The (2,0) mode were carried out with the large wave-guide. Observed and calculated values of $\alpha_{2,0}$ are given in table 5.3. The plot of $\tanh^{-1} S$ against x are also shown in figure 5.5 and 5.6. The results are about 6-7% above the theoretical values which was again caused by the high internal friction in the sand which covers this guide.

The variation of $\alpha_{2,0}$ as a function of the ratio of $\frac{(\delta_c)_{2,0}}{\delta}$ is shown in figure 5.7. $\alpha_{2,0}$ has large values near the cut-off frequency of the (2,0) mode where wavelength of the (2,0) mode is very large.

Attenuation of Sound in Helium Filled Wave-guide: Measurements with the small wave-guide filled with helium was also done. Helium is a monoatomic gas so the non-classical attenuation is avoided. Helium has also a high value of thermal conductivity with a high sound velocity compared with that of air. Gas coefficients for helium (see references 41, 42, 43, 44 and 45) are: $(c_o)_{he} = 97970$ cm/sec, $(\chi)_{he} = 1.60$, $(\lambda_p)_{he} = 1.25$ cal/ gm degC, $(\rho_o)_{he} = 0.17 \times 10^{-3}$ gm/cm , $(\mu)_{he} = 194$ micropoise and $(K)_{he} = 14.61 \times 10^{-4}$ cal/cm sec degC.

From a helium cylinder the gas admitted into the guide through a 0.08cm. orifice near the reflector plate. At the loudspeaker end a special glass tap system and a vacuum pump have been used to flush out the gas from the inside of the guide and from the rubber tubes which connects the loudspeaker units and the source end of the wave-guide. Apart from the probe tubes, the guide was well

sealed. Hence, the end of the probe tubes near the travelling microphone were also closed.

For about 15 minutes the gas inside the guide were flushed out for several times and helium was maintained in the guide. The gas pressure inside the guide was read by using U-tube gauge which was connected to an orifice in the tube wall.

Experiments were carried out for plane waves and for frequencies from 6889 to 7512 c/s. Results were about 3-6% above the theoretical values which are given table 5.4. $\text{Tanh}^{-1} S$ against x is also plotted in figure 5.8 for the frequency of 7003 c/s.

The classical attenuation in the body of the gas has been calculated by using the equation (4.4). It wass found that at 7 Kc/s, $\alpha_{clas.}$ has the value of about 3.4% of the total boundary layer attenuation. Therefore, theoretical values should be somewhat higher than given in table 5.4 and experimental values of attenuation coefficients should be accepted as close to its theoretical values.

The value of the boundary layer thickness for helium can also be determined from the equations (4.9) and (4.16). At a frequency of 7 Kc/s, $\xi_{vis} = 0.007$ cm and $\xi_{th.} = 0.0073$ cm which are very small compared with tube dimensions and therefore the boundary layer theory can be applied.

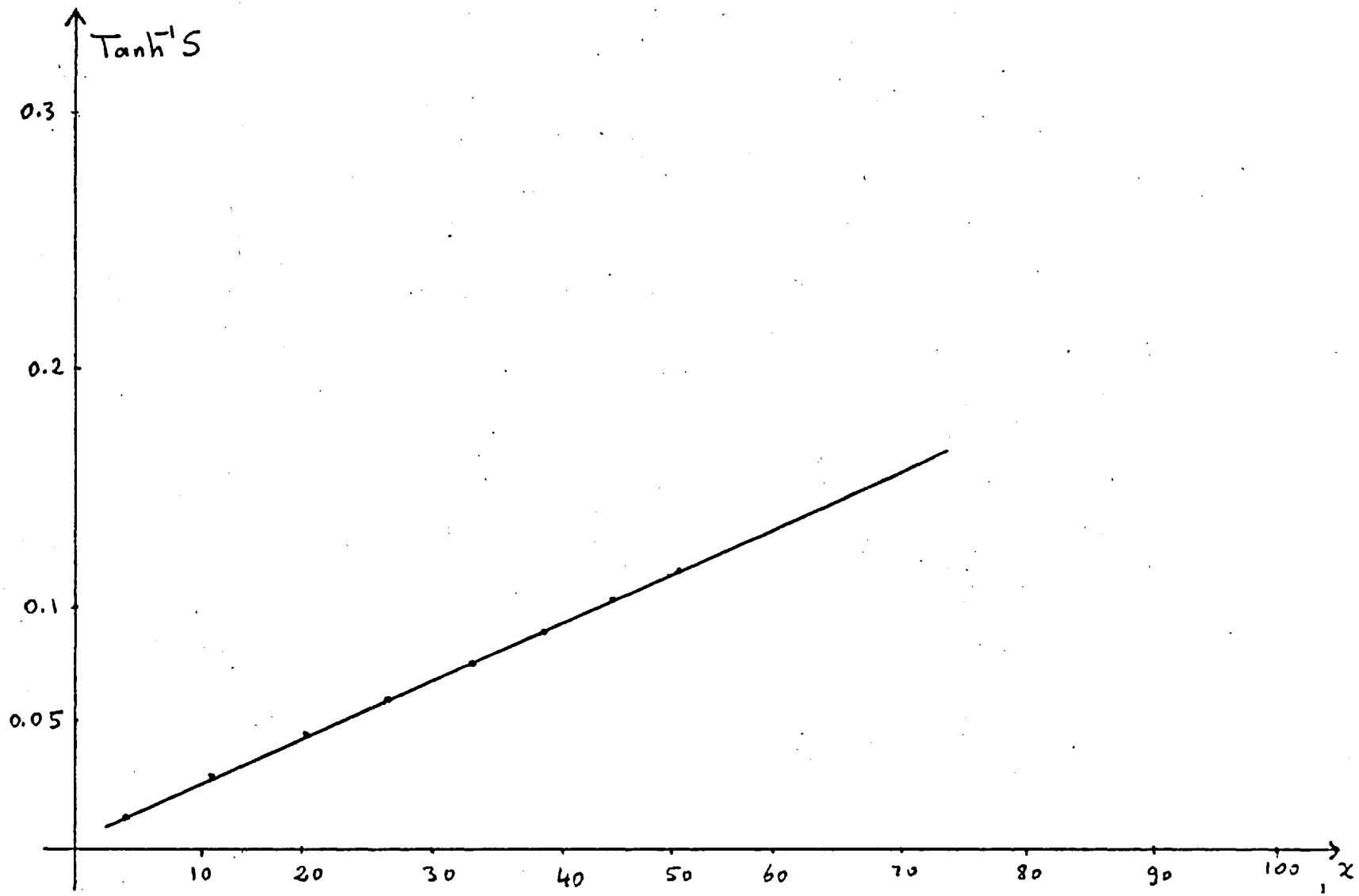

Figure 5.8

CHAPTER VI

THE MEASUREMENT OF THE SPECIFIC ACOUSTIC IMPEDANCE OF POROUS MATERIALS AT OBLIQUE INCIDENCE.

6.I. INTRODUCTION. Measurement at oblique incidence implies the use of a parallel beam of radiation incident at one definite angle to the surface normal so that randomly incident sound waves are excluded in the present discussion.

Various experimental methods have been employed but before describing these the conditions to be fulfilled by the "ideal method" will be defined.

a) Any desired frequency can be used,

b) The measurements can be carried out at any desired angle of incidence,

c) Any size of material can be used for the measurements,

d) A good experimental accuracy is attainable.

Condition (d) is, of course, the most important one. The several methods which are used in practice may be divided into three groups:

Free Wave Method. This type is the earliest method which has been used to measure the absorption coefficient of materials at oblique incidence. It is similar to the optical reflection and absorption measurement method. Conditions (b), (c) and part of (a) is fulfilled by this method but the results are not accurate for these reasons:

(i) At audible frequencies the wavelength of sound wave is large and ray optics formulas are not strictly applicable with an apparatus of feasible dimensions. So, lower frequencies cannot be used.

(ii) Diffraction effects.

Chamber Methods. In one procedure a small rectangular chamber has been used with one wall covered with a sound absorbing material. Bhatt[46](I939) and Harris[47](I945) have used such chambers and made observations on a single mode enabling the impedance to be evaluated. The incidence angles depend on the modes which are excited, and so frequencies and angle of incidences cannot be chosen at will. The results here are not expected to be accurate. This may be due to ambient temperature changes which are very difficult to control. The chamber method is advantageous if a large surface is required as often e.g. in panel resonators, the materials do not respond uniformly all over their surface. This method can also be used at frequencies as low as I00 c/s, where the other two methods become impracticable.

Acoustic Wave-Guide Method. This method was first suggested by Hartig and Swanson[8] (I938). In this method three techniques are possible:

(i) Study of the resonance curves obtained when the frequency of the source is varied. This technique is unlikely to allow accurate measurements in the case of highly absorbent surfaces, since the resonance curves of individual modes then tend to merge making discri-

mination difficult.

(ii) Study of the resonance curves obtained when the tube length is varied. (Beranek[10]). This technique leads to mechanical difficulties.

(iii) Exploration of the standing wave pattern in a tube. Paris[49](I927), Scott[9](I946), Shaw[11](I953) and others used this method.

This technique does not have any serious disadvantage if the sound generator system ensures the excitation of the desired mode only, as explained in chapter III.

The second and third techniques are termed acoustic transmission techniques.

The standing wave method has been applied in the present work. This method of impedance measurement consist simply of determining the pressure amplitudes at a maximum and minimum of the standing wave pattern, together with the distance from the specimen surface to the first minimum.

The specific acoustic impedance of the specimen can than be found from charts as will be explained in the next section.

The advantages and disadvantages of the acoustic waveguide method may best be understood by comparison with the " ideal method".

a) In order to excite a propagated mode, the frequencies which are above the cut-off frequency of that mode must be used as explained in chapter II. Therefore, only a limited frequency range can be used.

for a particular propagated mode in the tube. If the transverse dimensions of the tube is small, higher frequencies can be used for that mode but it is also necassary to choose a tube which has transverse dimensions large enough to accommodate a suitable test material. If one uses several tubes with different transverse dimensions a large frequency range can be used but this is, of course, rather impractible. On the other hand, the dimensions of the guide become rather large for frequencies less than about 300 c/s.

b) The angle of incidence depends on frequency and the dimensions of the wave-guide section. Therefore, it can be continuously varied by altering the frequency of excitation, but it is not possible to measure over a range of incident angles at one frequency with one tube. From the observed values of mode wave-lengths the angle of incidences can be determined accurately. When the frequency is increased, this angle gets less but at the same time the possibility of excitation of other modes in the tube, which are unwanted, put a lower limit on the value of the angle of incidence. This lower value for normal-sized tubes is about 25° - 30°. Beranek[49] (I942), derived an approximate formula for the acoustic impedance of thin porous layers. He showed that, important change, with increasing the angle of incidence is an increase in the resistive part of the impedance, the reactance remaining unchanged. Later experiments have confirmed these results. Therefore, the value of impedance does not change very much at lower values of the angle of

incidence. (i.e. between 0° - 25°). In fact, the wave-guide apparatus can be used for normal incidence (i.e. $\theta = 0$), measurements employing the (0,0) mode. These considerations indicate condition (b) can assumed to be fulfilled.

c) Wave-guides are not suitable for large-scale acoustic materials, unless corridors are used as sound-channels.

d) The wave-guide has the great advantage that it is capable of the high accuracy of the normal incidence tube methods. It can become a precision method and was used in the present experiment.

Normal incidence tube methods have been described by Beranek[10], in full detail.

6.2. DETERMINATION OF SPECIFIC ACOUSTIC IMPEDANCES OF MATERIALS AT OBLIQUE INCIDENCE, USING THE STANDING-WAVE METHOD.

In this experiment, impedance measurements have been carried out using the (I,0) mode. The impedance formula , therefore, will be evaulated here, for this particular mode.

When the tube is terminated by a test material a standing wave pattern developed along the tube. The complex reflection coefficient at the surface of the material is given by:

$$r_{1,0} = e^{-(2\psi + j\Delta)} \qquad (6.1)$$

where $e^{-2\psi}$: the ratio of the amplitudes of the reflected to incident wave, and $\Delta = 2\delta - \pi$: the phase angle, (6.2)

From equations (6.I) and (6.2) :

$$r_{1,0} = e^{-2(\psi + j\delta) + j\pi} = -e^{-2(\psi + j\delta)} \qquad (6.3)$$

The specific acoustic impedance of the material, $Z_{1,0}$, depends on the reflection coefficient and the characteristic mode impedance $W_{1,0}$ of the medium. This relationship is given by:[11]

$$r_{1,0} = \frac{Z_{1,0} - W_{1,0}}{Z_{1,0} + W_{1,0}} \qquad (6.4)$$

Substituting equation (6.3) into equation (6.4) gives,

$$\frac{Z_{1,0}}{W_{1,0}} = \tanh(\psi + j\delta) = p + jq \qquad (6.5)$$

Therefore, in order to find the value of $Z_{1,0}$ of a material, first ψ and δ must be determined. This can be done by observing the standing wave pattern in the tube as will be explained later in this section. However, at the cut-off frequency of the (I,0) mode $W_{1,0}$ is infinite and equation (6.5) becomes zero. Therefore, this equation does not give directly required impedance ratio.

Thus the ratio,

$$\frac{Z_{1,0}}{W_{0,0}} = \frac{R}{W_{0,0}} + j\frac{X}{W_{0,0}} \qquad (6.6)$$

has to be determined. The value of $W_{0,0}$ is given in equation (2.II.a) which is: $W_{0,0} = \rho_0 C_0$. By defination

$$W_{1,0} = \frac{\omega \rho_0}{\beta_{1,0}} = \frac{\omega \rho_0}{\frac{2\pi}{\lambda_{1,0}} - j\alpha_{1,0}} \qquad (6.7)$$

Substituting this value into equation (6.5) gives:

$$\frac{Z_{1,0}}{W_{1,0}} = \frac{Z_{1,0}}{W_{0,0}} \frac{\lambda_{0,0}}{\lambda_{1,0}} \left(1 - j\frac{\alpha_{1,0}\lambda_{1,0}}{2\pi}\right)$$

$$= \left(\frac{R}{W_{0,0}} + j\frac{X}{W_{0,0}}\right) \frac{\lambda_{0,0}}{\lambda_{1,0}} \left(1 - j\frac{\alpha_{1,0}\lambda_{1,0}}{2\pi}\right)$$

$$= p + jq \qquad (6.8)$$

So, from this equation, the resistance and reactance ratios are gi-

ven by:

$$\frac{R}{\rho_0 c_0} = \frac{\lambda_{1,0}}{\lambda_{0,0}}\left(p - q\,\frac{\alpha_{1,0}\,\lambda_{1,0}}{2\pi}\right) \qquad (6.9)$$

and:

$$\frac{X}{\rho_0 c_0} = \frac{\lambda_{1,0}}{\lambda_{0,0}}\left(q + p\,\frac{\alpha_{1,0}\,\lambda_{1,0}}{2\pi}\right) \qquad (6.10)$$

$\lambda_{1,0}$ and $\lambda_{0,0}$ can be measured with high accuracy from observation of the standing wave pattern. $\frac{\lambda_{1,0}}{2}$ and $\frac{\lambda_{0,0}}{2}$ are the distance between two successive pressure minima points.

When the values of ψ , $\alpha_{1,0}$ and the distance between the position of first pressure minimum and the material $(x_1)_{min}$ are found the values of p and q are obtained using a Smith chart, described by Willis, Jackson and Huxley[50] (1944). Values of ψ are defined by concentric circles intersecting the radial lines of constant $\left[\frac{(x_1)_{min}}{\lambda_{1,0}}\right]$. The values of p and q may than be found drectly which are important for the equations (6.9) and (6.10).

In the presence of appreciable tube attenuation the interpretation of the standing wave pattern becomes more difficult.

The expressions derived by Scott, for the maximum and minimum pressure amplitudes and their positions along the tube have been given in chapter V, by equations (5.2), (5.3), (5.8) and (5.9). It can be seen that, the effect of attenuation is to shift each minimum towards the reflecting surface by an amount

$$\xi_{(1,0)} = \frac{\alpha_{1,0}}{2\beta_{1,0}^2}\sinh 2(\alpha_{1,0}\,x + \psi) \qquad (6.11)$$

The standing wave ratio can be given by the modified for-

mula, which is from chapter V,

$$S = \frac{P_{min}}{P_{max}} \cong \tanh\left(\alpha_{1,0}\, x + \Psi\right) \qquad 6.12$$

Plot of $\tanh^{-1}S$ against x is a straight line and the slope of this line gives $\alpha_{1,0}$. The intercept of the $\tanh^{-1}S - x$ line at $x=0$ gives the value of Ψ.

In experiment, the distance $(x_1)_{min}$ can easly be measured but effect of tube attenuation should also be considered. So, $\xi_{(1,0)}$ must be added as a correction term to $(x_1)_{min.}$ i.e.

$$\left[(x_1)_{min.}\right]_{Corrected} = \left[(x_1)_{min}\right]_{measured} + \xi_{(1,0)} \qquad (6.13)$$

Corrected value of $(x_1)_{min.}$ is used in impedence formulas.

After these measurements and calculations all terms in equations (6.9) and (6.10) become known and results can be obtained.

6.3. EXPERIMENTAL WORK:

The specific acoustic impedance of a specimen of mineral wool with 2.45 cm thickness and 0.12 gm/cm^3 density has been measured at oblique and normal incidence in the large wave-guide.

The observed values of $R/\rho_0 c_0$ and $X/\rho_0 c_0$ for this specimen are given in figure (6.1). The angle of incidence is a function of $[f_c / f]$ and the values of f are also included in this figure where $(f_c)_{1,0} = 1204$ c/s.

If the velocity of sound in a porous medium is very low the impedance of the medium does not change considerably with the

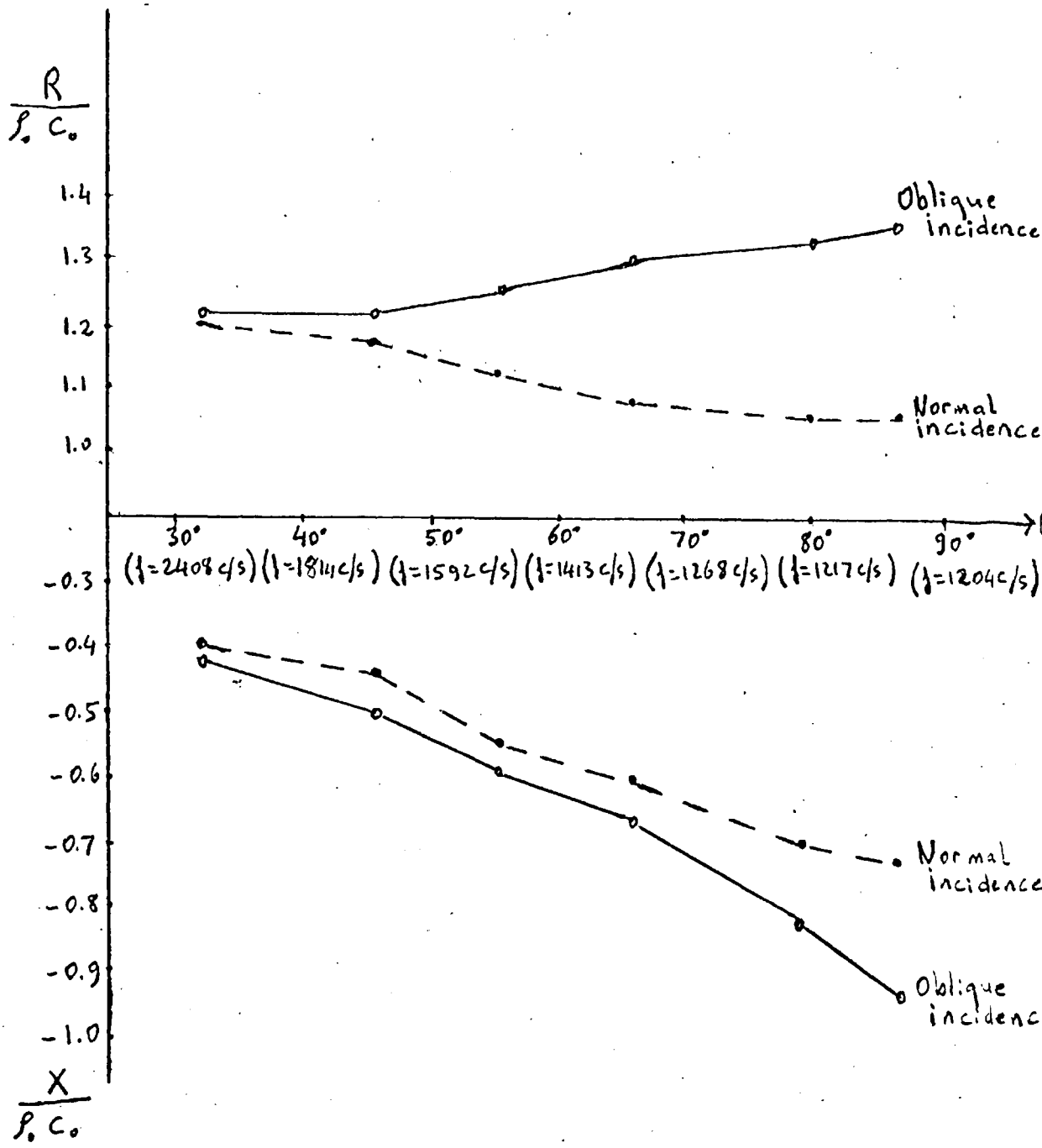
R / ρ₀ c₀
1.4
1.3
1.2
1.1
1.0
Oblique incidence
Normal incidence
30°
40°
50°
60°
70°
80°
90°
θ
(f=2408 c/s)
(f=1814 c/s)
(f=1592 c/s)
(f=1413 c/s)
(f=1268 c/s)
(f=1217 c/s)
(f=1204 c/s)
-0.3
-0.4
-0.5
-0.6
-0.7
-0.8
-0.9
-1.0
Normal incidence
Oblique incidence
X / ρ₀ c₀

Figure 6.1

angle of incidence. This condition is fulfilled at very low frequencies or in a medium with very fine pores. In this condition viscous forces are large compared inertial forces.

In mineral wool, at high frequencies the velocity of sound is nearly equal to its free value. Therefore, the impedance of this material gives an angle of incidence dependent impedance values. From figure (6.I) it can be seen that the impedance of the specimen at oblique incidence is different from the normal incidence impedance. The resistance ratio shows the greater divergence which was pointed out by Beranek.

CHAPTER VII

SOUND ABSORPTION BY POROUS MATERIALS.

7.I. INTRODUCTION. Sound absorption by porous materials is always a question of conversation of incident sound energy into heat. Lord Rayleigh showed that in porous materials sound was absorbed through the viscous and thermal conduction effects occuring in pores.

For plane waves, the mode impedance in the loss free case is

$$W_{0,0} = \rho_0 c_0 \qquad (7.1)$$

When acoustic absorption takes place in a material a parameter termed the absorption coefficient is used to define this acoustic property. It is defined as the ratio of the absorbed acoustic energy to the total acoustic energy incident on the given material.

For normal incidence the absorption coefficient of the specimen is given by:

$$A(0) = 1 - \left| \frac{Z(0) - \rho_0 c_0}{Z(0) + \rho_0 c_0} \right|^2 \qquad (7.2)$$

Z(0) is the impedance of the specimen measured at normal incidence.

If the measurements are carried out with a higher order modeat an angle of incidence θ, in the loss-free case, the mode impedance becomes:

$$W_{mn} = \frac{\rho_0 c_0}{\cos\theta} \qquad (7.3)$$

Paris[48] (I927), has obtained an expression for the absorption coefficient as a function of angle of incidence θ, i.e.

$$A(\theta) = 1 - \left| \frac{Z(\theta)\cos\theta - \rho_0 c_0}{Z(\theta)\cos\theta + \rho_0 c_0} \right|^2 \qquad (7.4)$$

where $Z(\theta)$ is the impedance of the specimen measured at an angle of incidence θ.

Sometimes the value of the absorption coefficient is wanted for random angles of incidence. This value can be measured directly by the reverberation method.[51] In a reverberant test room, the time of reverberation decreases when the absorbing sample is inserted. From the times of reverberation before and after the application of the sample, its coefficient of absorption for random angles of incidence can be calculated. The various absorption mechanisms can be divided into four main groups. These are:

a) Porous materils with rigid frame,

b) Porous materils with flexible frame,

c) Panel absorbers, and

d) Resonators.

Only rigid porous materials will be considered in this thesis, but a brief mention will be made about others.

The skeleton of a flexible material vibrates with the air borne sound and a separate elastic wave propagates in the skeleton. Therefore, the compression modulus of the frame is an important constant for such materials, apart from other parameters which will be given in the next section. The surfaces of these skeletons may be coated by a light and thin damping material, so the physical properties of the surface coatings are also important for their behaviour.

Light panel absorbers are usually mounted at some distan-

ce in front of a rigid wall and they will possess a resonance frequency at which the absorption has the highest value.

Perforated panels are also used and the main variables are the perforation and the thickness of the air layer. Perforations may be filled by another suitable absorbing material.

For further details about sound absorbing materials see Zwikker and Kosten[52] and Richardson.[53]

7.2. GENERAL EQUATIONS GOVERNING THE WAVE PROPAGATION IN A POROUS MATERIAL WITH A RIGID FRAME.

The acoustic parameters of rigid porous materials are:

a) Porosity (ξ),

b) Flow resistance (∇),

c) Structure factor (k).

a) Porosity is given by the ratio of the volume of accessible pores to the volume of the specimen. The porosity is independent of frequency and always less than unity. It can be measured directly by non-acoustic methods.

b) Flow resistance is the ratio of the pressure gradient, in the direction being considered, to the volume velocity in that direction where the volume velocity (U) is defined as the volume, crossing unit area perpendicular to surface per unit time. The flow resistance varies with frequency and can be measured by non-acoustic methods.

c) Structure factor depends on various parameters and is rela-

ted to the microscopic structure of the material. The factor varies with frequency, is always equal or greater than unity and is dependent on:

(i) The direction of the pores,

(ii) Existance of some closed pores,

(iii) Vibration of skeleton. This is small for rigid materials but can cause high values of k,

(iv) The influence of velocity distribution.

For many porous materials k has a value between one and two but is sometimes higher.

In the earlier papers various authors used a porosity and a flow resistance to specify the acoustic propertes of material. Zwikker and Kosten, have introduced a structure factor. When a microscopic volume of air in the material is subjected to an accelerating force, it may be constrained by the solid skeleton, to move in directions other than that of the force, so that the component of acceleration in that direction is less than if the air were unconstrained. Thus, air in the pores appear to have an increased inertial density. This increase is expressed in terms of a structure factor.

Zwikker and Kosten (1948) have introduced effective density (ρ) and effective bulk modulus (K) to replace all the other parameters of the porous materials.

In free air, in the loss free case ρ and K are real.

In a medium with internal damping, density variation is

no longer in phase with the pressure variation. This means $d\rho_0/dp$ is complex.

Equation of continuity is given by:

$$\nabla u = -\frac{\xi}{\rho_0}\frac{d\rho_0}{dp}\dot{p} \qquad (7.5)$$

The effective bulk modulus may be introduced by:

$$K = \frac{\rho_0}{\xi}\frac{dp}{d\rho_0} \qquad (7.6)$$

The equation of continuity may now be written in the simple form,

i.e. $$\nabla u = -\frac{1}{K}\dot{p} \qquad (7.7)$$

The equation of motion in an isotropic medium is given by [52]

$$-\nabla p = \frac{k}{\xi}\rho_0 \dot{u} + \nabla u \qquad (7.8)$$

The effective density may be introduced by:

$$\rho = \frac{k}{\xi}\rho_0 + \frac{\nabla}{j\omega} \qquad (7.9)$$

so, the equation of motion can be written in its simple form, i.e.

$$-\nabla p = \rho \dot{u} \qquad (7.10)$$

and, ρ becomes frequency dependent.

The effective bulk modulus and the effective density have limiting values. Assume a medium, composed of cylindirical capillaries. If η and L are defined as:

$$\eta = \left(\frac{\omega \rho_0 r_p}{\nu}\right)^{\frac{1}{2}} \qquad (7.11)$$

where, r_p: the pore diameter, and

$$L = \left(\frac{\nu}{\rho_0}\frac{\chi_p}{K}\right)^{\frac{1}{2}} \text{ (Prandtl Number)} \qquad (7.12)$$

Limiting values of K are found as follows:

If, $\eta L \ll 1$ i.e.

$$\left(\frac{\omega r_p \chi_p}{K}\right)^{\frac{1}{2}} \ll 1 \qquad (7.13)$$

then at very low frequencies or, $\left(K/\omega r_p\right)^{\frac{1}{2}}$ large compared with the pore diameter, K has the limiting value:

$$K = \frac{1}{\xi} \rho_0' \left[1 + j \frac{\chi - 1}{8\chi} (L\eta)^2\right] \cong \frac{\rho_0'}{\xi} \qquad (7.14)$$

If, $\eta L \gg 10$, i.e.

$$\left(\frac{\omega r_p \chi_p}{K}\right)^{\frac{1}{2}} \gg 10 \qquad (7.15)$$

then at very high frequencies, or $\left(K/\omega \chi_p\right)^{\frac{1}{2}}$ is small compared with the pore diameter, K has the limiting value:

$$K = \frac{1}{\xi} \chi \rho_0' \left[1 + \frac{2\sqrt{-j}(\chi - 1)}{L\eta}\right] \cong \chi \rho_0'/\xi \qquad (7.16)$$

At intermediate frequencies, the value of K can only be determined by measurement.

The variation of K with frequency is shown in figure (7.I)

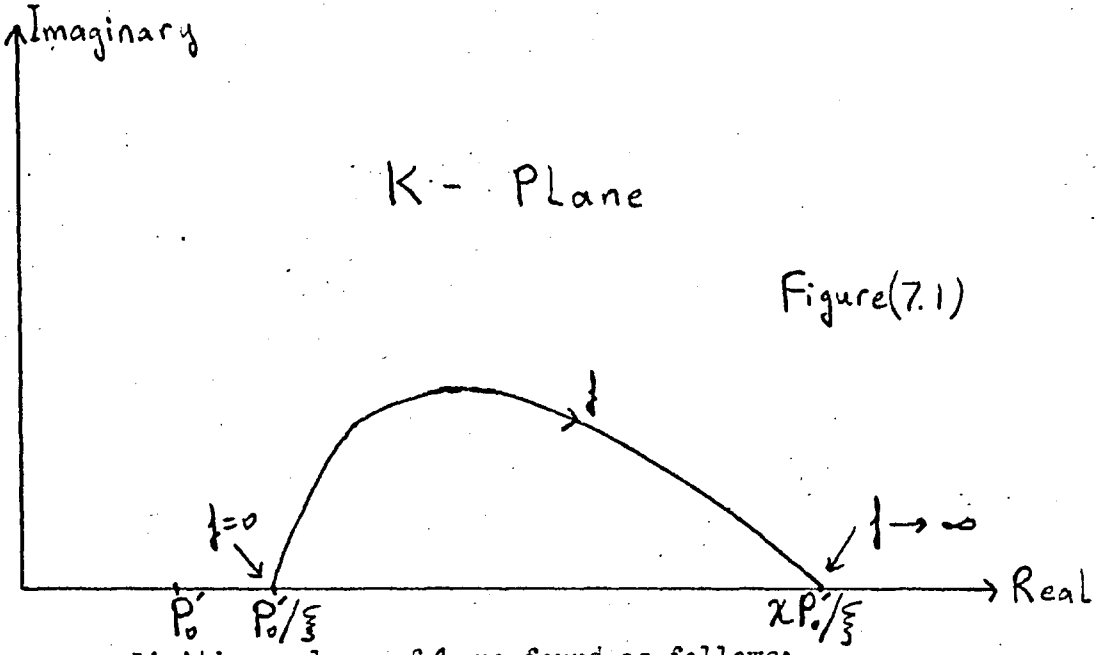

Figure(7.1)

Limiting values of ρ are found as follows:

If, $\eta \ll 1$ i.e. $\left(\frac{\omega \rho_0 r_p}{\mu}\right)^{\frac{1}{2}} \ll$ (7.16)

This means that at very low frequencies, or $(\mu/\omega\rho_0)^{\frac{1}{2}}$ is large compared with pore diameter, ρ has the limiting value:

$$\rho = \frac{k}{\xi}\rho_0\left[\frac{4}{3} - j\frac{8}{\eta^2}\right] \qquad (7.18)$$

This equation shows that, at very low frequencies, ρ is predominently imaginary.

If, $\eta \gg 10$, i.e.

$$\left(\frac{\omega\rho_0 r_p}{\mu}\right)^{\frac{1}{2}} \gg 10 \qquad (7.19)$$

This means that at very high frequencies, or $(\mu/\omega\rho_0)^{\frac{1}{2}}$ is small compared with pore diameter, ρ has the limiting value:

$$\rho = \frac{k}{\xi}\rho_0\left[1 + (1-j)\sqrt{\frac{2}{\eta}}\right] \simeq \frac{k}{\xi}\rho_0 \qquad (7.20)$$

Therefore, at very high frequencies ρ is real and motion is inertia controlled. Since, $k \gg 1$ and $\xi \ll 1$ the values of ρ at very high frequencies is greater than ρ_0.

The nature of the frequency dependence of ρ is shown in figure (7.2).

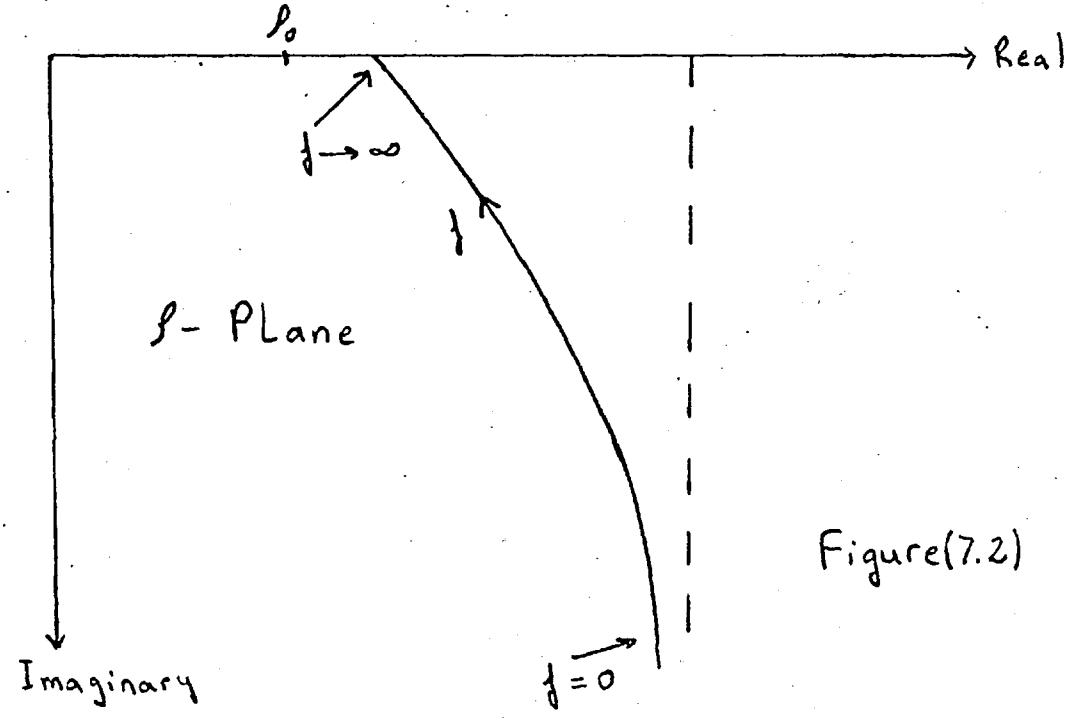

Figure(7.2)

The above values of ρ and K have been derived for a medium composed of cylindirical capillaries. Campbell,[54] has done the calculations for a medium composed of parallel plates.

ρ and K in fact depend on various properties of practical materials so that mathematical analysis can only be qualitative.

7.3. PROPAGATION CONSTANT AND WAVE IMPEDANCE OF A MEDIUM IN TERMS OF EFFECTIVE DENSITY AND EFFECTIVE BULK MODULUS. The impedance of a layer of a specimen, backed by a rigid material may be written in terms of its wave impedance (W) , propagation constant (γ) and its thickness. Hence, W and γ determine acoustical behaviour of a medium alternatively ρ and K. Regarding ρ and K as fundamental material constants and applying the equation of motion and equation of continuity for the vibrating air, one can find values of W and γ in terms of ρ and K.

These values are given by:

$$\gamma = \alpha + j\beta = j\omega\sqrt{\frac{\rho}{K}} \qquad (7.21)$$

and,

$$W = \sqrt{\rho K} = \rho c \qquad (7.22)$$

The velocity of acoustic waves in the medium is:

$$c = \sqrt{\frac{K}{\rho}} \qquad (7.23)$$

From these three equations ρ, K and c can be found. Since ρ and K are complex, c is also complex.

7.4. EXPERIMENTAL WORK:

The absorption coefficients of the mineral wool and an artifical sample have been measured at normal and oblique angles of incidence. The results of measurements with mineral wool are shown in figure 7.3. At angles of incidence near to the normal only a small divergence from the normal value is found for the absorption coefficient which was expected. At higher angles (above 80°), because of the $\cos\theta$ term in equation (7.4), the absorption coefficient has small values.

An artifical sample was made from perforated zinc metal. 30 plates were held together by four rods with a distance of about 0.2 mm. The measured absorption coefficient at normal and oblique incidence is shown in figure 7.4. Because of the high anisotropy of this medium, its absorbing properties was different from the normal incidence value.

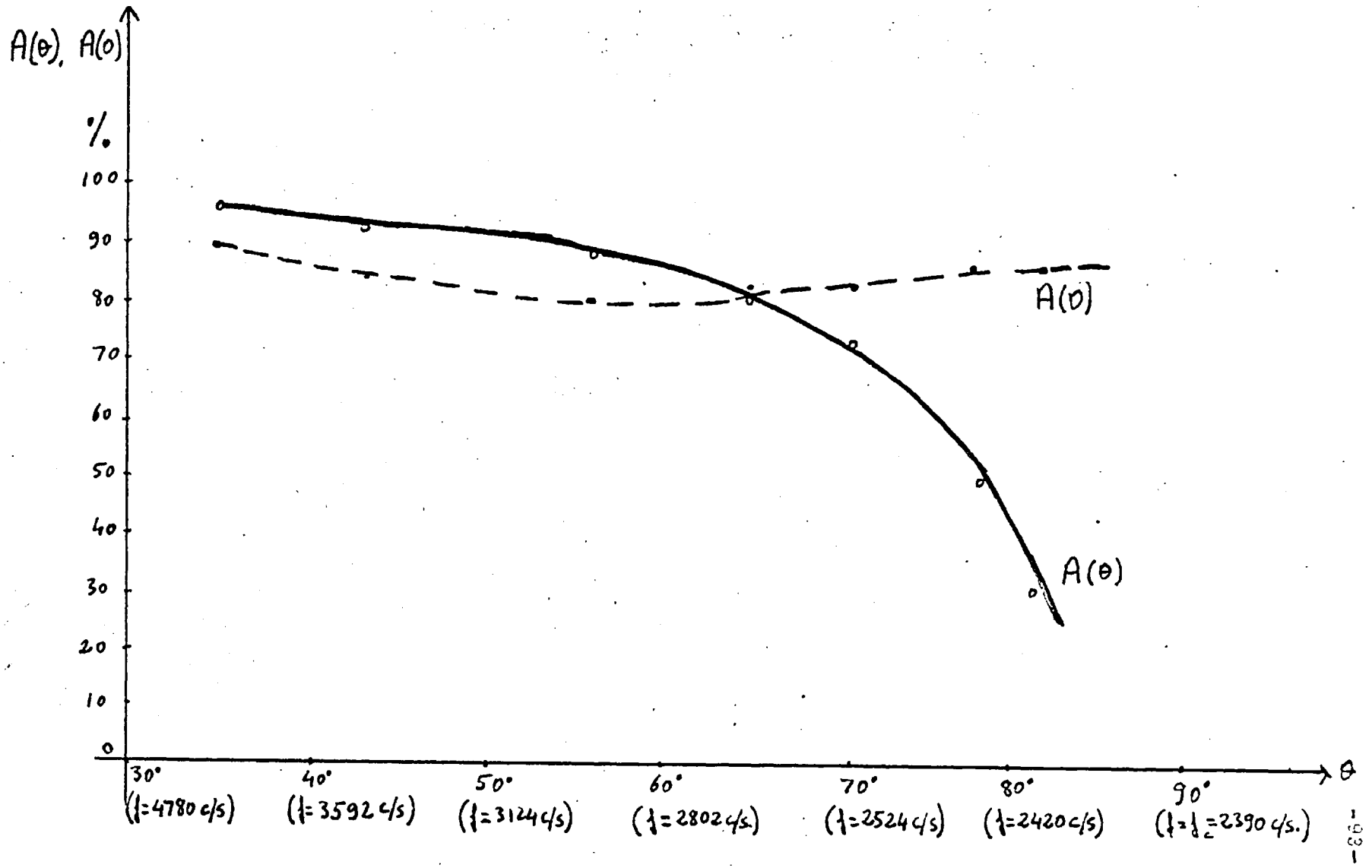
A(θ), A(0)
%
100
90
80
70
60
50
40
30
20
10
0
A(0)
A(θ)
θ
30°
(f=4780 c/s)
40°
(f=3592 c/s)
50°
(f=3124 c/s)
60°
(f=2802 c/s)
70°
(f=2524 c/s)
80°
(f=2420 c/s)
90°
(f=f_c=2390 c/s.)

Figure 7.3

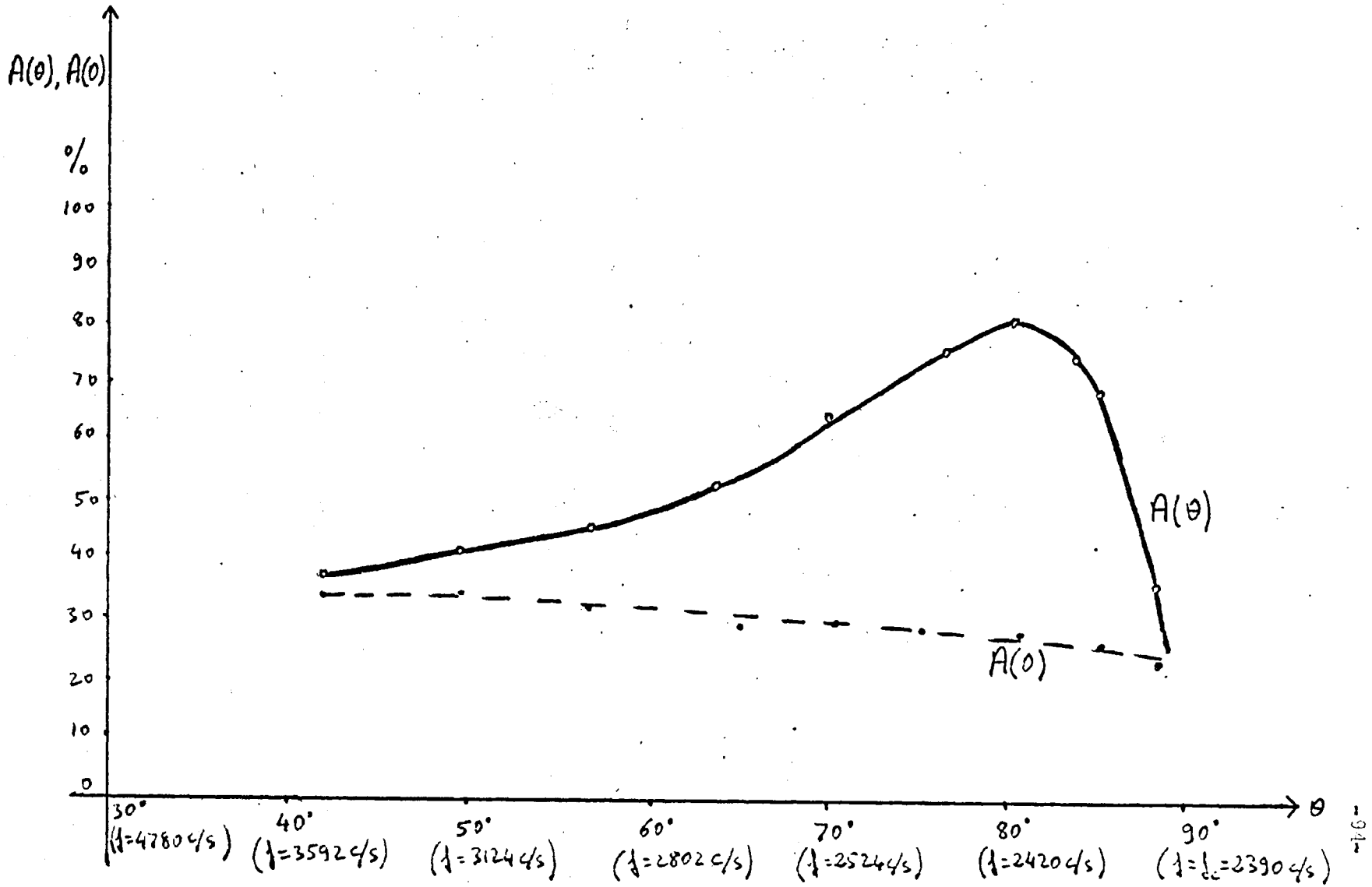
A(θ), Ā(θ)
%
100
90
80
70
60
50
40
30
20
10
0
A(θ)
Ā(θ)
θ
30°
(f=4780 c/s)
40°
(f=3592 c/s)
50°
(f=3124 c/s)
60°
(f=2802 c/s)
70°
(f=2524 c/s)
80°
(f=2420 c/s)
90°
(f=f_cc=2390 c/s)

Figure 7.4

CHAPTER VIII

PRESSURE-RELEASE MATERIALS UNDER HIGH HYDROSTATIC PRESSURES:

Elementary consideration of impedance tells us that reflection will occur if sound waves in one medium strike the boundary with another medium if there is a difference of characteristic impedance.

Therefore, to obtain a good reflector the first condition to be fulfilled is a large difference of characteristic wave impedances of the two adjoining media, i.e. water and reflector.

In the case of water/water or water/solid insulation, insulators which have a sufficiently high impedance are not available and a reflector which has a low impedance is needed. These low impedance materials are the so-called "pressure-release materials".

The amplitude reflection coefficient R_a for sound waves in water incident normally on a reflecting layer,[55]

$$\frac{\sqrt{1-R_a^2}}{R_a} = \frac{M_d}{\pi d f \rho_w c_w} \qquad (8.1)$$

where d : thickness of the layer,

c_w : velocity of sound waves in water,

f : the frequency of the sound waves, and

M_d : the dynamic elastic modulus of the layer.

It follows from equation (8.I) that,

$$R_a = \frac{\pi d f \rho_w c_w}{\sqrt{M_d^2 + (\pi d f \rho_w c_w)^2}} \qquad (8.2)$$

The medium is pure water, therefore, $\rho_w c_w$ is constant and

independent of frequency. Frequencies up to 6 Kc/s were used.

Therefore, the dynamic elastic modulus and the thickness of the layer are the most important parameters concerned in the achievement of good reflection. The thickness of the reflector is limited by practical considerations.

It follows, therefore, that a good reflector should possess a low dynamic elastic modulus.

The dynamic elastic modulus of the materials are given by

a) For solid medium

$$M_d = K_m + \frac{4}{3} \nu_m \qquad (8.3)$$

where K_m: the dynamic bulk modulus of the material,

ν_m : the rigidity coefficient of the material.

The lowest value of M_d for solids is not less than some 10^{11} dyn/cm.^{2}

b) For liquid medium: Liquids do not have value of M_d less than some 10^{10} dyn/cm.^{2}

c) For gas medium: The value of M_d increases with pressure and is given by:

$$M_d = \chi P \qquad (8.4)$$

where χ: ratio of principal specific heats,

P: pressure.

For air $\chi = 1.4$ and when the pressure is equal to 20 atms., which corresponds to 200 m. of water, the value of M_d becomes:

$$(M_d)_{air} = 2.8 \times 10^7 \ \text{dyn/cm}^2 .$$

In order to obtain a reflection coefficient of 97% or more in wa-

ter at a frequency of 3 Kc/s and a pressure of P= 20 atms. (From equ.8.1):

$$\frac{M_d}{d} \leq 3.5 \times 10^8 \ \text{dyn/cm}^3. \qquad (8.5)$$

where d is in cm.

From the above relation, it may be deduced that to use a metal or liquid as an efficent reflector requires a very thick layer of about 100cm. which is not a reasonable value in practice.

It is, therefore, necessary to use a layer which contains gas.

In the case of air-filled sponge with negligible skeletal stiffness at a pressure of 20 atms. and at a frequency of 3 Kc/s, $\frac{M_d}{d} = 2.8 \times 10^7$ dyn/cm^2 for air, thus, equation (8.5) can be fulfilled for layer thicknesses down to about 0.1 cm.

The range of critical thickness for different pressures and frequencies is illustrated in the table (8.I). The large variation of critical thicknesses with pressure is inconvenient in practice and alternative means must be adopted.

One procedure which can be adopted is to use a solid reflector which has pores filled with air. The stiffness of the reflector will no longer be small and the dynamic elastic modulus is necessarily greater than that for the air itself. This increase in M_d will involve slightly greater layer thickness to maintain a constant value of the reflection coefficient but the layer will have adequate resistance to high hydrostatic pressures.

A suitable material to satisfy the above conditions is

Frequency	Pressure	Critical Thickness
500 c/s.	1 atm.	9.4 cm.
	20 atms.	4.7 mm.
1 Kc/s.	1 atm.	5.6 cm.
	20 atms.	2.8 mm.
2 Kc/s.	1 atm.	2.4 cm.
	20 atms.	1.2 mm.
3 Kc/s.	1 atm.	2.0 cm.
	20 atms.	1.0 mm.
4 Kc/s.	1 atm.	1.2 cm.
	20 atms.	0.6 m.m.
5 Kc/s.	1 atm.	1.0 cm.
	20 atms.	0.5 m.m.
6 Kc/s.	1 atm.	0.8 cm.
	20 atms.	0.4 m.m.

Table 8.1

foamed rubber or stiff plastic containing air and will therefore, be suitable as reflector material in deep water.

However, the escape of air from the reflector and penetration of water into the reflector under high hydrostatic pressures has to be avoided. Hence the reflecting materials should possess closed pores.

Bocker[56] (I96I), has done work on pressure-release reflectors and found that among the tested samples, cellular rubber with closed pores had the best reflecting properties at the pressures from zero to 20 atmospheres.

Another important application of equation (8.2) relates to the reflection, in water, of sound waves from a thin film of air. If the thickness of this air film is 0.I cm. and it is enclosed between thin metal plates, from equation (8.2) it is found that the air film reflects at 20 atms. pressure above 95% of the incident energy at low frequencies. A possible pressure-release medium can be formed, therefore, from ribbed metal sheet(figure8.I) As a result of the flexibility of the sheets between ribs, the sample can be used at high hydrostatic pressure in the water.

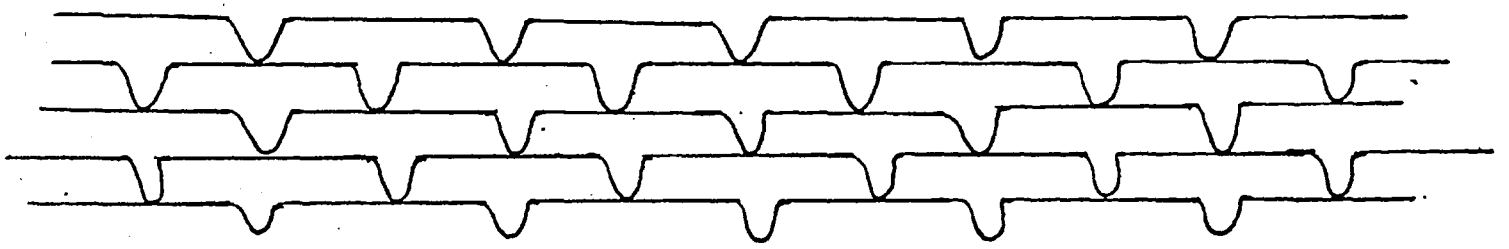

Atmospheric Pressure

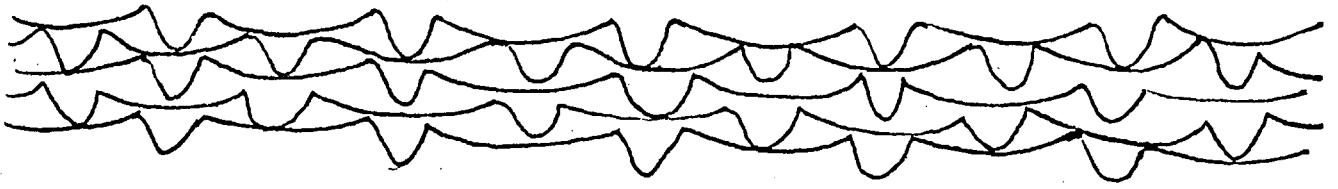

Compressed

Figure 8.1

CHAPTER IX

LIQUIDS IN CYLINDIRICAL TUBES WITH HARD WALLS.

In order to investigate the reflecting properties of materials under high hydrostatic pressures, it is necessary to use a measurement chamber and this may be conveniently provided by a closed rigid steel tube containing a water column, at one end of which is situated the test specimen.

The agreement between the analytical and experimental results of Fay, Brown and Fortier[57] indicates that a water filled tube is practicable for use in measuring the impedance of underwater acoustic materials.

In air acoustics, it is relatively easy to obtain an enclosure with rigid walls, that is, with walls whose specific acoustic impedance is large compared with that of air and, therefore, it can be that no energy is transferred from the sound field to the solid enclosure. For sound propagation in water, in fact, no practical boundary can be assumed to be completely rigid, since the specific acoustic impedance of the walls of the tube cannot be assumed very large compared with that of water.

Therefore, relatively thick walls are necessary to provide sufficiently rigid boundaries for the water column in the tube.

It has been shown that for the case of forced vibrations of a fluid, contained in a cylindirical tube, the waves become plane if:

$$\frac{c_w}{f} \geq 3.413 \times D \qquad (9.1)$$

where D : internal radius of the tube,

c_w : velocity of sound in the fluid and

f : the frequency.

Below this frequency, the sound waves in the tube are plane.

The yielding of the tube near the liquid nodes results in a lowering of the wave-velocity in the liquid. H. Lamb has shown that the relationship between velocity of sound in the tube, thickness of the tube walls and inside diameter of the tube is given by:[58]

$$c_{free} = c_{actual} \left(1 + K_m D / d_t E\right)^{\frac{1}{2}} \qquad (9.2)$$

where E: Young's modulus for the material of the tube,

K_m : volume elasticity of the liquid,

c_{free} : the velocity of sound in the free liquid,

c_{actual} : actual velocity of sound in the tube,

d_t : thickness of the tube walls.

At frequencies within the audible range, the resonance within the liquid can be heard by ear. Figure (9.I) shows the reduction of sound velocity in a steel tube filled with water.[59] It can be seen that (as Helmnoltz had predicted and from equation (9.2)), the actual velocity of sound in the tube increases with increase in the thickness of the tube walls and with decrease in the diameter of the tube.

In order to make measurements in liquid filled tubes it

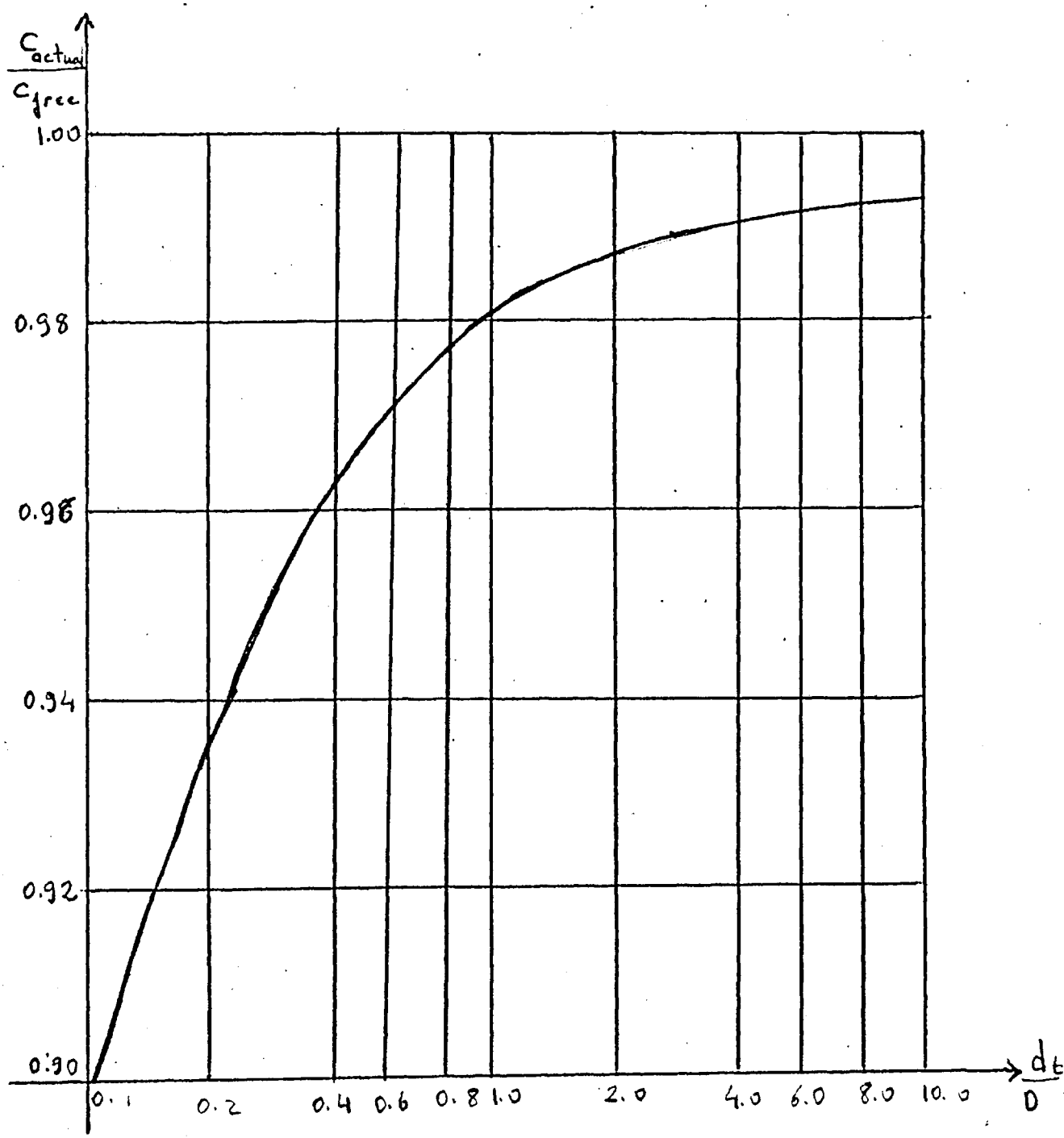
C actual / C free
1.00
0.98
0.96
0.94
0.92
0.90
0.1
0.2
0.4
0.6
0.8
1.0
2.0
4.0
6.0
8.0
10.0
dt / D

Figure 9.1

is essential to remove any dissolved air from the water in the tube, so that when the temperature or pressure changes, no air bubbles are released. The presence of air bubbles can modify appreciably the velocity of sound waves in water.

The dissolved air can be removed by heating the water or by pumping out the air from the space between the water and the top plate of the tube using a vacuum pump.

CHAPTER X

CHOICE OF METHOD OF MEASUREMENT AND DETERMINATION OF THE SPECIFIC ACOUSTIC IMPEDANCES USING THE METHOD OF THE RESONANCE ANALYSIS.

IO.I. CHOICE OF METHOD OF MEASUREMENT:

To investigate the reflecting properties of materials under hydrostatic pressures necessitates a measurement chamber which is closed and of moderate size. Because of this, the method of measurement must be chosen from the standard impedance tube techniques i.e.

a) Progressive wave or pulse,

b) standing wave,

c) Resonance analysis.

The pulse technique, which requires several wavelengths within the tube, is not applicable to this experiment. The reasons are:

(i) Limited length of the impedance tube,

(ii) Low audible frequencies will be used.

A standing wave pattern requires a moving sound probe or a telescopic tube which may lead to measuring difficulties especially at high hydrostatic pressures.

Therefore, the resonance method was adopted in this experiment. This method has also the advantage of causing the least mechanical troubles.

In the case of resonance analysis method, the resonance

frequencies of the water column, contained in the tube, and the bandwidths are measured for each of the modes in the desired frequency range. From these readings, the real and imaginary parts of the terminating impedance can be derived (see the next section).

Pooler[60]'s work indicated that the resonance curves are very sharp when there is a free water surface to air at the top of the tube.

10.2. DETERMINATION OF THE SPECIFIC ACOUSTIC IMPEDANCES USING THE METHOD OF THE RESONANCE ANLYSIS.

When the source of sound is at one end of the impedance tube and the sample under test is located at the opposite end, if the lateral dimensions are sufficiently small, the sound field can be represented by two plane waves travelling in opposite directions in the tube.

It has been shown that the dissipation constant k_t is made up of two components k_m and k_{na} where k_m is the damping constant of the sample under test and k_{na} is the damping due to the tube-wall losses e.t.c.[61,62].

i.e. $$k_m = k_t - k_{na} \qquad (10.1)$$

$$k = \pi (f'' - f') \qquad (10.2)$$

where f'' and f' are the frequencies on either side of the resonance at which the sound pressure is 3 dB. down from the resonance value. Hence, measurements of the bandwidths of resonance peaks, with and without sample in position give values of k_t and k_{na} respectively and

hence k_m. Therefore, the specific acoustic impedance of the termination may be determined by obtaining two resonance curves, one with the material in place and another without the material.

The specific acoustic impedance at the surface of the sample under test is given by:

$$\frac{Z}{\rho_w c_w} = C\coth(\psi_1 + j\psi_2) = \frac{R}{\rho_w c_w} + j\frac{X}{\rho_w c_w} \qquad (10.3)$$

where Z : specific acoustic impedance of the sample,

$\rho_w c_w$: characteristic impedance of the medium,

$R/\rho_w c_w$: resistance ratio for the sample,

$X/\rho_w c_w$: reactance ratio for the sample.

Then,

$$\frac{R}{\rho_w c_w} = \frac{\tanh\psi_1(1+\tan^2\psi_2)}{\tanh^2\psi_1 + \tan^2\psi_2} \qquad (10.4)$$

and

$$\frac{X}{\rho_w c_w} = \frac{\tan\psi_2(1-\tanh^2\psi_1)}{\tanh^2\psi_1 + \tan^2\psi_2} \qquad (10.5)$$

For high values of impedance ψ_1 and ψ_2 less than 0.1, the following relations may be used:

$$\frac{R}{\rho_w c_w} = \frac{\psi_1(1+\psi_2^2)}{\psi_1^2 + \psi_2^2} \qquad (10.6)$$

$$\frac{X}{\rho_w c_w} = \frac{\psi_2(1-\psi_1^2)}{\psi_1^2 + \psi_2^2} \qquad (10.7)$$

where

$$\psi_1 = \frac{k_m l}{c_w} \qquad (10.8)$$

$$\psi_2 = \frac{2\pi f_0}{c_w}\left[\frac{m c_w}{2 f_0} - l\left(1 - \frac{k_t^2}{4\pi^2 f_0^2}\right)\right] \qquad (10.9)$$

where f_0 : the resonance frequency,

c_w: velocity of sound in the water in the impedance tube,

m: an integer, equal to the number of one-half wave-lengths in the tube,

ℓ : the length of the tube (measured from the sample to the sound source).

In order to determine the impedance of sample in the tube, we must first find the values of Ψ_1 and Ψ_2.

CHAPTER XI

EXPERIMENTAL WORK.

II.I. THE APPARATUS OF THE WATER FILLED CYLINDRICAL TUBE EXPERIMENTS:

The apparatus which has been used in this experiment is shown in figure (II.I) and figure (II.2). Impedance tube should have a ratio of wall thickness to inside diameter as large as possible. It is also necassary to choose a tube which has an inside diameter large enough to accommodate a suitable test material.

An impedance tube which has a length of 305 cm. has been used for this experiments. It is a cadmium plated steel tube of wall thickness I.6 cm. and I0.8 cm. internal diameter. From equation (9.1), the frequencies up to 7 Kc/s can be used to produce plane sound waves in this tube.

Equation (9.2) and figure (9.1) shows that the velocity of sound in the contained water is constant under same conditions but less than the velocity of sound in the free water. The sound velocity in the tube, therefore, is about 95% of the free velocity.

There is an extra 30.5 cm. tubing and it may be bolted to the main tube, if wanted. In this experiment, the main tube has been used only, and from the length of the tube, it appears that the fundamental quarter-wavelength resonance should occur at the frequency about I20 c/s and the higher order resonances should be sepe-

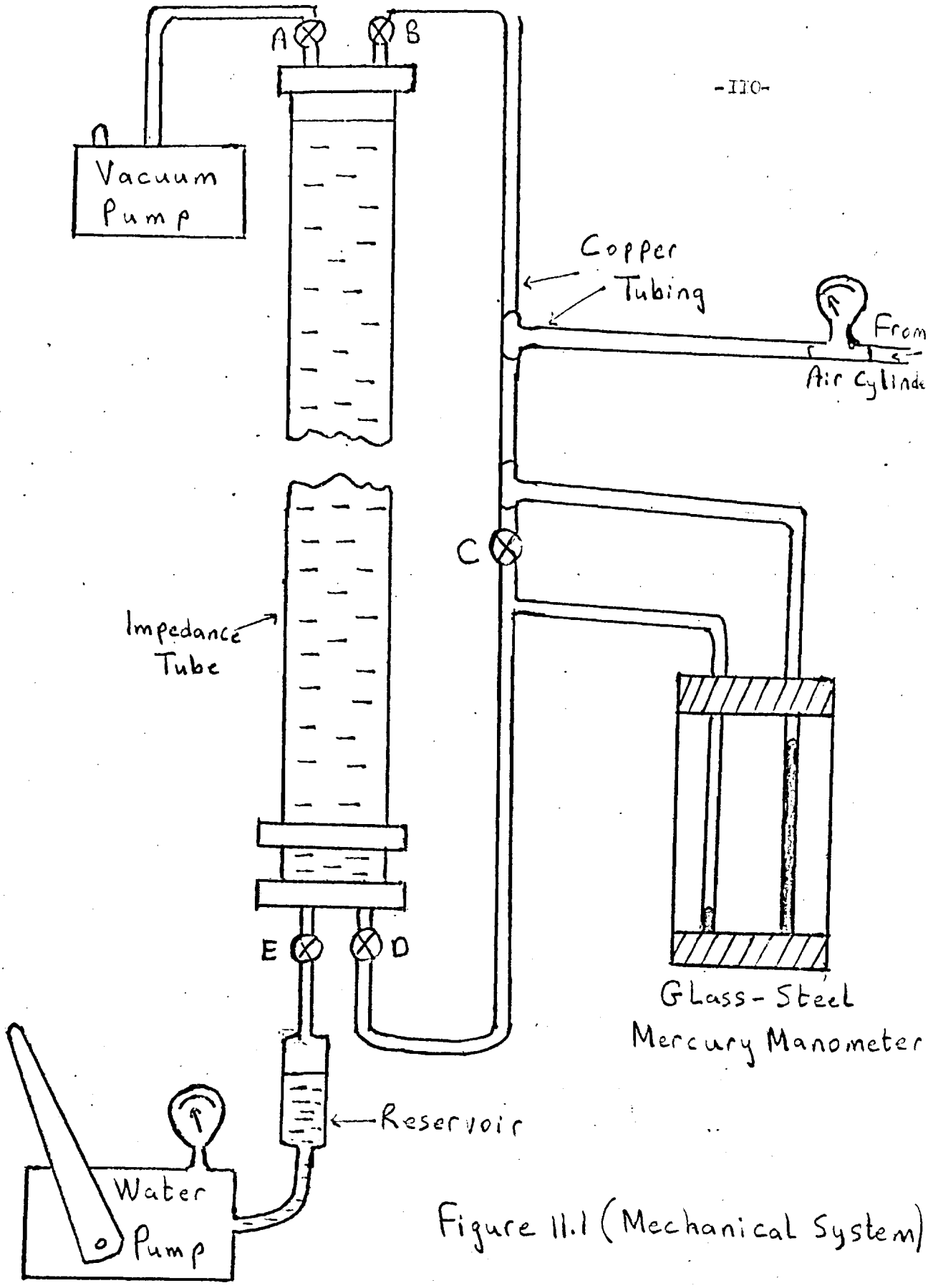

Figure 11.1 (Mechanical System)

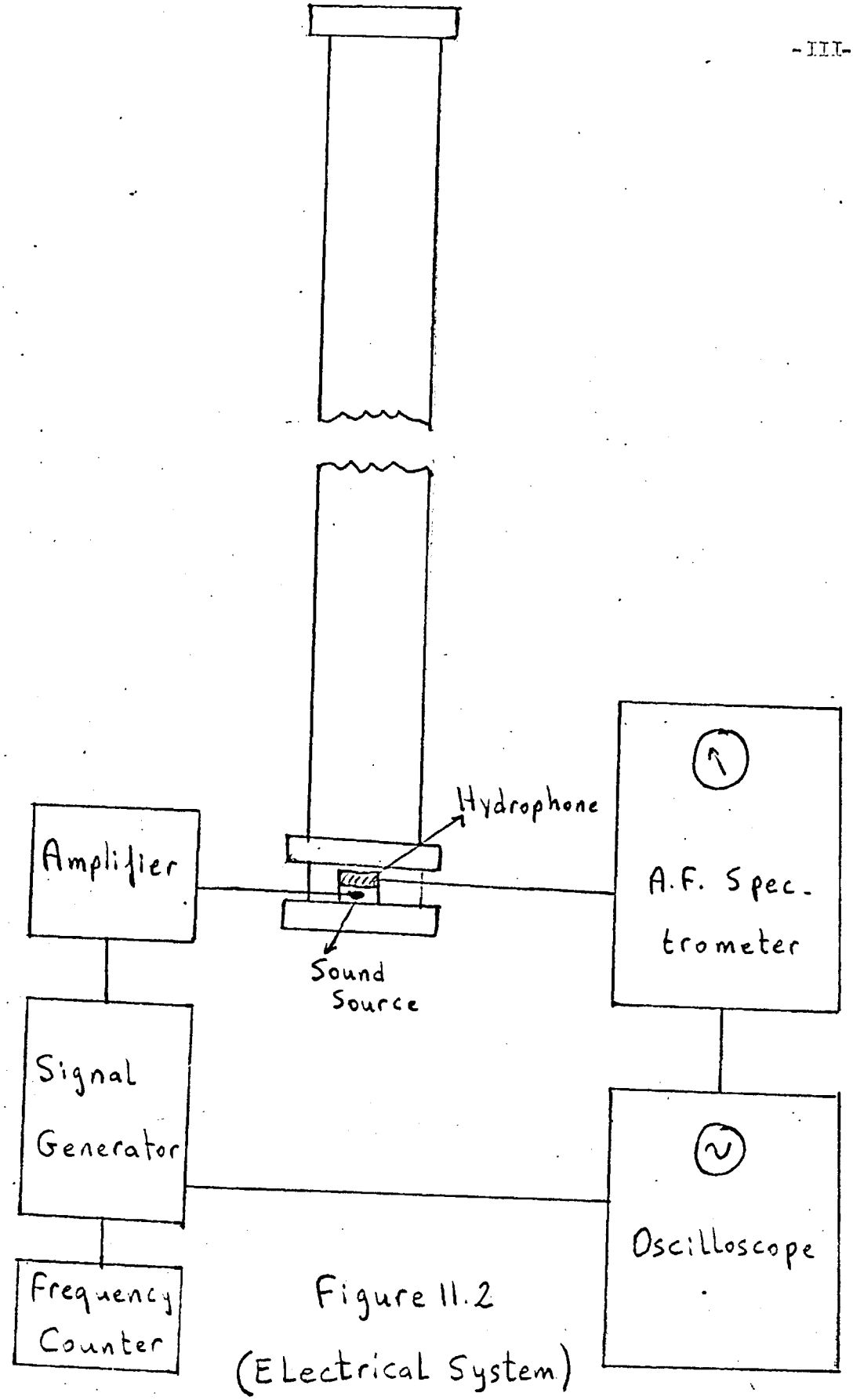

Figure II.2

(ELectrical System)

rated by about 240 c/s.

A permanent fixture to support the tube was built and it was fixed in a vertical position. (see figure II.3). There are two steel end plates which are 5 cm. thick and they can be bolted to flanges screwed on to the bottom and the top ends of the tube. (see figure II.4 and figure II.5). Each of the end plates has two taps. (A) is used to de-gas the water using a vacuum pump and (B) is used to apply pressure to the water column. (E), when open, is employed to apply a balancing pressure to the water column at atmospheric pressure. (D) is opened when it is required to apply a balancing pressure when the water column is itself subjected to an additional external pressure (via B).

The hydrophone is put on the internal rubber diaphragm which is at the bottom of the water column. This diaphragm prevents coupling of the tube walls and the transducers and there is an air cavity under this diaphragm.

The sound source is not rigidly connected to the tube walls or end plate, in order to keep the direct excitation of the tube walls to a minimum.

The joints are sealed with O-rubber rings, therefore, the water and pressurized air cannot come out from the tube.

By using a hand operated water-pump, the air space below the diaphragm could be compressed. A pressure equivalent to the

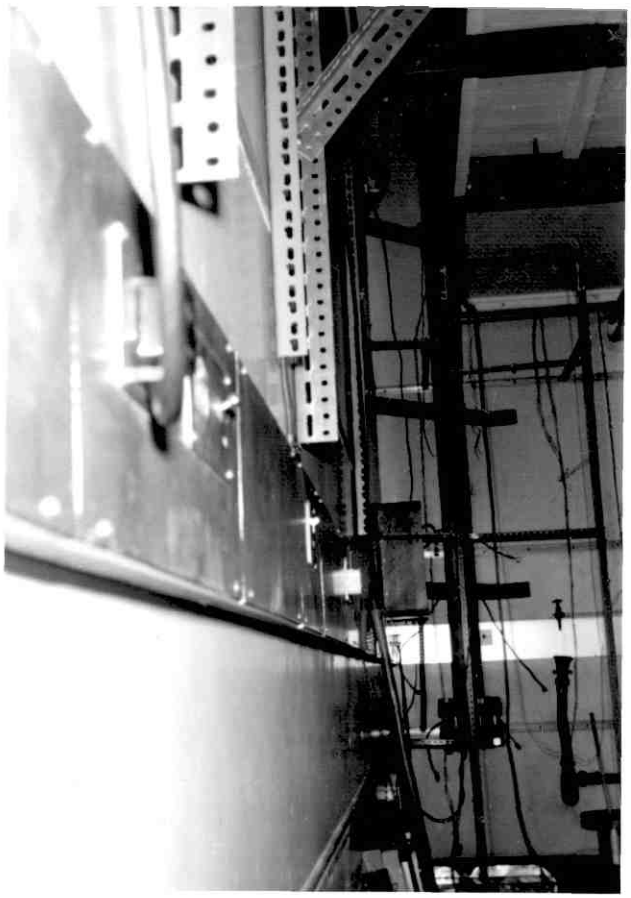

Figure II.3

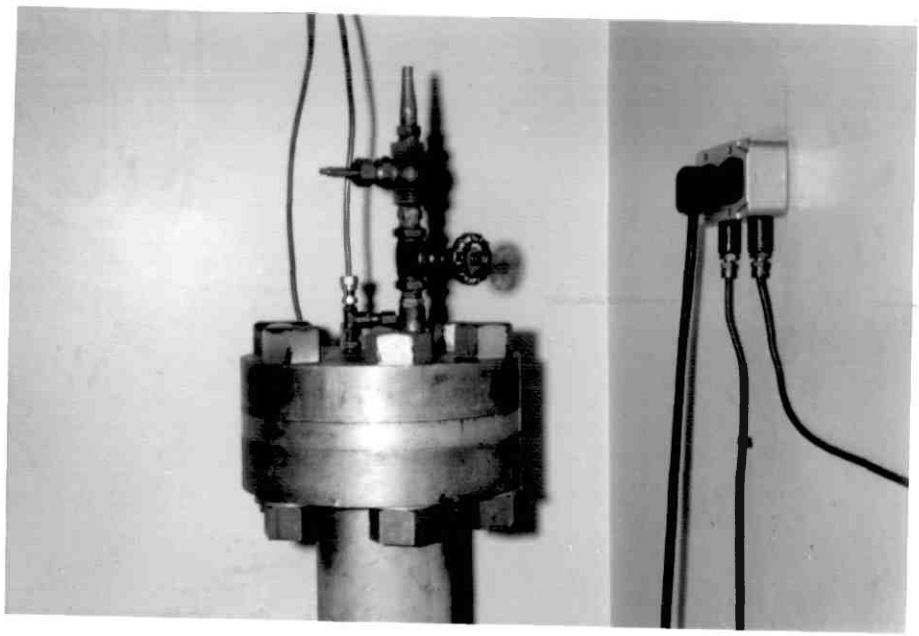

Figure 11.4 (Top end)

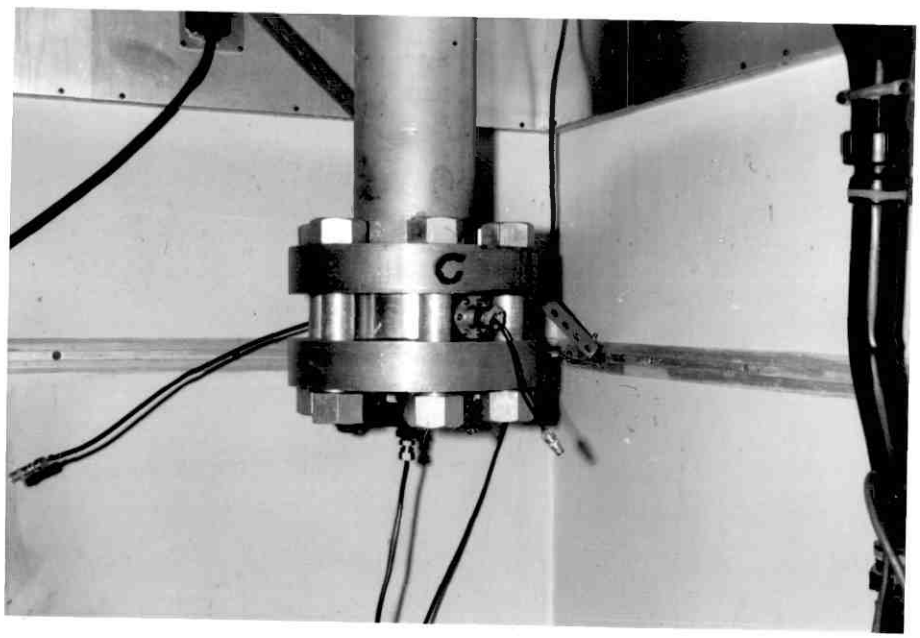

Figure 11.5 (Bottom end)

contained water column pressure could be obtained to balance the downward pressure on the upper side of the diaphragm. The value of this balancing pressure is measured by a glass-steel mercury manometer.

A vacuum-pump was used to de-gas the contained water.

The pressure on the top of the water column which now filled the tube could be increased by opening (B) to connect with a gas cylinder under pressure; at the same time, the (D) was also opened so as to maintain the pressure balance on the diaphragm. In this operation, (A) and (E) are closed and (C) is opened.

The electronic equipment consists of a AF Signal Generator and power amplifier to drive the sound source and an AF Spectrometer with a Cathode Ray Oscilloscope to detect the hydrophone signal. The input signal from the generator was also displayed on the screen of the Oscilloscope to ascertain the waveform.

The sound source was a barium titanate sphere, 2.5 cm. in diameter. The hydrophone was constructed by using lithium sulphate crystals 2.5 cm. in diameter by 0.9 cm. thickness. They were lightly clamped inside a cylindrical brass case 3.6 cm. in diameter by 3.7 cm. deep. This was then filled with castor oil and sealed with a stout rubber diaphragm. A length of co-axial out-put cable was sealed through the case.

Details about the AF Signal Generator and the AF Spectrometer have been given in chapter III.

A Venner counter has been used to read the frequency more accurately which was necessary because of the sharpness of the resonances.

II.2. MEASUREMENTS AND RESULTS:

In the first instance, The hydrophone and the sound generator were mounted in the bottom of the tube with both end plates closed. The manometer and water pump were connected to the tube by the copper tubing. With tap (A) open, the tube was filled by water. With only tap (A) open, using the vacuum pump, the water column in the tube was de-gassed. Tap (A) was then maintained closed for the rest of the experiment.

Then, tap (E) and tap (D) were opened and tap (C) was closed. Using the water-pump, an excess air pressure was produced under the rubber diaphragm. This pressure was increased until it became equal to the water column pressure and the value of this pressure was read by the manometer. By this means, the rubber diaphragm was maintained horizontal.

The electronic circuit was connected as shown in figure (II.2). To minimise background noise, the cables used were made as short as possible.

The system was left undisturbed for a day , for each measurement to ensure that thermal equilibrium was established. With the upper water surface free, measurements were made to find the water column resonance frequency and bandwidth for every mode.

As expected, sharp water column resonances with frequency intervals of about 240 c/s have been obtained. The frequency of resonances were very close to their theoretical values with a Q (i.e. quality factor) of about 300.

The Q of resonances have been calculated and a plot of Q against frequency is given in figure (II.6)

One particular resonance curve has been plotted in figure (II.7).

It is most desirable to minimise coupling between tube ends and the water column and, hence, a brass cylinder was suspended from the upper end plate of the tube. The test specimens were mounted on this brass-cylinder which was 5 cm. thick and I0.2 cm. diameter.

The measurements then were made using brass-cylinder with attached samples, in terms of the change in resonance frequency and bandwidth caused by the presence of samples.

It was shown in chapter X that the specific acoustic impedance of the sample can be determined by obtaining two resonance curves, one with the sample in place and another without the sample. Therefore, resonance curves have been obtained for the samples to determine their specific acoustic impedances at the frequencies from 3.5 Kc/s to 5.5 Kc/s and at hydrostatic pressures from zero to 25 atmospheres.

Using the equations (10.1), (10.2), (10.3), (10.4), (10.5), (10.8)

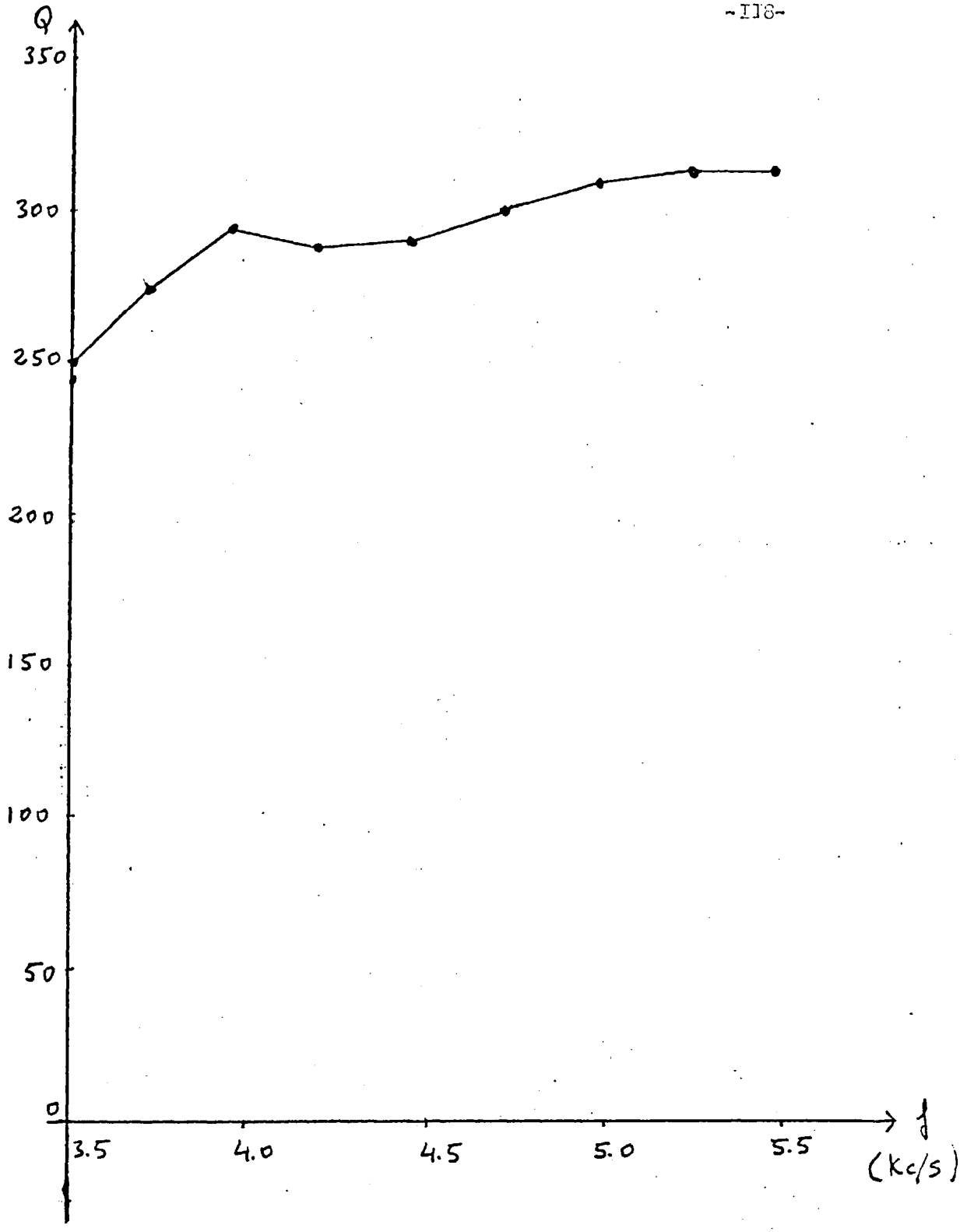

Figure 11.6

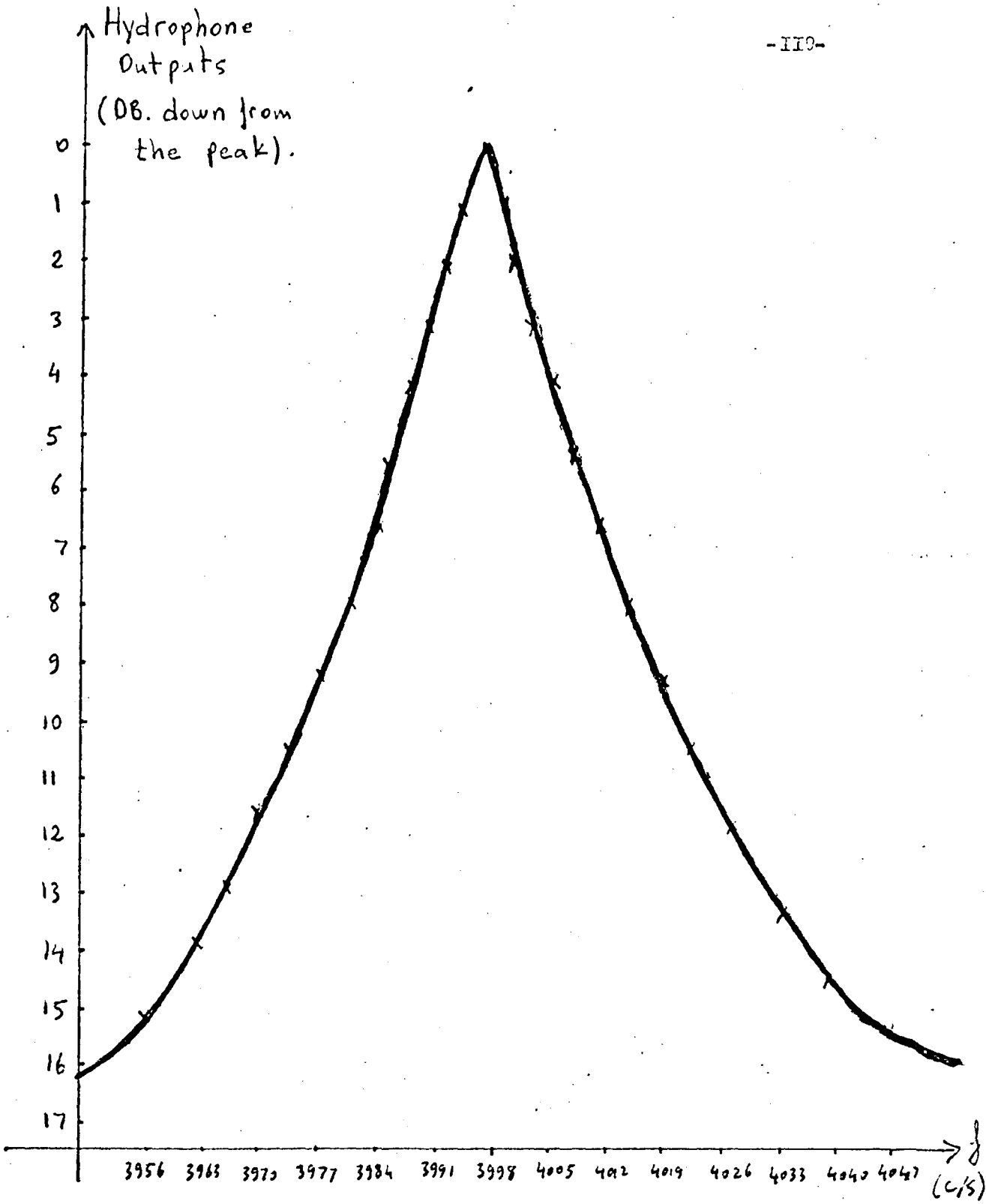
Hydrophone Outputs (DB. down from the peak).
0
1
2
3
4
5
6
7
8
9
10
11
12
13
14
15
16
17
3956
3963
3970
3977
3984
3991
3998
4005
4012
4019
4026
4033
4040
4047
f (c/s)

Figure 11.7

and (10.9), the resistance and reactance ratios of the materials, have been calculated.

From the values of resistance and reactance ratios of the materials, the reflection coefficient of the materials can be found from the equation:

$$R = \left| \frac{\frac{Z}{\rho_w c_w} - 1}{\frac{Z}{\rho_w c_w} + 1} \right|^2 \qquad (11.1)$$

The Samples:

(a) Closed Rubber Tubes (Thick Walled): Five rubber tubes of I.25 cm. in outside diameter were sealed on a circular rubber sheet which was 0.I cm. in thickness and had the same value of diameter as brass-cylinder. (see figure II.8). The wall thickness of the rubber tubes was 0.47 cm. and they were clamped at both ends to prevent the escape of air and the penetration of water into the tubes.

The sample was backed by the brass-cylinder and immersed in the water. From the readings, two resonance curves have been obtained at atmospheric pressure and IO atmospheres. By the aid of these two curves and the water column resonance curve with free surface to air, the resistance and reactance ratios against frequency for this sample have been calculated and plotted in figure (II.9). Variation of reflection coefficient against hydrostatic pressure has also been calculated for this material and plotted in figure (II.IO). Reflection coefficient against frequency of this sample

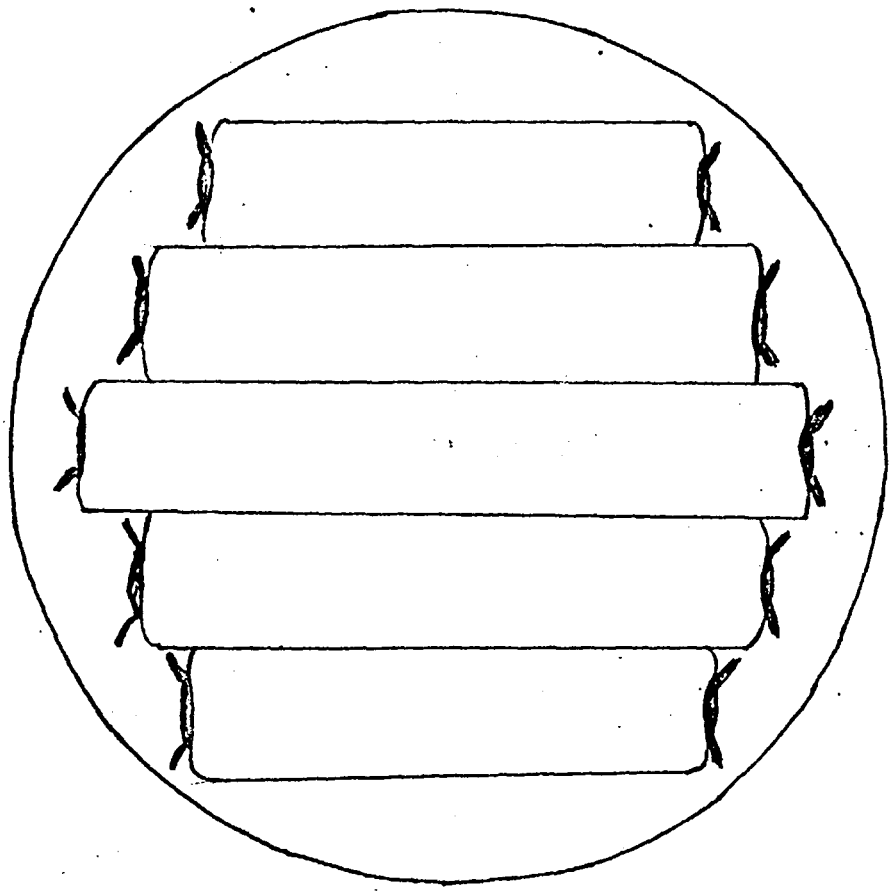

Figure 11.8

at zero and IO atmospheres hydrostatic pressures have been plotted in figure (II.II).

(b) Closed Rubber Tubes (Thin Walled): A similar sample as with the thick walled rubber tubes were used, the tubes having 0.24 cm. wall thickness.

Similar measurements were made on this sample and resistance and reactance ratios against frequency for this sample have been plotted in figure(II.I2). Variation of reflection coefficient agains hydrostatic pressure is shown in figure (II.I3). Reflection coefficient against frequency for this sample was plotted in figure (II.I4).

(c) Rubber Slab With Closed Pores: A circular disc of I.0 cm. thick rubber having cylindirical pores set perpendicular to the end faces, and 0.2 cm. diameter was used as a test samle.

To prevent the penetration of water in the pores and the escape of air from the pores, the samle was covered with 0.I cm. rubber sheet.

The variation of reflection coefficient against hydrostatic pressure at a frequency of 4 Kc/s has been measures and plotted in figure (II.I5).

(d)Foamed Plastic(I): A circular disc of 2.4 cm. thick foamed plastic was used. Density of this sample is 0.32 gm/cm. The reflection coefficient of this sample is plotted as a function of hydros-

rostatic pressure in figure (II.I6).

(e) Foamed Plastic(II): A similar sample with (d) was used, The density of this material is 0.I7 gm/cm. The reflection coefficient of this sample is plotted as a function of pressure in figure (II.I7).

(f) Foamed Plastic (III): The density of this material is 0.06 gm/cm. Tests showed that this material was inadequate to the pressures above I5 atmospheres. Therefore, measurements were carried out at the pressures from zero to I0 atmospheres. The reflection coefficient of this sample as a function of pressure is shown in figure (II.I8).

As a result of these measurements, it is evident that the reflection coefficient decreases with rising pressure. This decrease in reflection coefficient is caused by the high static load on the solid structure containing air. Under high pressure, compression of the solid structure of the foamed material leads to the formation of increasing numbers of sound bridges allowing for better transmission of sound.

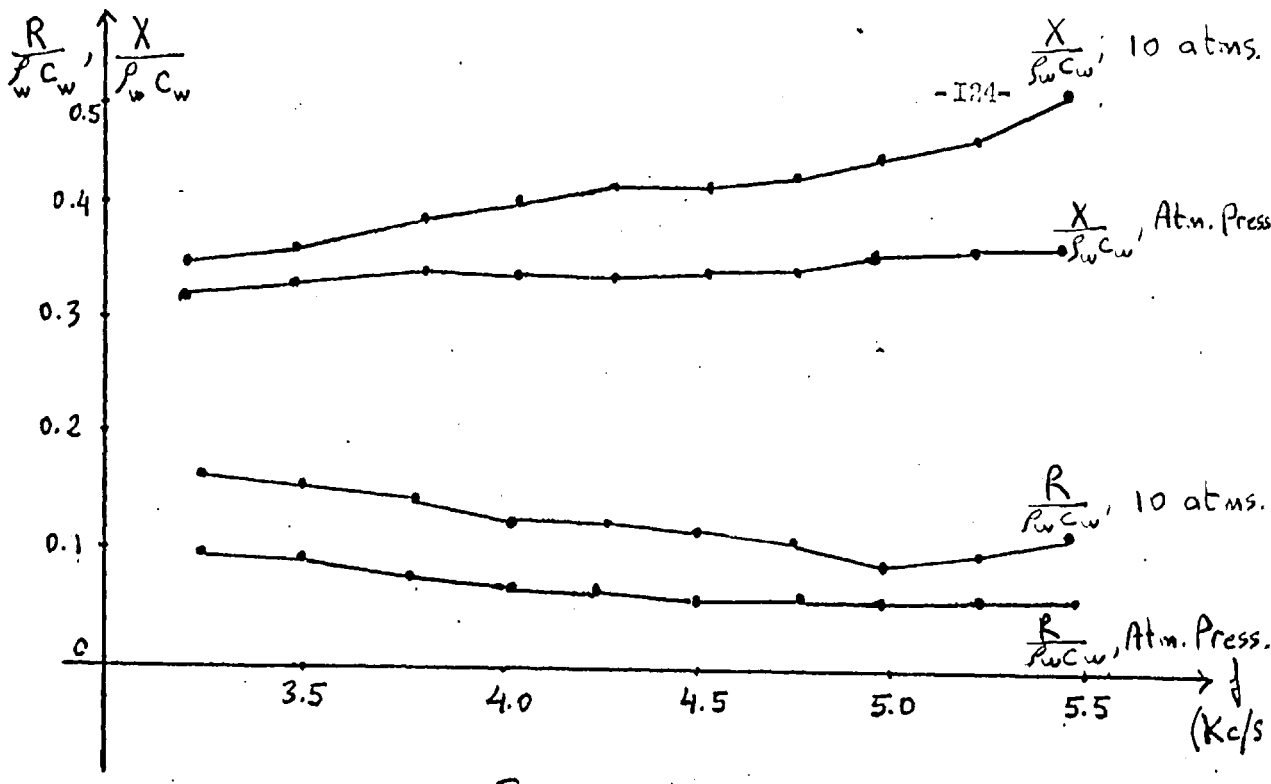

Figure 11.9

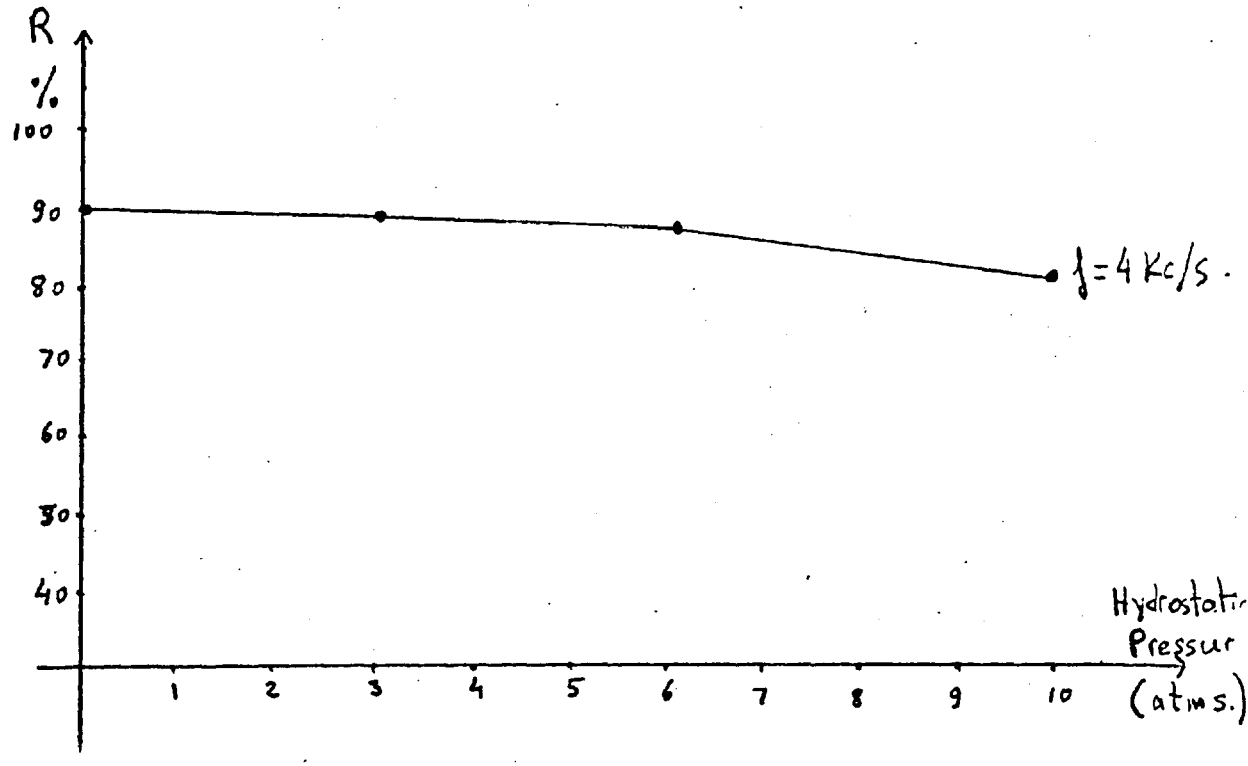

Figure 11.10

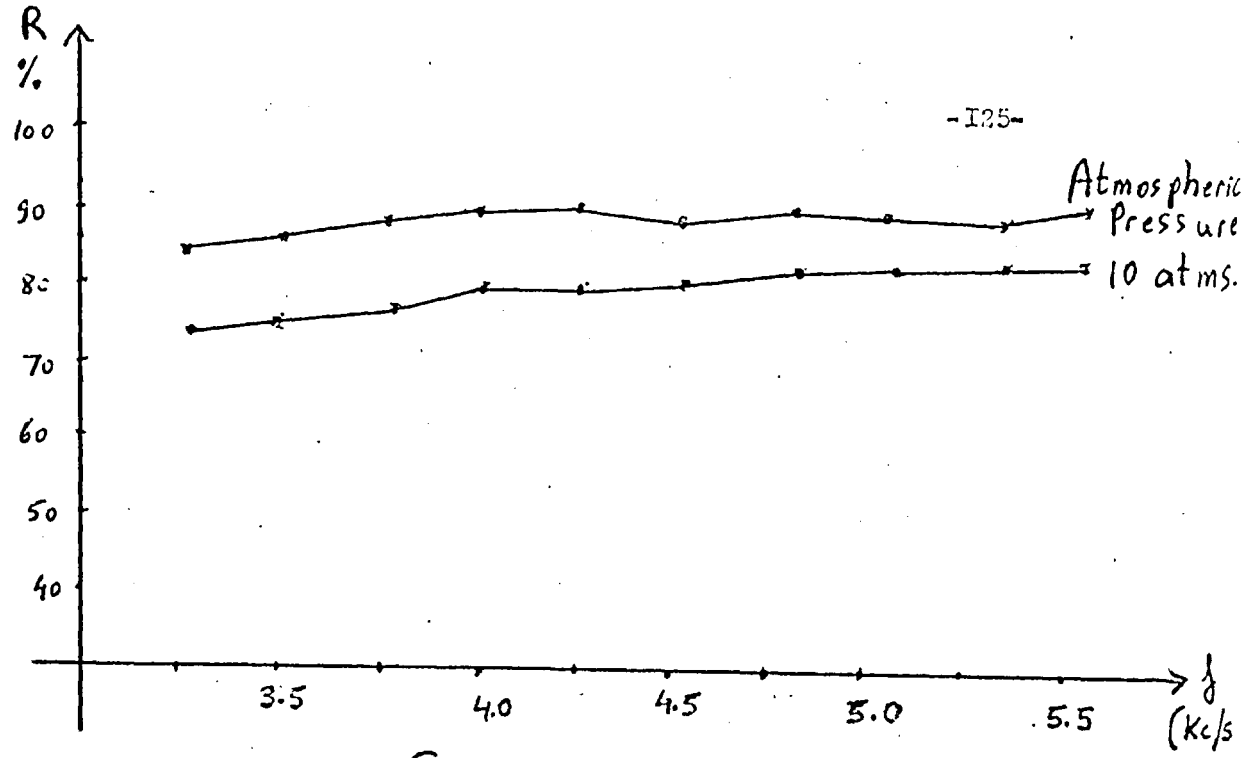

Figure 11.11

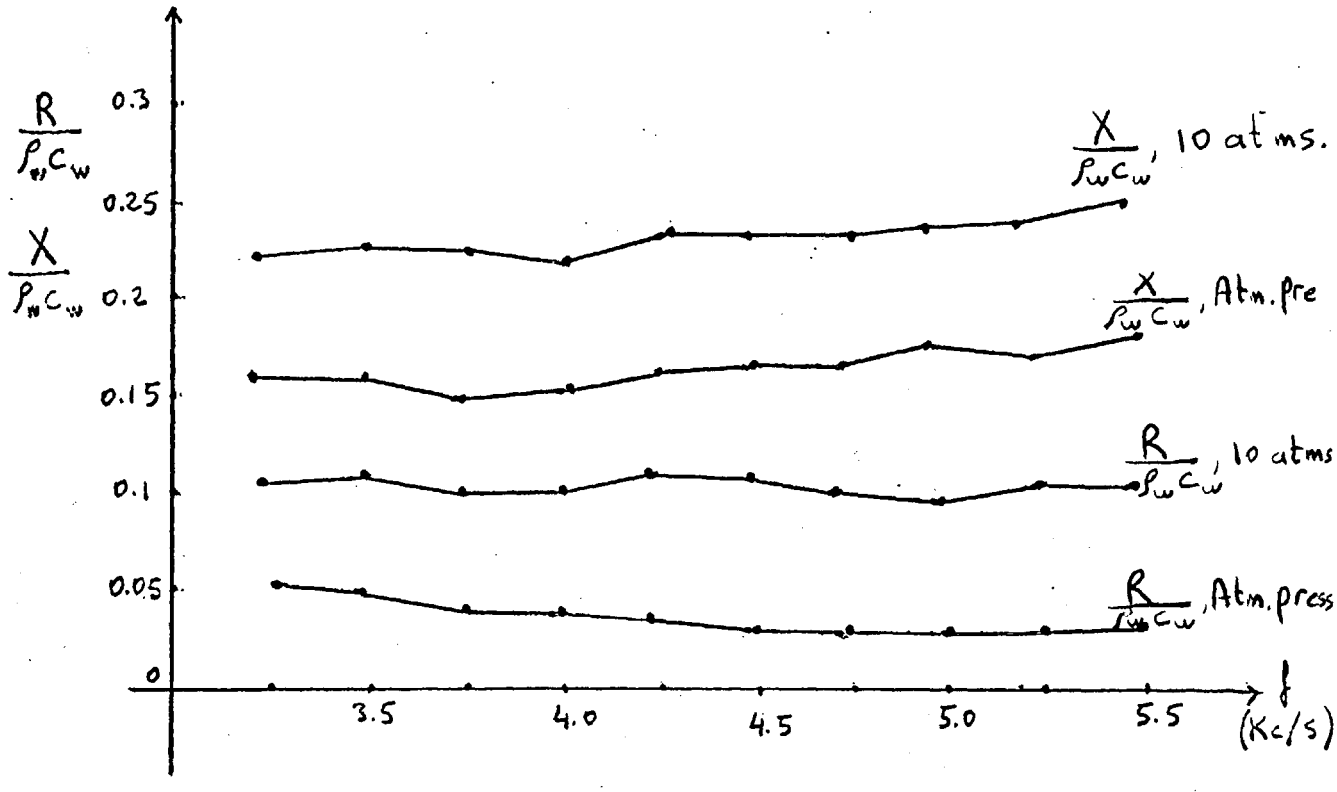

Figure 11.12

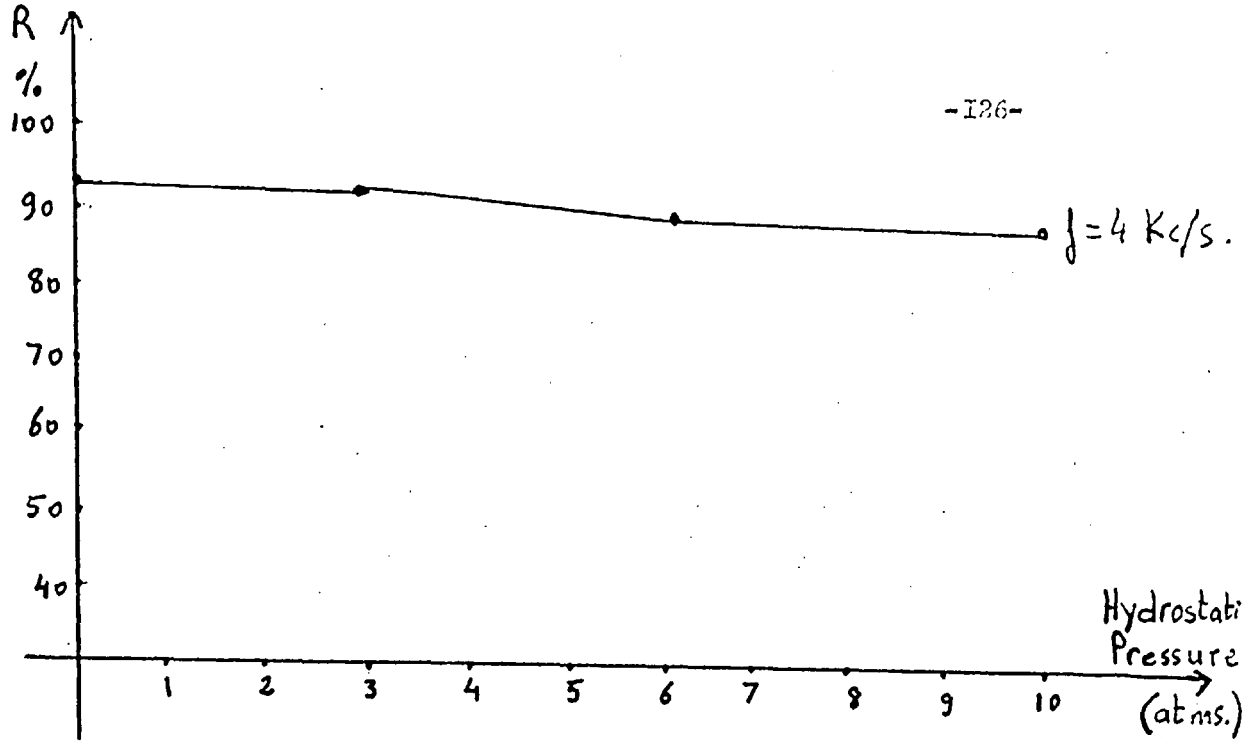

Figure 11.13

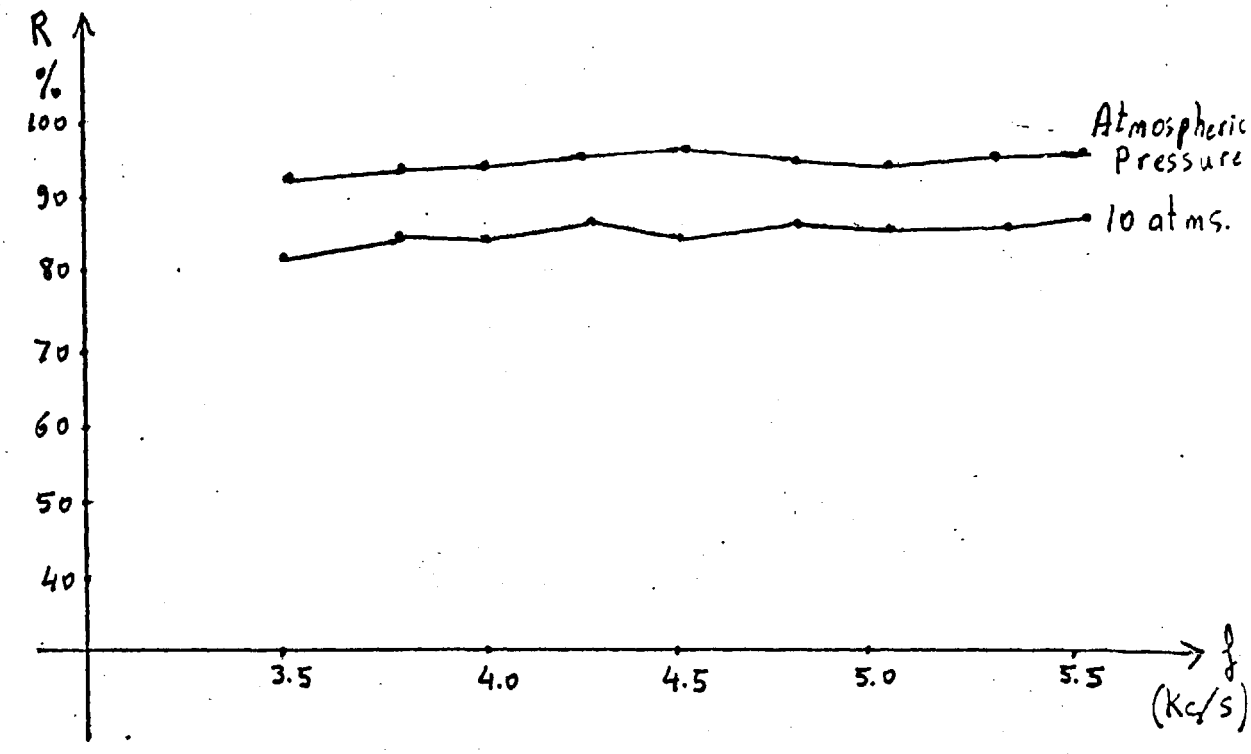

Figure 11.14

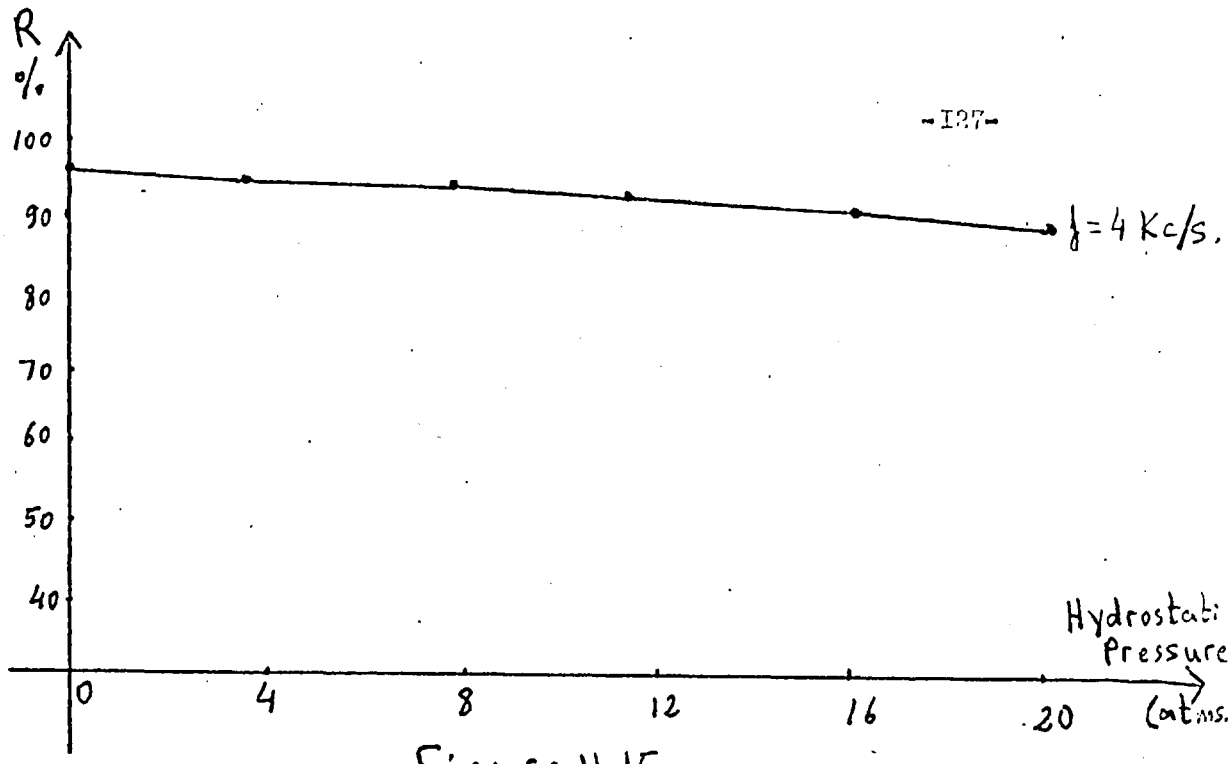

Figure 11.15

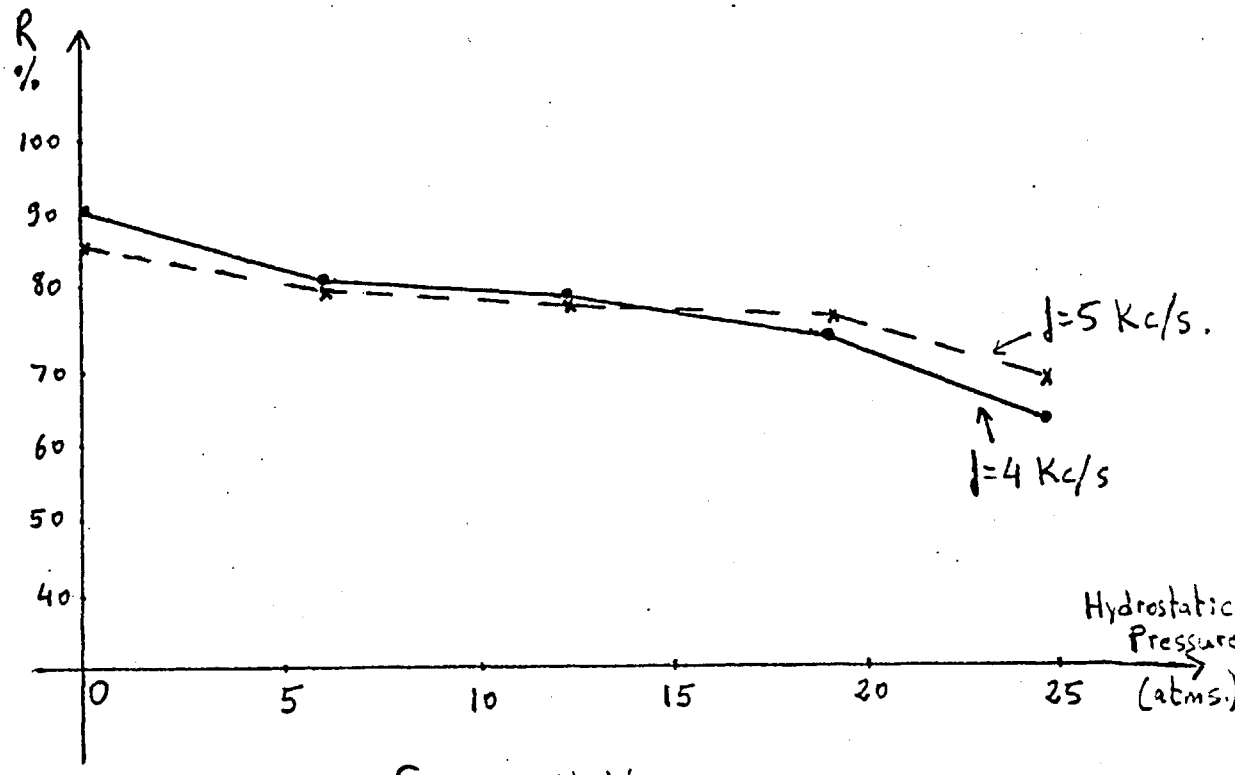

Figure 11.16

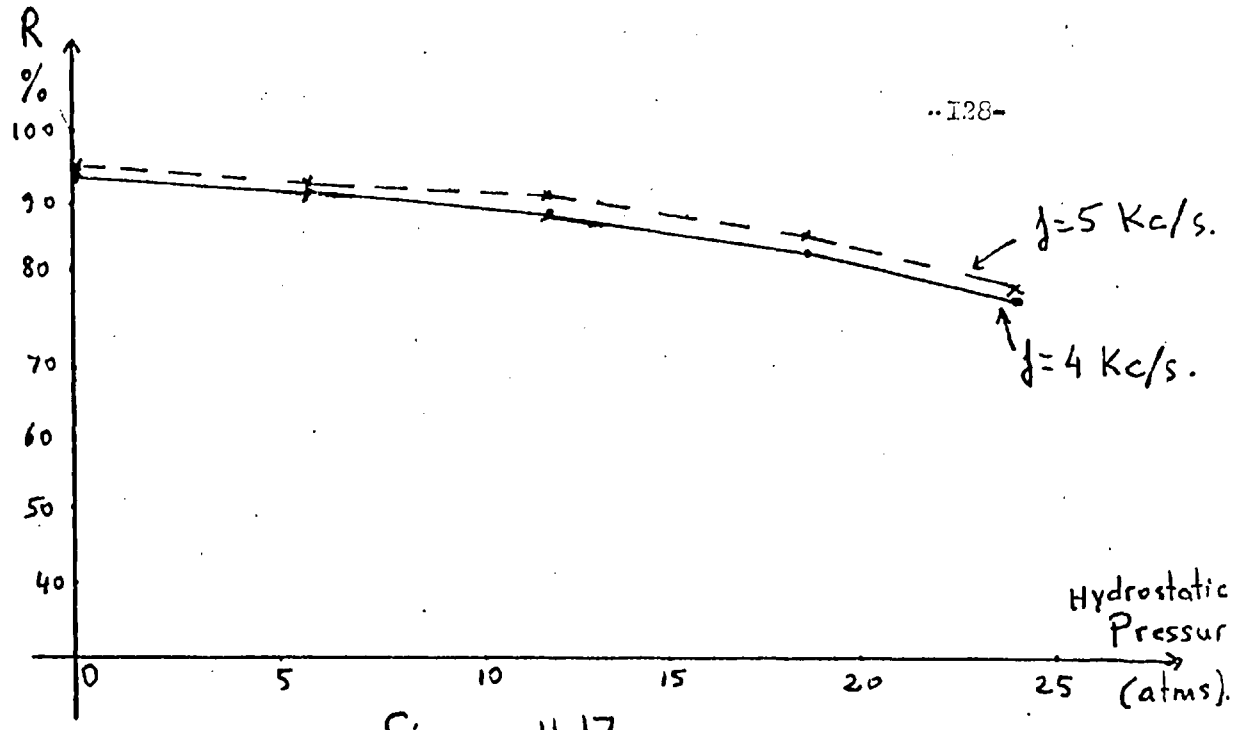

Figure 11.17

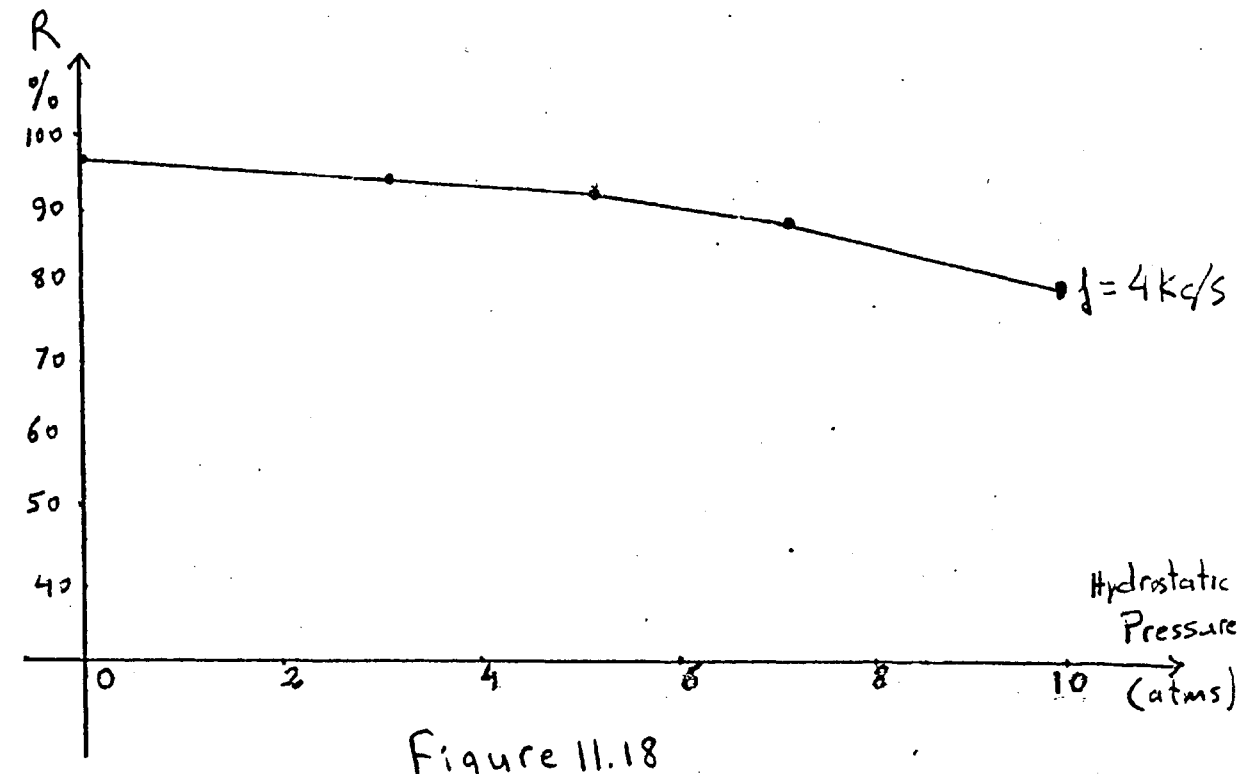

Figure 11.18

REFERENCES.

(I) Lord Rayleigh(I896), The Theory of Sound, p.72.

(2) P.M.Morse(I948), Vibration and Sound, 2.ed. p.368.

(3) R.Rogers(I940), The Attenuation of Sound in Tubes, J.A.S.A. II, p.480.

(4) M.Redwood(I960), Mechanical Wave-guides.

(5) K.G.Budden(I96I), The Wave-guide Mode Theory of Wave Propagation.

(6) S.N.Rschevkin(I963), Course of Lectures on The Theory of Sound.

(7) R.W.B.Stephens and A.E.Bate(I966), Acoustics and Virational Physics, p.525.

(8) H.E.Hartig and C.E.Swanson(I938),Transverse Acoustic Waves in Rigid Tubes, Phys. Rev. 54, p.6I8.

(9) R.A.Scott(I946), An Apparatus for Accurate Measurement of The Acoustic Impedance of Sound Absorbing Materials, Proc. Phys. Soc. p.253.

(I0) L.L.Beranek(I949), Acoustic Measurements, p.326.

(II) E.A.G.Shaw(I953), The Acoustic Wave-guide. An Apparatus for The Measurement of Acoustic Impedance Using Plane Waves and Higher Order Waves in Tubes, J.A.S.A. 25, p.224 and p.23I.

(I2) Stokes(I845), Camb. Trans. 9, or see (I), p.3I5.

(I3) Kirchhoff(I868), Pogg. Ann. I34.

(I4) L.J.Sivian(I947), High Frequency Absorption in Air and in Other Gases, J.A.S.A. I9, p.9I4.

(I5)Helmholtz(I863), Verh.d.nat.hist.med.III,S,I6.

(I6)W.P.Mason(I928), The Propagation Characteristics of Sound Tubes and Acoustic Filters, Phys.Rev.3I, p.283.

(I7)L.L.Beranek(I940), Precision Measurement of Acoustic Impedance, "Tube Dissipation", J.A.S.A.I2,p.IO.

(I8)R.D.Fay(I940), Attenuation of Sound in Tubes,J.A.S.A.I2,p.62.

(I9)R.A.Scott(I946),The Absorption of Sound in a Homegeneous Porous Medium, Proc.Phys.Soc.58,P.I65 and p.253.

(20)P.M.Morse(I948), reference(2),p.38I.

(2I)L.Cremer(I948), Arch.Elekt.Ubertraung 2,p.I36.

(22)A.K.Nielsen(I949),Acoustic Resonators of Circular Cross-Section and with Axial Symmetry, Trans.Danish Acad.Tech.Sci.No:IO.

(23)A.E.Hartig and R.F.Lambert(I950), Attenuation in a Rectangular Slotted Tube of (I,0) Transverse Acoustic Waves,J.A.S.A.22,p.42.

(24)E.A.G.Shaw(I950),Attenuation of (I,0)Transverse Acoustic Waves in a Rectangular Tube,J.A.S.A.22, p.5I2.

(25)B.P.Bogert(I950),Classical Viscosity in Tubes and Cavities of Large Dimensions,J.A.S.A. 22, p.639.

(26) Beatty(I950),Attenuation of (n,0) Transverse Modes in a Rectangular Tube,J.A.S.A.22,p.850.

(27) Beatty(I950),Boundary Layer Attenuation of Higher Order Modes in Rectangular and Circular Tubes,J.A.S.A.22,p.850.

(28)R.F.Lambert(I95I), Wall Viscosity and Heat Conduction Losses

in Rigid Tubes, J.A.S.A. 23, p.480.

(29) J.C. Slater (I950), Microwave Electronics, p.48.

(30) E.A.G. Shaw (I953), The Attenuation of The Higher Order Modes of Acoustic Waves in a Rectangular Tube, Acoustica 3, p.87.

(3I) I.D. Champbell (I953), The Transmission of a Plane Wave Between Parallel Plates, Acoustica 5, p.298.

(32) A.M. Ghabrial (I955), Attenuation of The (I,0) and (2,0) Modes in Rectangular Ducts, Acoustica 5, p.I87.

(33) R.F. Lambert (I953), A study of The Factors Influencing The Damping of an Acoustical Cavity Resonator. J.A.S.A. 25, p.I068.

(34) D.E. Weston (I953), The Theory of The Propagation of Plane Sound Waves in Tubes, Proc. Phys. Soc. B. 66, p.695.

(35) R.F. Lambert (I955), Acoustical Propagation of Higher Order Modes in The Region of Cut-off, J.A.S.A. 27, p.790.

(36) V.O. Knudsen (I935), The Absorption of Sound in Gasses, J.A.S.A. 6, p.20I.

(37) H. Lamb (I932), Hydrodynamics, 6. ed.

(38) J.S. Pyett (I954), The Propagation of Sound in a Porous Medium, Ph.D. Thesis, University of London.

(39) P.M. Morse (I948), Vibration and Sound, 2. ed. p.I54.

(40) E.A.G. Shaw (I950), A Study of Higher Order Modes of Acoustic Waves in Rectangular Tubes, D.I.C. Thesis, Imperial Colloge.

(4I) L.L. Beranek (I948), Acoustic Measurements, p.37.

(42) Handbook of Chemistry and Physics.

(43) G.W.C.Kaye and T.H.Laby (I966), Tables of Physical and Chemical Constants.

(44) International Critical Tables.

(45) F.E.Fowle(I933), Physical Tables.

(46) N.B. Bhatt(I939), Effect of an Absorbing Wall on The Decay of Normal Frequencies, J.A.S.A.II, p.67.

(47) C.M.Harris(I945), Application of The Wave Theory of Room Acoustics to The Measurement of Acoustic Impedance, J.A.S.A.II, p.67.

(48) E.T.Paris(I927), On The Reflection of Sound from a Porous Surface, Proc. Roy Soc. A II5, p.407.

(49) L.L.Beranek(I942), Acoustic Impedance of Porous Materials, J.A.S.A. I3, p.248.

(50) W. Jackson and L.C.H. Huxley(I944), The Solution of Transmission-Line Problembs By Use of The Circle Diagram of Impedance, Journal of The Inst. of Elect. Eng. Vol 9I, Part3, p.I05.

(5I) E.G.Richardson(I953), Technical Aspects of Sound, Chap. 5.

(52) C.Zwikker and C.W.Kosten (I948), Sound Absorbing Materials.

(53) E.G.Richardson(I953), Technical Aspects of Sound, Chap. 4.

(54) I.D.Champbell(I954), Boundary Layer Phenomena, Ph.D. Thesis, University of Lomdon.

(55) G.G.Parfitt and J.D.Rands(I96I and I962), Pressure-Release materials, Report Nos. I and 2.

(56) E. Bocker(I96I), Pressure-Release Reflectors for Water Borne Sound at High Hydrostatic Pressures, Acoustica 4,p.I90.

(57) R. Fay, R. Brown and C.V.Fortier(I947),Measurements of Acoustic Impedances of Surfaces in Water, J.A.S.A. I9, p.850.

(58) A.B.Wood, Text-Book of Sound, p.267.

(59) E.G.Richardson(I953), Technical Aspects of Sound, Vol.2,p.209.

(60) L.G.Pooler(I930), Physical Review,Vol.35, p.832.

(6I) L.L.Beranek(I948), Acoustic Measurements, p.329.

(62) L.L.Beranek(I940), Precision Measurement of Acoustic Impedance, J.A.S.A. I2,p.3.

W.J.Toulis, J.A.S.A. 29, p.I02I and p.I027,(I957)

H.Sussman, On The Use of Unicellular Rubber for Underwater Acoustic Devices, J.A.S.A. 29,p.I45,(I957).

SYMBOLS.

$A_{m,n}$: The amplitude constant of the (m,n)th mode, A(0) : Absorption coefficient at normal incidence, A(θ): Absorption coefficient at oblique incidence, dA: An elemental area, C: A constant, 2D: Diameter, K_o: Bulk modulus, K: effective bulk modulus, L: See equ.7.II, M_d: The dynamic elastic modulus, P: Pressure, P_o: Amplitude of the sound pressure, R: Reflection coefficient, $R/\rho_o c_o$: resistance ratio, S: The standing wave ratio, W: The rate at which the acoustic energy crossing the section at x = 0, and wave impedance of a medium, $W_{m,n}$: Characteristic impedance of the (m,n) th mode, $dW_{vis.}$: See equ.4.I2, $dW_{th.}$: See equ.4.23, $X/\rho_o c_o$: Reactance ratio, Z: Specific acoustic impedanc Z(0): Spe. aco. imp. at normal incidence, Z(θ): Spe. aco. imp. at oblique incidence.

2a, 2b: Transverse dimensions of the wave-guide (see fig.2.I), c_o: Velocity of sound in air, c: Vel. of sound in a medium with internal damping, c_p: Phase vel., c_g: Group vel., c_w: Vel. of sound in water, c_1: Vel. of flexural wave in a bar, d: Thickness of the material, d_t: Thickness of the tube walls, f: Frequency, f', f'' : See chapter X, f_c : The cut-off frequency, f_o: Resonance frequency, h: An axis (see fig.4.I), $j=\sqrt{-1}$, k: Structure factor, k_t, k_m, k_{na} : The damping constants (see section IO.2), l: The length of the tube, m,n: Mode numbers, p: Sound pressure, $r_{1,0}$: The reflection coefficient of the (I,0) mode, t: Time, u: Particle vel., u_x, u_y, u_z : The components of the particle vel., v : A volume element, x_N : The distance between the N th minimu

and the face of the reflector, x_M : The distance between the Mth maximum and the face of the reflector.

ϕ :The velocity potential, $\gamma_{m,n}$: The propagation constant, $\lambda^{\circ}_{m,n}$: Wavelength of the (m,n)th mode in the loss free case, $\lambda^{\alpha}_{m,n}$: Wavelength of the (m,n)th mode in the case of energy dissipation, f : Cut-off frequency, $\Delta = (2\delta - \pi)$: Phase change accompanying reflection, τ : Period of the acoustic cycle, K : Thermal conductivity, χ :The Ratio of specific heats, χ_p : Specific heat of the gas at constant pressure, $\Psi = \tanh^{-1} p_{min}/p_{max}$ at $x = 0$, Ψ_1 and Ψ_2 : See equations 10.8 and 10.9, η : See equ. 7.12, ω : Angular frequency, $\beta_{m,n}$: Wavelength constant of the (m,n)th mode, ρ_a : Density of air, ρ_w : Density of water, ρ : effective density, θ : angle of incidence, $\alpha_{m,n}$: Attenuation coefficient of the (m,n)th mode, μ : Shear coefficient of viscosity, ξ_{vis} : The viscous boundary layer thickness(see equ.4.9), ξ_{th} : The thermal boundary layer thickness(see equ. 4.16), $\xi_{1,0}$:The shift of pressure minima towards the reflecting surface, ξ : Porosity, ∇ : Flow resistance.